UNIVERSITÀ DEGLI STUDI DI PADOVA

DIPARTIMENTO DI INGEGNERIA DELL'INFORMAZIONE

DIPARTIMENTO DI INGEGNERIA DELL'INFORMAZIONE

CORSO DI LAUREA MAGISTRALE IN BIOINGEGNERIA INDUSTRIALE

"DEVELOPMENT OF AN INTEGRATED METHODOLOGY FOR THE FUNCTIONAL EVALUATION OF MODERN SKITOURING SKIS"

Relatore: Prof. Nicola Petrone

Correlatore: Dott. Giuseppe Zullo

Laureando: Matteo Rinaldi

ANNO ACCADEMICO 2023-2024

24 Aprile 2024

Abstract

Aim of this work is the development of an integrated methodology for the functional evaluation of modern ski touring skis. Indoor and outdoor tests were conducted on three pairs of Blizzard skitouring skis to assess differences in skiing performance and at the same time to validate the method. At first indoor test in Padova on Slytech bench were made to evaluate the edge load profiles of the skis, a characteristic 'footprint' representative of the force distribution on the ski edges during a turn. Bench tests were carried out on a surface representative of hard snow, while softer surfaces with behavior similar to soft snow were characterized for future trial. Subsequently, outdoor tests were conducted on skis instrumented with load cells in Nassfeld, focusing on the loads acting at the ski-snow interface. At the end subjective evaluation of the performances of the three skis were collected in Madonna di Campiglio with a questionnaire filled from ski instructors. The results of the bench and track tests were then compared with the subjective ratings obtained to confirm their representativeness. This workflow gave a complete set of objective and subjective parameters to evaluate the ski performances of skis with different shape, geometry and stiffness.

Index

1. Introduction

Skiing is a quintessential winter sport where athletes navigate across snow-covered terrain with the aid of skis. It encompasses various disciplines, each distinguished by unique features and objectives. For instance, in alpine skiing, athletes carve their way down groomed slopes, while in Nordic skiing, they propel themselves forward along designated tracks using a combination of skis and poles. Skitouring, on the other hand, involves ascending off-piste terrain before descending back down. Given the distinct demands of each discipline, appropriate attire is paramount for optimal performance. Alpine skiing calls for robust and stable skis that facilitate precise carving, whereas Nordic skiing necessitates lightweight, glide-enhancing skis to propel skiers swiftly along the course. Skitouring demands skis that are lightweight for uphill travel yet sturdy enough to provide stability during the descent.

1.1 Skitouring

Skitouring is a sport performed in mountain during the winter season, usually off-piste, using the appropriate typology of ski and skiboots and the help of seal skins. Seal skin is a band of synthetic tissue adhesive on one side and covered with oriented textile fiber on the other. Applied under the skis, it allows, due to the anisotropic orientation of the fibers, to slide only forward without then sliding backward, and thus to cope with a snowy ascent even steep. Seal skins are applied only when going uphill.

Figure 1.1: uphill and downhill use of skitouring skis

Skitouring garments are:

- Skitouring skis: these are skis similar in size to those for alpine skiing but lighter with bindings that allow the heel to be free, thus facilitating the uphill movements and then locked for skiing downhill.

Figure 1.2: skitouring bindings and boots

- Skitouring boots: similar to alpine ski boots but lighter, equipped with a rubber sole to facilitate walking should be necessary. Skiboots are designed with consideration of the requirements for both going uphill and skiing down.
- Ski poles: very similar to those for alpine skiing, but also lighter. Can be telescopic. During the ascent help the arm push while during the descent help the stability.
- Seal skins: made of synthetic material (polyester), they have an adhesive side and should be applied to the base of the ski when you want to undertake an ascent by being removed and stored in the backpack before the descent.

Figure 1.3: seal skins

- There are also several other tools such as: crampons, ice axe and more generally any mountaineering equipment needed to overcome any mountaineering difficulties along the way.

Skitouring can be approached mostly in two ways. A huge amount of people intends it as a way to approach big mountains during the winter in order to climb them. So skitouring became a vehicle with which people can cross mountains, glaciers and valley to approach alpinistic routes while carrying with them climbing material. Skiers need a solid base of technical skills when skitouring is intended as an high altitude sport. Other people prefer skitouring as a stand-alone activity and practice it nearby alpine skiing's slope or in terrain less difficult than glaciers and big mountains. Different approach of the same sport need difference in sports equipments: in the first case ski must be lighter because of the big drop that has to be covered while in the second case a ski with better performance downhill is requested by users.

1.2 Ski Construction

This chapter provides a summary of the construction and production of skis. The ski is the piece of equipment that is responsible for allowing the skier to glide uphill and downhill and for providing speed and trajectory control during the descent.

1.2.1 Ski Elements

A ski usually consists of:

- **Core [1]:** internal part of the ski that determines its mechanical behavior. It can be made of various materials such as wood, synthetic foams, or honeycomb composites. Its construction gives the ski the behavioral characteristics for which it is designed. Wood is the most used material for its mechanical behavior.
- **Surface [2]:** upper outer part of the ski, can be made of metal or plastic material. Its function is to cover and enclose the load-bearing part of the ski called core. The surface is in charge of the cosmetics of the ski. It can be either painted or printed by means of techniques such as sublimation. In some cases, it can also play a structural role as in the construction called "monocoque."
- **Sidewall [3]:** lateral elements that run on both sides along the entire longitudinal development of the ski. Together with the surface they have the task of closing the core. During the descent they allow the movements of the skier to be transmitted to the edges and, conversely transmit terrain information to the skier. They can be made of different materials, generally plastics. Different hardnesses affect the mechanical behavior of the ski, changing its torsion and flex.
- **Running base [4]:** polyethylene sheet that allows sliding on snow. To increase glide, polyethylene can also be enriched with graphite (black insoles).
- **Steel edges [5]:** these are metal elements, usually made of steel, that are intended to cut through the hardest and/or icy snows to ensure speed control, trajectory set up, and skier safety.
- **Reinforcement elements [6]:** various types of metal and/or fiber reinforcements are also used in ski construction. Generally, these reinforcements are inserted between the surface, the base and the core. In many cases above the wood core is also enclosed inside a fiber wrap (glass and/or carbon, called an anti-torsion case). This processing is intended to increase torsional strengths. Fiber orientation plays a key role in achieving different torsional strength results.

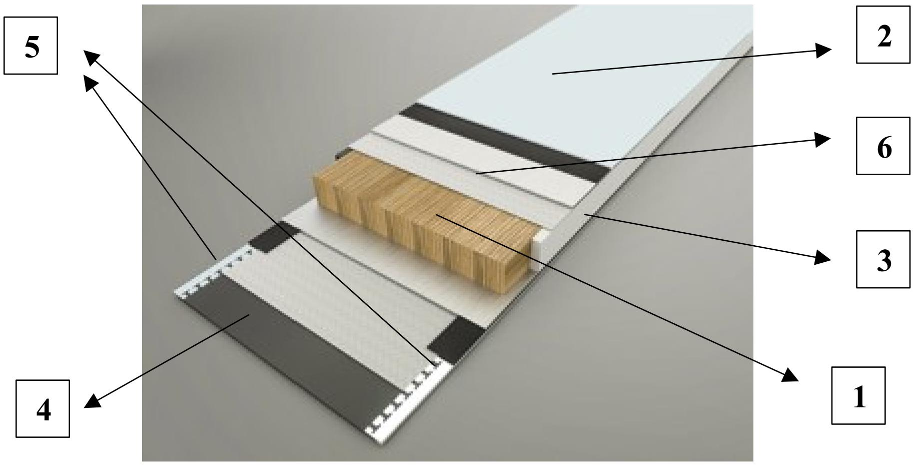

Figure 1.3: ski construction elements

The upper ski construction elements can be combined to modify characteristics of the ski. For a ski the most important characteristics are:

- **Sidecut:** geometric shape determined by the difference in width between the ends (paddle and tail) of the ski and the center. Joining these points will produce an arc that determines the static curve radius of a ski (also called the sidecut radius).
- **Ski width:** indicates the ski's ability to be used on different types of terrain. Narrow skis (with values between 63-70mm) are best suited for on-piste use. Wider skis increase flotation aptitude for use on freshly fallen or melting snow;

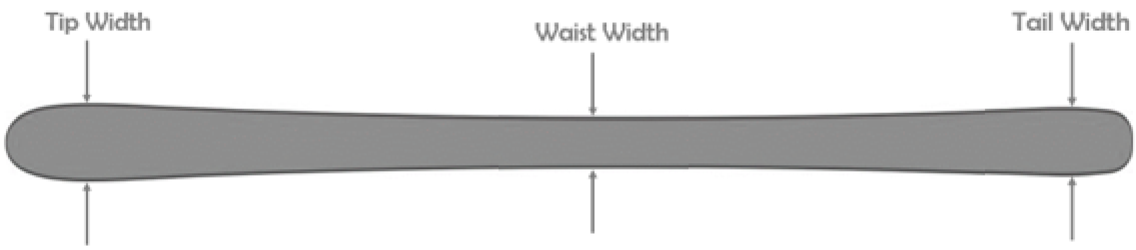

Figure 1.4: definition of tip, waist and tail width from Soothski website

- **Flex:** property of the ski to deform longitudinally when appropriately stressed by pressure. Different structure materials gives different results in bending. For skis intended for competitive or high-performance use, a structure capable of resisting high loads is made. When a ski is designed for light skiers or those with low technical ability, a softer flex is preferred. For skis intended for Freeride use, differentiated hardnesses are opted for, with softer ends facilitating floating, while the harder middle area allows for better ski grip in more compact snows;

- **Torque:** deformation in a helical direction that the ski undergoes when resting on edges. Skis that are particularly resistant to this deformation are suitable for on-piste use on compact or hard snow. The skis are very precise in their handling but are particularly nervous and require excellent technique to manage the execution of turns. Conversely, skis that are less resistant to this deformation increase handling at low speeds, forgive any technical shortcomings but offer less grip on hard snows
- **Elastic rebound:** property of the ski to return to its initial condition after being stressed. Skis that have a faster return (elastic response) are better suited for execution of short arc turns. Conversely, a less rapid return characterizes skis intended for execution of long arcs.

1.2.2 Ski Materials

Under the most reproducible conditions offered by a prepared slope, skiing means traversing a slope consisting of a succession of planes inclined at different angles to a horizontal reference plane. These planes also have an undulating lateral profile: therefore locally depressions and reliefs change the slope from the average slope. The skier alternates between straight downhill sections along the maximum slope, curves of different amplitudes, and straight diagonal sections, varying speed according to his or her ability, taste, and environmental conditions.

Considering three sequences of turns executed on the same wide, medium-gradient slope by the same skier using a defined pair of skis: snowplow turns, base turns, and conducted turns; these are turns of very different levels from each other in which the motor gestures performed selectively exploit different properties of the implement. The ski must therefore be constructed in such a way that it is still satisfactory with respect to stability, maneuverability, damping of mechanical vibrations produced by the movement in contact with the ground, and precision in the execution of trajectories. As with many other high-tech products, there is no such thing as a ski with optimal performance with respect to every characteristic: different types of equipment, targeting different categories of users with different skill levels, favor some characteristics at the expense of others. A historical retrospective shows that evolution in ski construction, during the 20th Century, progressed in parallel with the introduction of new structural materials: in order metals, fibers, particularly glass and carbon, polyurethane foams (polymers), replaced, or were variously combined with, the original wood. Of equal importance, though less well known, has been research into bonding techniques and materials.

Consider a current ski: it must exhibit certain characteristics of bending stiffness, maximum possible torsional stiffness, and high yield strength. The tool must be waterproof, offer performance indifferent to possible variations in environmental temperature, and maintain performance over long periods of use, under proper conditions of use and maintenance; maintenance cannot be complex or time-consuming.

The experience accumulated in the past, when skis were made entirely of wood, remain true. In fact, wood is a natural composite where cellulose gives high elasticity and mechanical strength, while lignin is the resin matrix with significant stiffness and brittleness. Wood, seasoned and with balanced moisture content, has excellent mechanical vibration damping capabilities, high reactivity and elasticity, and stable properties over time even at low temperature, which facilitate ski deformation and elastic recovery. One shortcoming is its relatively high density, so wooden skis are heavy and of limited maneuverability. This is also why modern skis are made following two main schemes: sandwich and torsion box, or monocoque (cap). The former scheme is adopted for high level and competition skis, the latter for low to medium level skis.

The sandwich structure consists of a central core and several layers of structural and, or protective materials. The purpose of the core is to establish and maintain a distance between these layers, increasing the rigidity of the structure, with a limited increase in weight. It is made of laminated wood: it has consistent stiffness and resistance to shear and compressive stresses and has low density. The laths, made of two or more types of wood of different hardness and flexibility, are laminated vertically, arranged alternately, aligned with the longitudinal axis of the ski and glued together. Beech, ash, maple and birch give the tool stiffness; poplar and paulownia flexibility and lightness. Occasionally other woods are used, for example cedar.

With respect to the core, looking at a cross-section of skis, proceeding outward are arranged, either upward or downward, at least one layer of fiber-reinforced polymer matrix composite material. These may be glass, carbon, boron, basalt, or Kevlar. All fibers impart strength and stiffness to the matrix. Widely dominant for reasons of quality-cost-ease of production are glass fibers. These are now beginning to be replaced by basalt fibers that perform similarly and are less toxic. Carbon fibers and Kevlar, which are very good in damping vibrations, have limited diffusion. Still niche is the adoption of boron fibers because of the high cost of production.

Metal layers, among which the most suitable is an aluminum alloy called Titanal (composition $Al_{88.7}Cu_{1.7}Mg_{2.5}Zn_{7}Zr_{0.1}$), help stiffen the structure and give it high elastic properties. Different construction strategies lead to variations in composite structure, thickness of individual layers, their number, and relative arrangement, thus corresponding to tools with significantly differentiated responses to the same stresses among them.

The support structure just described is externally protected from impact and moisture by a polymer coating, usually decorated. On the side, sidewalls made of ABS, or phenolic resins, protect the core from impact, abrasion, and moisture and transmit the force exerted by the skier to the edges.

On the underside, in contact with the snow, the ski features the base, currently made of ultra-high molecular weight polyethylene, UHMWPE, with added carbon compounds to which are associated the black color and the thermal and electrical conductivities necessary to optimize sliding on snow/ice. On both sides to the slab is attached a thin metal foil with a sharp and precise profile. The material used is C60 low-alloy steel, which offers a reasonable compromise between wear resistance and deformability. Unfortunately, it is easily oxidized in a humid environment (a layer of iron oxide, i.e., rust, is formed); the problem has been solved by sometimes adopting stainless steels, with worse mechanical performance, and higher cost, which have limited its widespread use. However, the mechanical performance, particularly hardness and fracture toughness of C60, appears to be inadequate for prolonged use on today's aggressive snows and requires continuous maintenance; as a result, in a short time the foils, whose initial thickness is on the order of 1.5 mm, wear out.

Often the life of a tool is limited precisely by the consumption of the foils. We observe again that, introduced in the 1960s, with soft natural snows, polyethylene, even in its UHMWPE evolution, has excellent sliding characteristics, further enhanced by additives, but as a polymer, it is inherently soft. As such it strongly suffers wear and irreversible physicochemical degradation if, under conditions of use on modern aggressive snows, the polymerization temperature is exceeded by heating caused by friction during sliding at high speed. One possible solution to the limitations of current slabs and foils is to make slabs from metallic materials, which have significantly superior mechanical properties. With this choice, the distinction between slab and laminae also falls. Under straight sliding conditions on snows of different consistencies, the performance of prototype skis made with metal slabs is comparable to, or better than, that of identical skis with UHMWPE slabs and conventional foils, prepared at the state of the art.

1.2.3 Ski Geometry

In order to change direction for skis with respect to straight motion, a force directed transverse to the direction of motion and oriented in the direction in which one wants to head is required. The cause of the curve is a muscular, voluntary force generated by the skier, oriented toward the center of the curve he or she wants to go through and for this reason called centripetal force. It is revealed by the fact that the skis are placed at a certain angle of edge grip with respect to the terrain. This requires the presence of the terrain binding reaction, the direction of which changes as the angle of edge grip changes. However, edge grip alone is not sufficient for skis to curve. In fact, if they were straight, undeformable bars, the edge grip would fail to make them deviate from a straight trajectory. Deformable skis, with a straight side profile, can travel a curved trajectory because they deform along their longitudinal axis. The greater pressure on the center part than on the paddle and tail causes the tool to elastically deform, which flexes and thus can change trajectory. For skis of similar length, however, all turns made in this way would be approximately equal arcs to each other.

The geometric properties of the tool then assume decisive importance. Sidecut, the parameter that gives the measure of the difference in width between the paddle, the center and the tail of the ski, allows the longitudinal deformation of the ski to vary greatly as the angle of edge grip varies. Considering a ski of fixed length, a given skier and the same terrain, for any given defined edge grip angle, the more the sidecut of the ski is accentuated, the more the arc of the curve drawn at the edge-snow contact is short and the more the tool is elastically deformed.

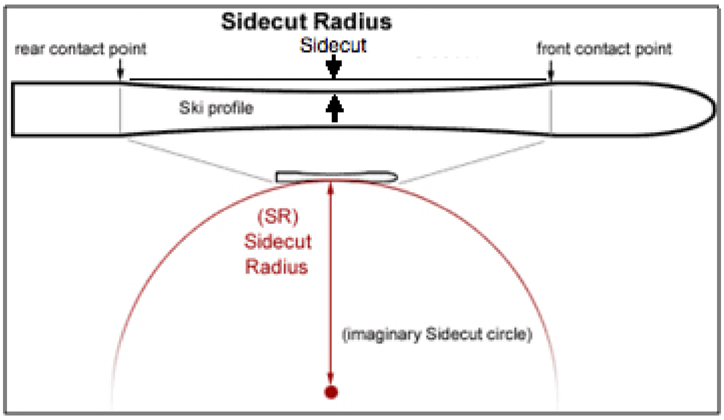

Figure 1.5: ski sidecut definition

If skiing in ideal conduction, the geometry of the ski (lateral profile) in continuous contact with the terrain completely defines the curve trajectory. For each sidecut, the maximum curve radius possible without skidding of the implement can be determined. The minimum value depends on the consistency of the snow and the skier's actions. Softer snow, which allows more sinking of the middle part of the ski, allows for shorter turns with a smaller edge grip angle. The more pronounced the sidecut, the shorter the cornering trajectories achievable with the same ski deformation and, at the same time, the greater the centripetal moment the skier must generate to balance the centrifugal moment.

The elastic deformation of the ski is further increased by the camber, the upward curvature of the central part of the tool with respect to the tip and tail: this can be clearly assessed when the ski, unloaded, is placed on a horizontal plane. The role of the camber is to distribute along the entire length of the ski the load exerted by the skier. As a matter of fact, when the skier is stationary on skis placed flat on the ground, the pressure affects the central part, under the boot, plus a small contribution to cancel the centina at the shovel and tail.

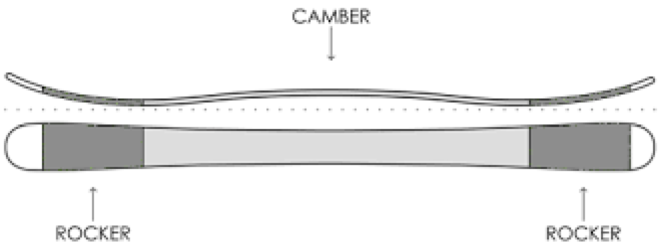

Figure 1.6: ski rocker and camber

When the ski, loaded by the skier, is resting on the edge on a slope of fixed gradient, on compact snow, the distribution of pressure between the shovel, center, and tail varies according to the stiffness of the tool: roughly speaking, in giant slalom and superG skis the pressure on the center of the ski is about equal to that on the shovel and tail; in slalom skis the pressure on the shovel is less than on the center and tail, while in touring skis the pressure is greater on the center than on the shovel and tail.

In general, the more rigid a ski is, the more intense are the forces required to deform it, and, at low speed, it becomes more difficult to direct it without skidding along a curvilinear trajectory, all the more, the more it consists of short-arc curves. On the other hand, the elastic response of the implement when it resumes its original lateral profile, or approaches it, is all the more intense and develops in a shorter time the more rigid it is. This contribution of mechanical energy that becomes available toward the end of the turn gives the skier a direct impulse along the longitudinal axis of the ski, providing him with extra acceleration and increasing his longitudinal speed.

1.2.4 Ski Production

There are several methods for constructing a pair of skis; the choice depends on the type of performance you want to achieve. “Sandwich Construction” is so called because several materials assembled are used. By adding materials or increasing the thickness of them, one can influence or change the elastic response of the ski, its flex and its torsional strength, thus changing the characteristics of the skis and achieving the desired market segment. This is the most complex construction to make, but also the one that offers the most solutions. “Single Shell Cap Construction” consist of an outer shell that functions as the structure of the ski. Variation in the thickness of the shell along the development of the shaft determines the different performance characteristics of the ski. The inner part of the ski below the shell, and above the edges and base is generally filled with inert synthetic material. “Injected Construction” is used for inexpensive, low-performance skis. The structure of the ski consists of synthetic material injected inside a mold where the surface, edges and base are already present.

Even the most modern construction systems do not allow for full automation of production. For Sandwich construction wood cores are used, process start by assembling the cores, placing the different wood laths side by side following the design. The laths may differ between model in size, shape, type of wood to obtain the core with the required characteristics. The resulting parallelepiped is machined by numerically controlled milling machines to shape it both laterally (sidecut) and longitudinally (tapering). In the case of Sandwich skis with a synthetic core, the same procedure is used with the substitution of the synthetic material chosen instead of wood. All other metal elements such as foils, sidewalls and steel edge are cleaned by special treatments to remove chemical residues from processing, elements that could generate cohesion problems with resins. The fibers are resined inside the mold during the hot assembly phase, or alternatively, already impregnated fibers are used in order to have a better distribution of the resins. If robotic or semi-automatic tools are used for the constituent elements, the assembly of the ski is done exclusively by hand. All the elements that make up the ski are placed manually inside the mold. It starts from the bottom with base and edge and rises to the top surface following the design sequence of the model. This artifact, thus assembled has no cohesion and requires what is known as "baking." The closed mold is placed in a hot press that allows the resins to melt and solidify. In addition, these presses, are set to generate the longitudinal curvature of the ski being able to give the skis different mechanical and behavioral characteristics. The resulting artifact, after cooling, is taken out of the mold and processed for surface finishing and grinding and preparation of the base and sharpening of the edges. Skis are born single and are paired into pairs only after careful inspection that finds, among individual rods, those with similar characteristics.

For single cell cap construction process starts from the mold of the upper shell structure. Then this element is assembled by resin bonding to the lower part of the ski (edges and base). The next step is to fill the gaps between the upper shell and the lower part of the ski with inert synthetic materials. During this operation, which is done hot inside a press, the longitudinal curvature is also generated.

For injected construction the ski is assembled in the molds and, during "baking," is injected a chemical compound which, due to temperature, expands by filling in the gaps.

1.2.5 Ski Choice

The combination of the above elements makes it possible to make skis intended for different types of use or indicated for specific technical needs. To recommend the best ski for a skier, it is essential to take into consideration technical skills of the skier, weight and height of the skier and type of use. Crossing this information helps in the best choice that can be made among the various categories:

- **Race:** ski intended for amatorial and professional's race. Geometric shapes are regulated by Federation.
- **Race Carve:** ski intended for amatorial skiers with high technical skills. This type of ski has high and equilibrated torsional stiffness and can have different shape to perform carved turns with different radius.
- **All Mountain:** ski intended for in-piste and off-piste use. They have lower flexional and torsional stiffness to perform better in every snow conditions.
- **Freeride:** ski indented for off-piste use. They present low stiffness modulus on the extremity while high in the middle. Tail can be raised.
- **Freestyle:** ski intended for snow-park use. Present twin tip to better perform in jump starts and landing.
- **Skitouring:** ski intended for an use uphill and downhill. They must be light but also stable during downhill.

1.3 Research topic

The main objective of this research is to examine in depth how differences in ski widths impact on the performances and on the loads exerted during the descent phase of skitouring skiing. Previous studies showed the possibility of using the Edge Load Profile bench present in the *University of Padova* laboratory as a method to evaluate differences in performance of alpine skis. In "The use of an Edge Load Profile static bench for the qualification of alpine skis" by Petrone N. (2012) are presented the curves of the distribution of forces along the ski edge when it is pressed over a hard surface. Each ski has a characteristics Edge Load Profile and differences in load distribution of various skis can be evaluated observing differences in the shape of their curves.

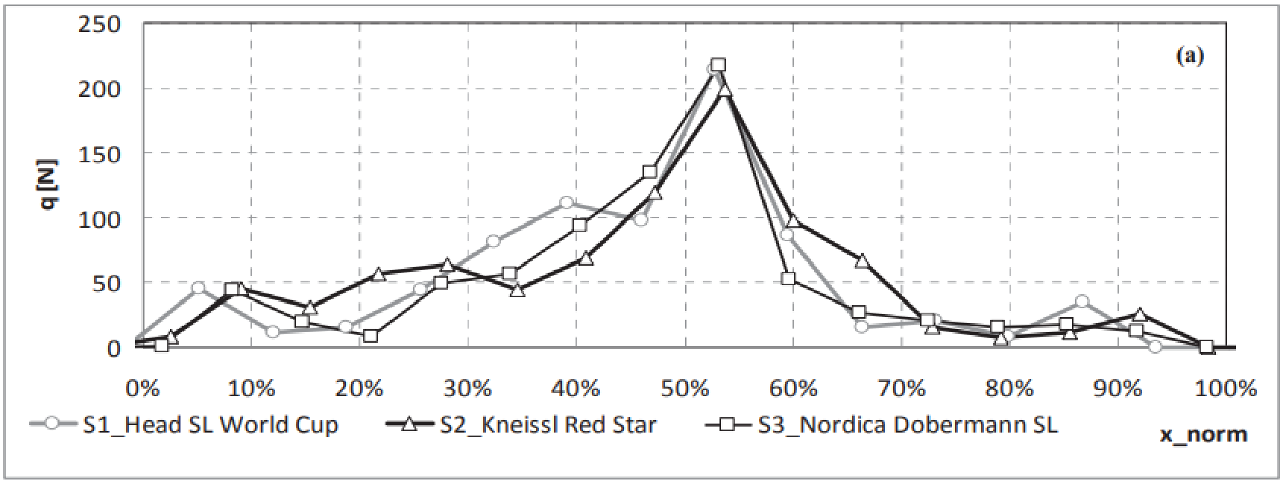

Figure 1.7: differences in Edge Load Profiles between three Special Slalom skis taken *from "The use of an Edge Load Profile static bench for the qualification of alpine skis" by Petrone N. (2012). q represent the Load of each portion of ski edge, while x_norm is the normalized ski length*

The Edge Load profiles are obtained by pushing the ski on a hard surface to maximize the critical points present in the turns. However, it is important to note that these curves do not exactly match the actual force profiles of a ski pressed on snow, as the surface used in the test has a different hardness than the one of the snow. Pilot tests with surfaces of different materials were conducted on the Edge Load Profile bench as part of Cherubin E.'s master thesis project titled "Polymeric Foams: A New Method for Ski Edge Load Distribution Evaluation". Several types of foam, different for manufacturer, nature and thickness, were tested to identify the foam more similar to snow. Then foam panels were sliced and applied as contact surface of the Edge Load Profile test bench. Results showed smoother Edge Load Profiles curves but foams similar to snow were not found. Another interesting work on foams characterization were made by La Chiesa G. during her 's master's thesis project titled "Characterization of snow impact properties and comparison with synthetic surrogates for the correct implementation of helmet safety standards". She performed impact tests over different snow and foams using a sensorized drop tower with an impactor equipped with five different designs of tip. The tests were performed both with the free fall of the impactor and with a preloaded spring to achieve a meaningful simulation of the forces that occur during a ski impact. As the results revealed interesting similarities between snow and foams tested, a similar technology without spring load will be developed in this study. Impact on snow and on phenolic foams will be carried out during this work to understand which foam can simulate different snow conditions.

After evaluating differences in Edge Load Profiles of different skis over hard surfaces and after the research of phenolic foams able to reproduce snow conditions on the bench, more test to evaluate differences in the ski performances of skis with various widths are carried on. In "An Innovative Compact System to Measure Skiing Ground Reaction Forces and Flexural Angles of Alpine and Touring Ski Boots" by Zullo, G.; Cibin, P.; Bortolan, L.; Botteon, M.; Petrone, N. (2023), was introduced a compact portable system able to measure the load under the skis during ski descent.

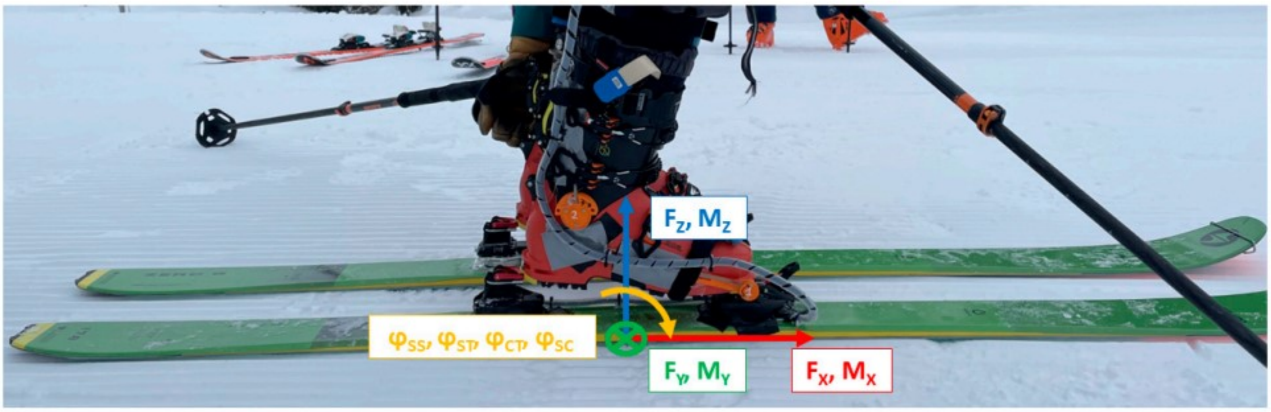

Figure 1.9: particular of the loads and the angles obtained by the instrumentation system developed in the article "An Innovative Compact System to Measure Skiing Ground Reaction Forces and Flexural Angles of Alpine and Touring Ski Boots"

The system was equipped both to skitouring skis and alpine skiing skis, showing as results the differences in loads between the two types of skis. Given the presence of the system in the *University of Padova* laboratory, it will be used in this work to search differences in the loads between different skitouring skis.

At the end also the subjective evaluation can be used to analyze differences in the ski performances. Subjective evaluation offers firsthand, intuitive sense of how well the ski aligns with one's unique style and skill level. Factors such as stability, responsiveness, maneuverability, and comfort, crucial for the skiing experience, are challenging to measure solely through objective means and are largely influenced by the individual preferences of the skier. Moreover, correlations between subjective evaluations and construction parameters of the ski can be searched as made by Brousseau, C.; Desbiens, A.L. in "A.L. Alpine Skiing Recommendation Tool and Performance Prediction".

Possible correlations will explain which construction parameter can influence the performance of the skis.

The combination of Edge Load Profile test bench, Load cell system and Subjective evaluation will be used in this work to understand how skis of different width behave in field conditions. Impact test will be also carried on to understand which foams can simulate the snow conditions during test on the Edge Load Profile bench. At end correlations between building parameters and measured response of the skis will be analyzed to search other parameters responsible of the ski behavior.

2. Materials and Methods

In this chapter are presented the skis used in the study and the test instrumentations used to evaluate the skis performances.

2.1 Skis, Bindings and Boots

Three different pair of *Blizzard ZeroG* skitouring skis were subjected to test to analyze their different behaviors: *Blizzard ZeroG 85, Blizzard ZeroG 95* and *Blizzard ZeroG 105.* These skis primarily differ in their tip, waist, and tail widths, although they have also minor discrepancies in their construction. The following table summarize the skis mainly characteristics:

	ZeroG 85	***ZeroG 95***	***ZeroG 105***
Turn Radius [m]	22	22	23
Length [cm]	178	178	180
Core	Paulownia	Paulownia	Isocore/Beech/Paulownia
Tip Width [mm]	117	127	133
Waist Width [mm]	85	95	105
Tail Width [mm]	101	111	119

Table 2.1: Blizzard ZeroG geometry and construction

The three skis have similar length and turn radius, differ in ski construction (only the *Blizzard ZeroG 105* has a different core material) but has important differences in the ski width and sidecut.

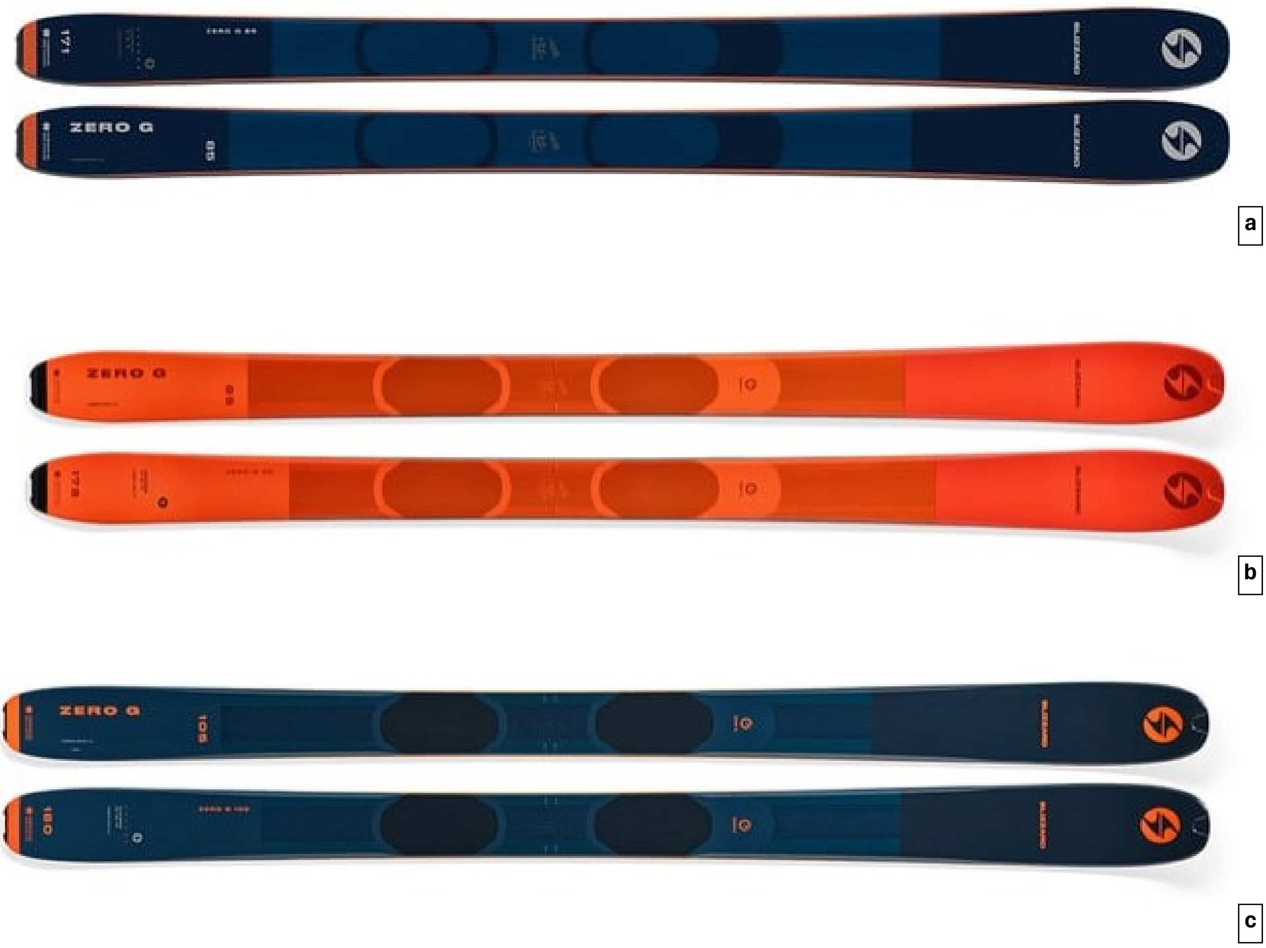

Figure 2.1: Blizzard ZeroG 85 (a), 95 (b) and 105 (c)

In total six pair of skis were tested during the work, two pair for each ski width. One pair was used for indoor test, while the other was used for outdoor sessions. Both pair were equipped with *Marker Alpinist 12.*

Figure 2.2: bindings Marker Alpinist 12 (a) and skiboots Tecnica ZeroG tour pro (b)

For the on-piste skiing *Tecnica ZeroG Tour Pro* skiboots (size 26.5) were used.

2.2 Indoor bench tests

The Slytech test bench is a lab equipment used at the *Department of Industrial Engineering, University of Padova*, for testing the ski edge load profile of different skis at different loads and different edge angles. The test bench is equipped with 21 uniaxial vertical load cells along the ski axis, sustaining each a squared rocking plate with side of 100 mm.

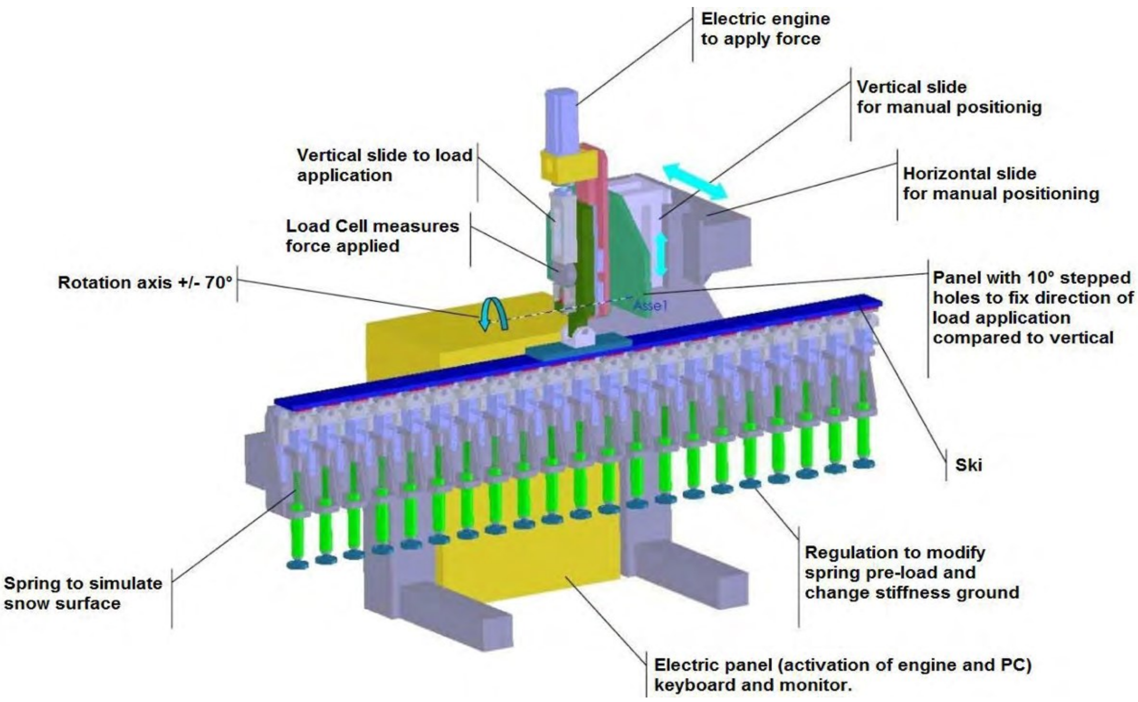

Figure 2.3: 3D model of Slytech testbench

A linear actuator load ski on this bed of load cells with different edge angle form 0° to +/- 70° with steps of 10°. The actuator can also slide vertically and horizontally (as in *Figure 2.3*). An aluminum boot sole designed for alpine skiing bindings. connects the ski to the actuator.

Slytech bench and dummy boot sole are designed for alpine skiing skis. It has been adapted to work as dummy boot sole for pin bindings.

Figure 2.4: dummy boot sole of Slytech bench

Toe and heel plates were removed from the whole body of the existing dummy and new plates were build. The two metal insert on the toe and heel were taken from old skitouring boots and have been welded and screwed to the new plates. The new plates were then added to the main dummy boot sole and the machine was ready to work with skitouring skis.

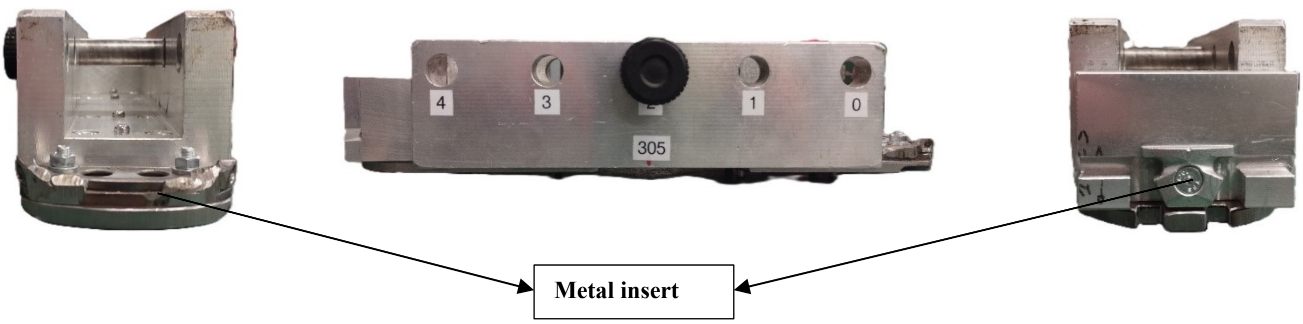

Figure 2.5: new dummy boot sole for pin bindings

When activated the actuator push the ski and the load cells measure the load of the portion of ski above. An additional load cell is mounted on the actuator to measure the applied. The operator can set the load of the actuator and see the results from a PC connected to the system.

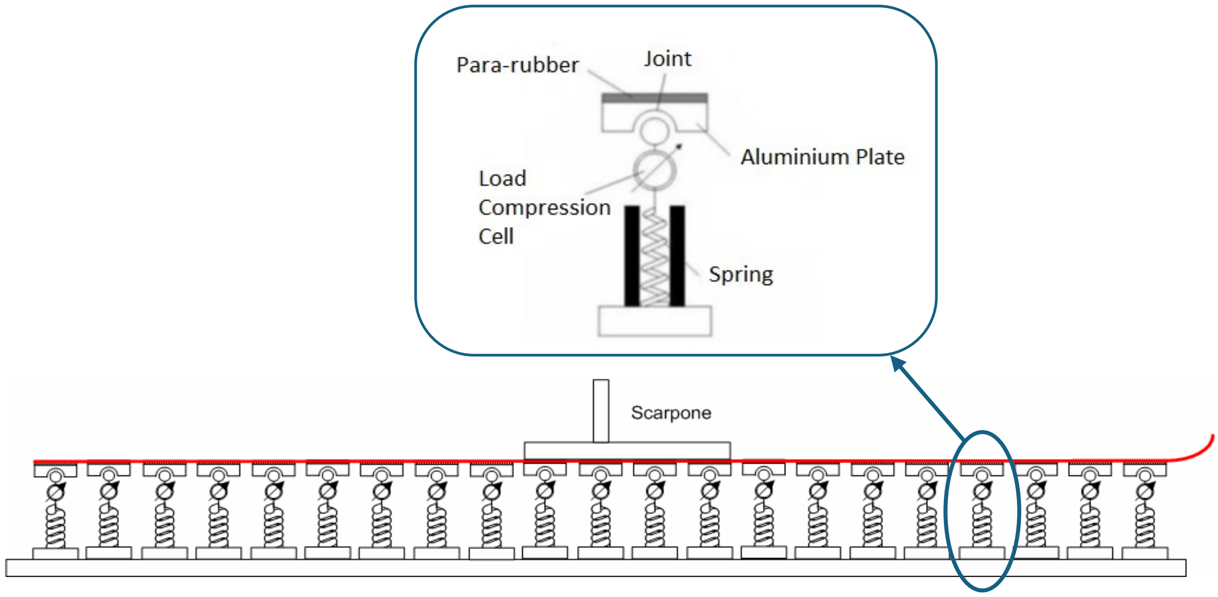

Figure 2.6: Frontal view of the load cell array of Slytech edge load bench

The actuator presses the ski over 21 aluminium plate of 110 mm x 100 mm x 8 mm covered with a layer of Para-rubber able to grip ski steel edge, deforming it and simulate a carved turn. Aluminum plate have free rotation on the axis orthogonal to the ski direction, allowing better adhesion of the ski to the para. Each uniaxial load cell collects the vertical force applied from the portion of ski edge over the plate.

The force applied from the actuator is the sum of skier bodyweight and centrifugal force and is increased as the edge angle grow. When the ski has edge angle equal to 0° the vectorial sum of forces is composed only by vertical forces, when the ski edge angle grows the horizontal centrifugal force appear and increase force orthogonal at the ski surface.

LabView software on the PC connected at the bench collect the output of each load cell, as load expressed in kilograms. A file.*txt* can be saved and imported in *Excel* for data processing. Edge Load Profiles of the ski are plotted for each ski.

Figure 2.7: Slytech test bench in use and detail of rocking plates

The test method consists in connecting the ski at the bench, manually set the ski edge angle at the machine, set the actuator force at the computer, adjust the position of the ski over the rocking plates and start the test after zeroing the system.

For each ski three test were performed at every inclination from 0° to 60° each 10°. At each edge angle correspond the force load expressed in the table.

Angle [°]	**Load [kgf]**
0	50
10	60
20	70
30	85
40	100
50	120
60	140

Table 2.2: applied load corresponding to edge angle on Slytech bench

The applied load is obtained as the vectorial sum of the skier bodyweight and the centrifugal force transferred to one ski.

The *LabView* software gave as output a *.txt* file with the load acquired from each uniaxial load cell. Data are processed with *Excel* and *Load over Distance from tail* graph are plotted.

2.3 Outdoor load cells measurements

During outdoor infield test two M3564F1 load cells by *Sunrise Instruments* were mounted under ski bindings to measure the GRF at the ski-snow interface. These load cells are low-profile cylindrical 6 axis load cells, able to collect forces and moments acting on them on X, Y and Z axis. Each load cell has a cylindrical shape of 10 mm height, 65 mm of diameter and weights 0.190 kg, forming a compact and low weight system. The reference system of each load cell has the Z axis on the cylinder axis, while X axis and Y axis on two orthogonal radial axes of the cylinder. Specific of the load cell are reported in the data sheet in *Figure 2.4*. These load cells have full scale force in X,Y axes of 2500 N, in Z axis of 5000 N, and full scale moment in X,Y axis of 200 Nm and in Z axis of 100 Nm. In outdoor tests where used the load cells with serial number SN13828 and SN13829.

Figure 2.8: Sunrise load cell

The system work with a circuit of 6 independent full Wheatstone bridges, powered with 5V. Output of the system are the mV signals of the bridges: when the load cell is loaded, the resistances of Wheatstone bridges are deformed, changing the resistance. Deformation of the resistance are thus collected as change in mV signals of the 6 bridges.

To obtain forces and moments, mV signals are divided by the voltage of the system, changing their measure unit to mV/V. The 6 channels are then multiplied by the calibration matrix given by *Sunrise Instrumentation* to obtain F_X, F_Y, F_Z [N] and M_X, M_Y, M_Z [Nm] in the reference system of the load cell. The relation to use is the following, assuming that ch_i and F_i, M_i are column vectors containing an element for each collected sample:

$$[F_X \quad F_Y \quad F_Z \quad M_X \quad M_Y \quad M_Z] = ([C] \cdot [ch_1 \quad ch_2 \quad ch_3 \quad ch_4 \quad ch_5 \quad ch_6]^T)^T$$

Calibration matrixes are reported below.

SN13828 calibration matrix

$$[C_{SN13828}] = \begin{bmatrix} 16.1339 & -1.3179 \cdot 10^3 & 11.9077 & 34.5778 & 0.5781 & 1.3000 \cdot 10^3 \\ -29.7976 & 775.8834 & -10.5230 & -1.5369 \cdot 10^3 & 31.6552 & 763.1357 \\ -805.8461 & -8.3500 & -828.3296 & -5.9820 & -823.3692 & -8.9155 \\ 16.7871 & 0.5249 & 0.1148 & -0.0658 & -16.9362 & -0.0709 \\ -9.5992 & -0.2174 & 20.0961 & 0.0453 & -9.6538 & -0.1043 \\ -0.1225 & -20.4818 & 0.2201 & -20.7976 & -0.2238 & -21.7562 \end{bmatrix}$$

SN13829 calibration matrix

$$[C_{SN13829}] = \begin{bmatrix} -5.1523 & -1.3299 \cdot 10^3 & 33.2533 & 24.2635 & -14.7065 & 1.2919 \cdot 10^3 \\ -29.6251 & 776.3958 & -6.4696 & -1.5311 \cdot 10^3 & 27.5223 & 756.4022 \\ -837.3353 & -20.0323 & -856.3873 & -9.4932 & -844.1284 & -5.3031 \\ 17.4557 & 0.3459 & 0.1831 & 0.0623 & -17.2548 & -0.2138 \\ -9.9916 & -0.1069 & 20.5139 & 0.2228 & -10.0826 & -0.0439 \\ -0.1535 & -20.4533 & -0.0695 & -20.5234 & -0.1822 & -21.1902 \end{bmatrix}$$

At the end of the operations a 6 columns matrix is obtained in which each column corresponds to F_X, F_Y, F_Z and M_X, M_Y, M_Z values.

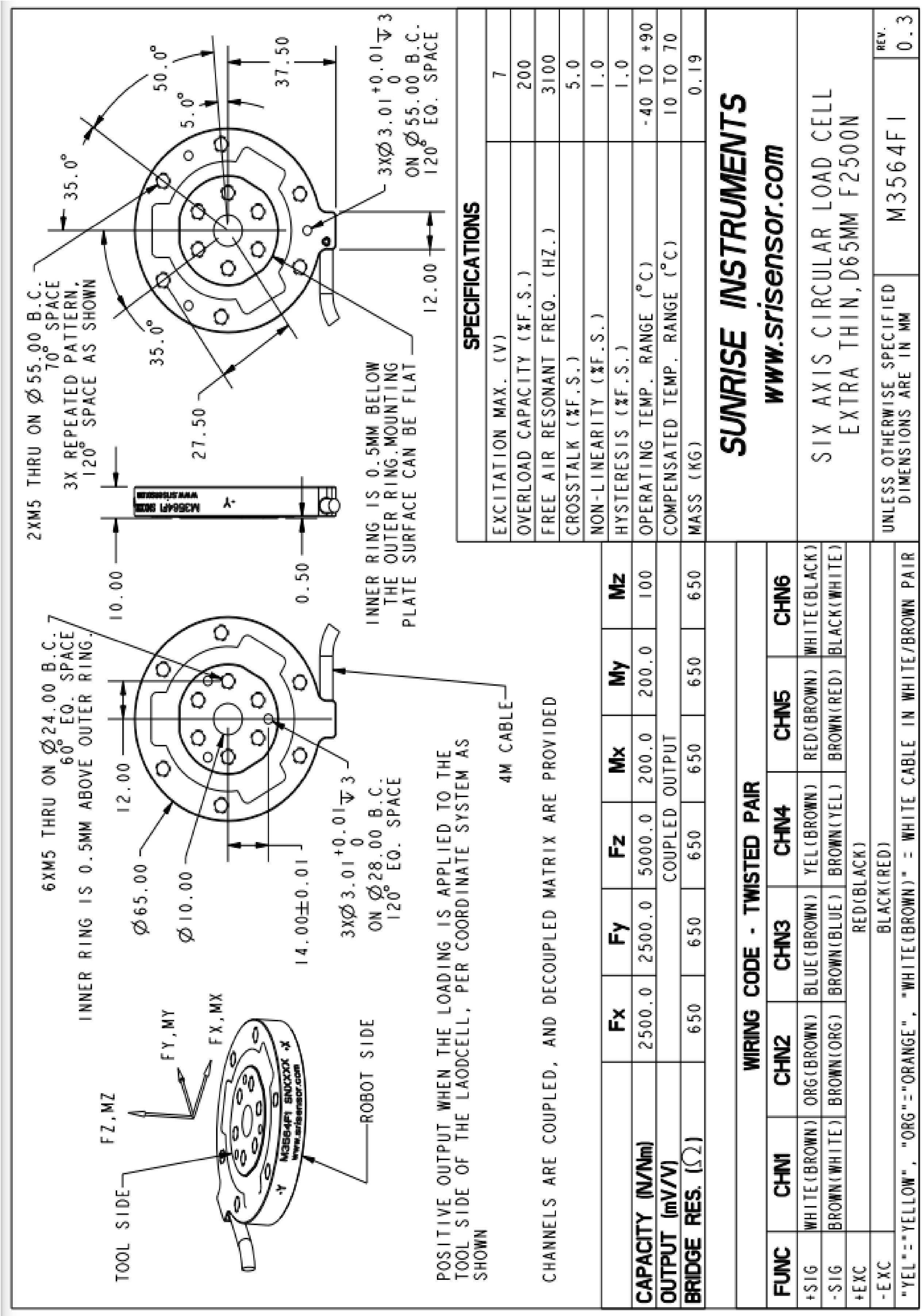

Figure 2.9: Sunrise load cell data sheet

Load cells signals were acquired and saved with *DTS Slice Nano* system. It is a compact, modulable acquisition system, functional for on field use. Each module is 26 mm wide, 31 mm depth and 8 mm tall and can collect up to 3 channels.

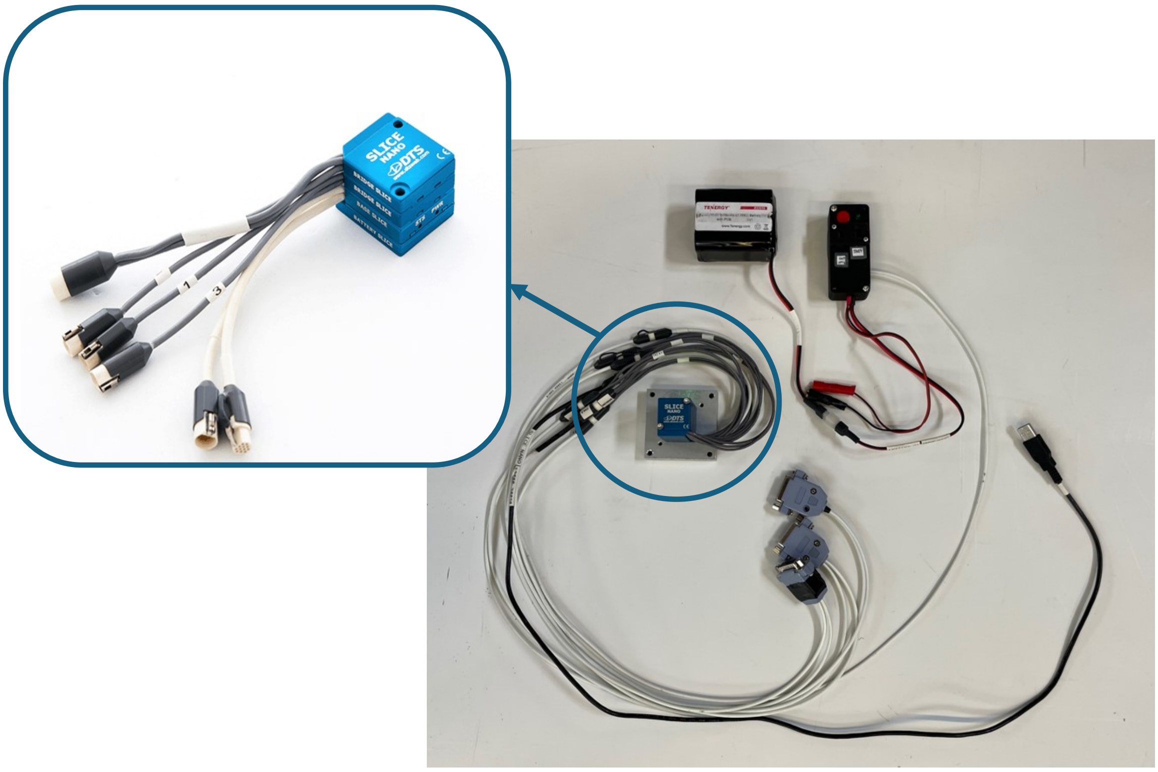

Figure 2.10: DTS Slice Nano acquisition system in the configuration used in the outdoor tests

The system can acquire data at a sample rate from 10 Hz to 500 kHz. On field were collected data from 12 channels, one for each force and moment. The sample rate was set at 1000 Hz.

During the tests one ski was instrumented with load cells, while on the other ski were mounted dummies load cells to reproduce the dimensions and weight of the first. Load cells and dummies load cells were screwed at the skis through aluminum plates which worked as interface between the ski and the bindings: it was not possible to directly screw bindings on the load cells to save their integrity. For all tests the instrumented ski was the right one. Lower plates connect load cells to skis, while upper plates connect load cells to ski bindings.

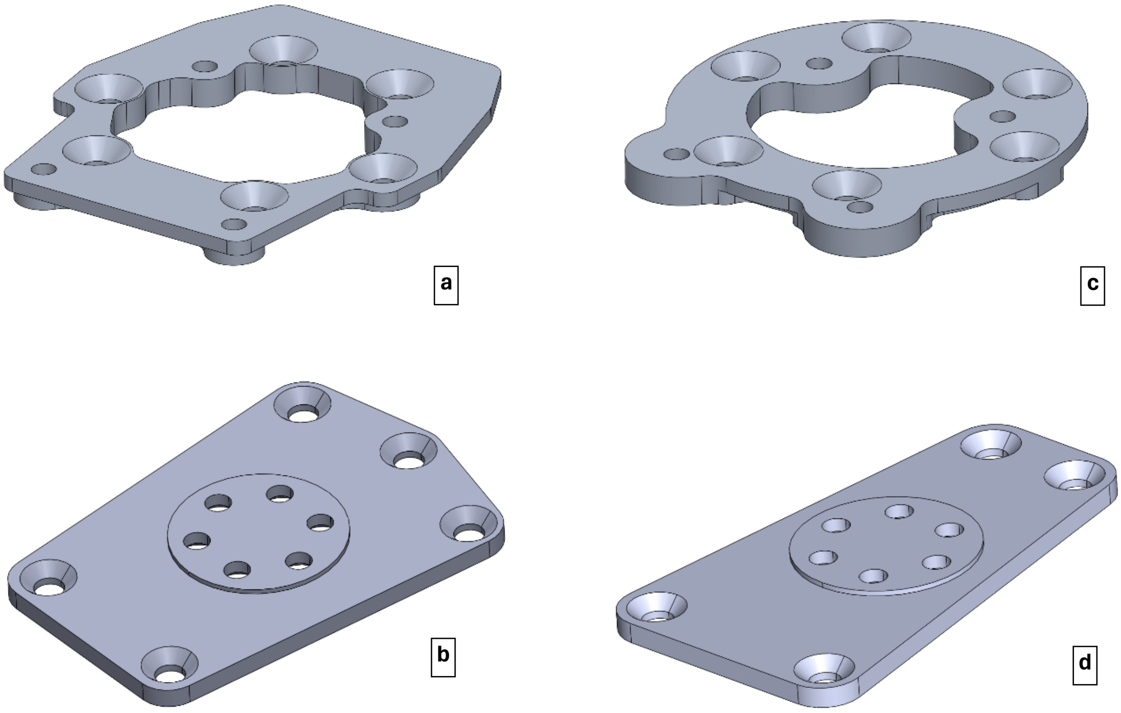

Figure 2.11: front upper (a) and lower (b) plates and rear upper (c) and lower (d) plates for load cell binding system

Interface plate in *Figure 2.6* were previously designed in the master thesis *Cibin P., Design and testing of an innovative data acquisition system for skitouring/alpine ski ski boots loads and deflections field measurements, Padova: Università degli studi di Padova, 2022* for similar research. In this research the front binding load cell N° SN13828 was equipped under the front binding, while cell N° SN13829 under the rear binding.

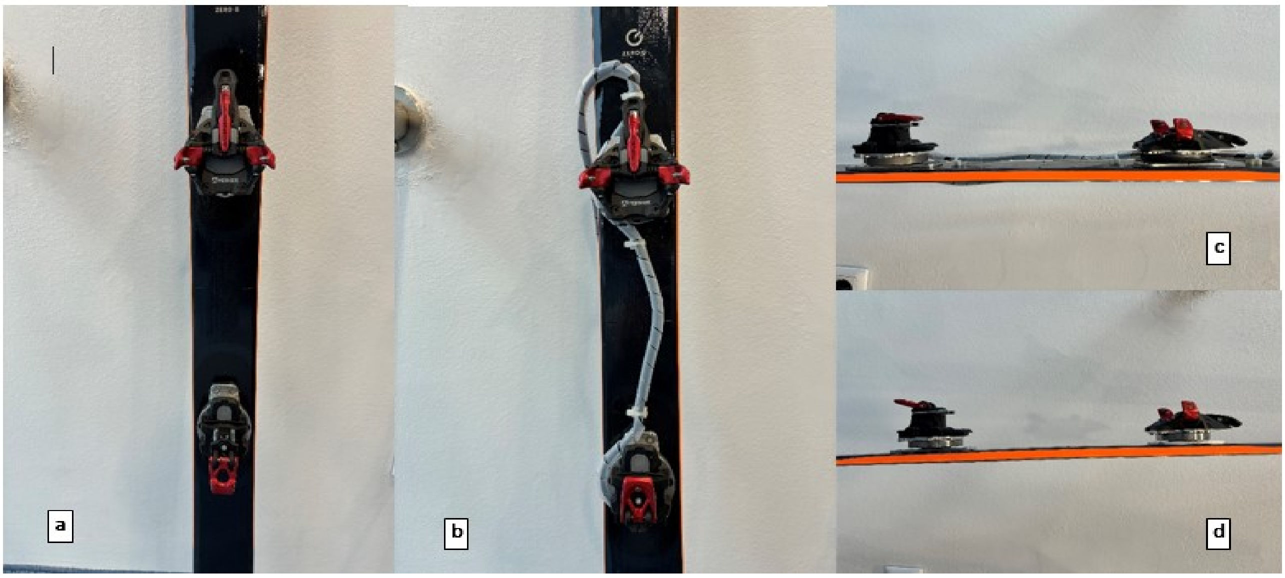

Figure 2.12: upper and lateral view of skis instrumented with load cell (b and c) and of skis equipped with dummy load cells (a and d)

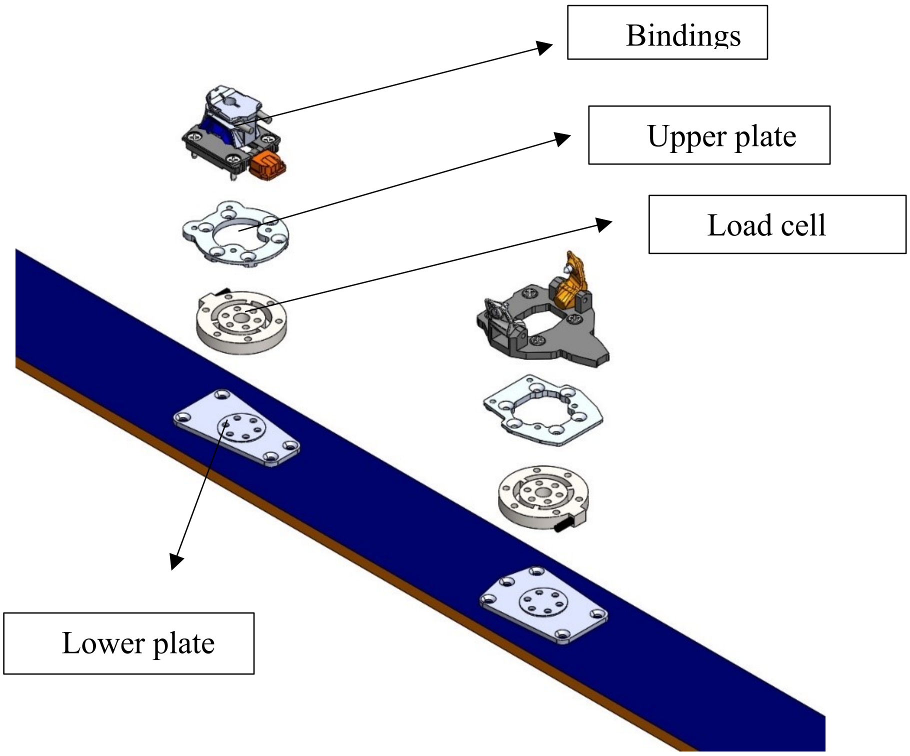

Figure 2.13: exploded view of bindings-load cell system

The plates-load cells system adds to each ski 20mm of height and 0.5 Kg. Most skier doesn't feel big differences between the skis with and without the instrumentation.

The origin of the reference system of the ski is located under the ski center given by construction company as can be seen in *Figure 2.14*. The X axis follows the ski length pointing forward, the Y axis is normal to X axis pointing left and the Z axis is normal to the ski plane pointing towards the boots. Loadcells were mounted with their reference system aligned to the reference system of the skis. The load cell-plates instrumentation and its reference system are described in: Zullo, G.; Cibin, P.; Bortolan, L.; Botteon, M.; Petrone, N. *An Innovative Compact System to Measure Skiing Ground Reaction Forces and Flexural Angles of Alpine and Touring Ski Boots*. Sensors 2023, 23, 836.

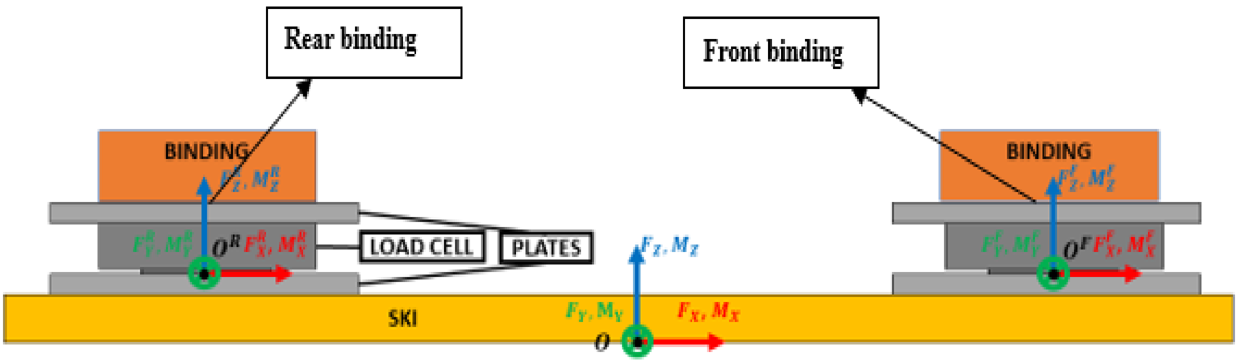

Figure 2.14: load cells and ski reference system

Once tests are done and data are acquired and processed the system gave as output 2 matrix of 6 columns each containing forces and moments in the load cells reference system. More precisely the front load cell matrix contain:

- In column 1 F_{XF};
- In column 2 F_{YF};
- In column 3 F_{ZF};
- In column 4 M_{XF};
- In column 5 M_{YF};
- In column 6 M_{ZF};

while the rear load cell matrix contain:

- In column 1 F_{XR};
- In column 2 F_{YR};
- In column 3 F_{ZR};
- In column 4 M_{XR};
- In column 5 M_{YR};
- In column 6 M_{ZR}.

In occasion of *ISEA WinterSchool* in *Kranjska Gora* during March 2024 international students and tutors meet spending four days of teaching, testing and analyzing activity in snow sport fields. This was also the occasion to perform on field test on the *Blizzard ZeroG 85, 95* and *105* instrumented with load cells as shown in *Chapter 2*.

On Friday 8th March on field tests were carried on in *Nassfeld- Passo del Pramollo*. 16 runs were recorded with the three *Blizzard ZeroG* skis driven by two different amatorial skiers with poles and normal ski conditions. Antropometric characteristics of the two subjects are reported in *Table 2.3*

SUBJECT ID	***GENDER***	***AGE***	***HEIGHT***	***WEIGHT***
SUBJECT 1	M	23 y	170 cm	68 Kg
SUBJECT 2	F	22 y	165 cm	60 Kg

Table 2.3: anthropometric characteristics of the two subjects

Different conditions of each run are specified in *Table 2.4.*

RUN NUMBER	***SKI***	***SUBJECT***	***CONDITIONS***	***SLOPE***
01	*Blizzard ZeroG 95*	Subject 1	Free	N° 67
02	*Blizzard ZeroG 95*	Subject 1	Poles	N° 67
03	*Blizzard ZeroG 95*	Subject 2	Free	N° 67
04	*Blizzard ZeroG 95*	Subject 2	Poles	N° 67
05	*Blizzard ZeroG 105*	Subject 2	Free	N° 67
06	*Blizzard ZeroG 105*	Subject 2	Poles	N° 67
07	*Blizzard ZeroG 105*	Subject 1	Free	N° 67
08	*Blizzard ZeroG 105*	Subject 1	Poles	N° 67
09	*Blizzard ZeroG 85*	Subject 1	Free	N° 67
10	*Blizzard ZeroG 85*	Subject 1	Poles	N° 67
11	*Blizzard ZeroG 85*	Subject 2	Free1	N° 67
12	*Blizzard ZeroG 85*	Subject 2	Poles	N° 67
13	*Blizzard ZeroG 85*	Subject 2	Free2	N° 67
14	*Blizzard ZeroG 85*	Subject 2	Off Piste	Off Piste
15	*Blizzard ZeroG 85*	Subject 2	Slope23 Free	N° 23
16	*Blizzard ZeroG 85*	Subject 2	Slope23 Free	N° 23

Table 2.4: different ski run made in Nassfeld

Tests subjects were two students of the *WinterSchool*: they were amatorial skiers with experience in alpine skiing. Subject 2 had also experience in skitouring and was very confident with *Blizzard ZeroG* skis, while Subject 1 had less experience and was salso less confident. They performed two runs for each ski, the first run on the lower part of the slope N°67 with free turns and the second run on the upper part of the slope N°67 prepared with poles.

Having only two load cells to instrument skis, between run 04 and 05 and between runs 08 and 09 were taken breaks to unscrew bindings, plates, load cells and dummy load cells from the pair of skis already used and transfer the setup on the other pair of skis. Other breaks were done between run 02 and 03, run 06 and 07 and run 10 and 11 to switch ski boots from one subject to the other because only one pair of *Tecnica ZeroG Tour Pro* was available for the test.

Figure 2.15: setup preparation after tester switch and ski preparation before tests

All data was acquired at a sample rate of 1000 Hz with the *DTS* data logger system. At the start and at the end of each run the skier hits three times the snow with the instrumented ski to have a sync reference and to set a zero offset value helpful for data processing. In all runs the instrumented ski was the right one.

As already mentioned in *Chapter 2* data analysis with *MATLAB* consist in the following steps:

a) Electrical output of each bridge was divided by the excitation of the bridge (5V) to obtain a measure in mV/V
b) Data in mV/V were filtered with a Butterworth lowpass filter (2° order, cut-off: 5Hz) to clean data from ski vibrations and electrical noise
c) The filtered data are firstly multiplied by the calibration matrix to obtain Forces and Moments in the load cells reference systems, then the results are multiplied by the rotational matrix to obtain Forces and Moments in the ski reference system in N and Nm. The applied formula is the following:

$$[F_X \quad F_Y \quad F_Z \quad M_X \quad M_Y \quad M_Z] = ([R]([C] \cdot [ch_1 \quad ch_2 \quad ch_3 \quad ch_4 \quad ch_5 \quad ch_6]^T))^T$$

d) Ski GRF and GRM are obtained from load cells forces and moments combined with the position of their reference system. From now all the Forces and Moments are referred as Ground Reaction Forces and Moments

e) Each run is divided in cycles to analyze data of different turns and runs. M_X is used to segment data: it signs positive when the skier is turning left and negative when he is turning right. Each turn cycle starts when M_X cross zero from negative to positive. In each cycle skier perform a right turn and a left turn

f) Of these cycles the better shaped, central, consecutive turns are manually selected from M_x plots

g) Each cycle is then resampled to 101 samples to overlap and compare ski turns of different length. Each sample rapresent the advancement in turn cycle from 0% to 100%

h) Data are normalized by skier's bodyweight and multiplied for the mean weight of the two subjects. Then the average curves of all Ground Reaction components in the normalized cycles are determined.

2.4 Impact tests on snow and foams

A portable impactor was developed to evaluate the hardness of snow and the hardness of different foams to understand if some foams can reproduce the snow behavior for indoor tests. The impactor is composed by a main PVC pipe of 50 cm height and with an inner diameter of 4.7 cm able to stay vertical with the help of support bars.

Figure 2.16: guide pipe of the impactor

The pipe work as a guide for a cylindrical mass of steel with a conical tip taking name of dart. The dart has a height of 10,2 cm and a diameter of 4,3 cm. At one extremity it has a conical tip of 90° with a height of 2,1 cm. The whole mass weight 1 Kg. At the opposite end of the tip was screwed a plastic plate made with a 3D-printer were an IMU sensor was placed.

Figure 2.17: steel dart used as impactor

The IMU used is a miniaturized multisensor IMU from *221e* called *MUSE*. The sensor is equipped with an inertial linear and angular accelerometer able to log at a data sampling up to 1600 Hz, a magnetometer (1000 Hz) and environmental sensors (25 Hz). The system is able to start and stop the acquisition both wireless and with a button.

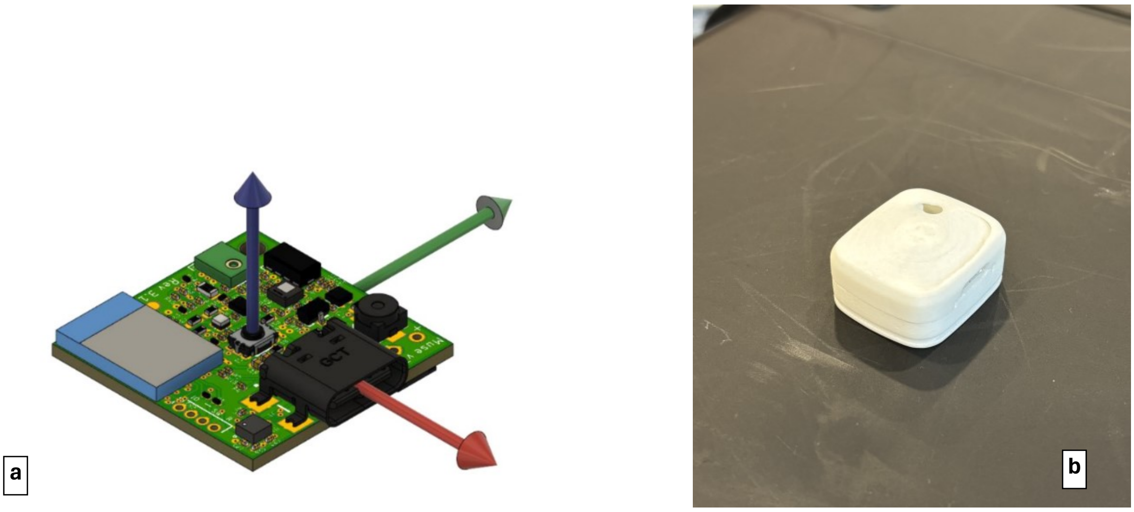

Figure 2.18: MUSE reference system (a) and MUSE with his case (b)

The MUSE complete with the white case has a rectangular base of 3,3 cm x 2,8 cm and a height of 1,6 cm. Its small dimensions allowed us to mount it on the dart.

MuseV3 Viewer is the software that sets the sensor acquisition parameters and downloads the data on the computer. Only the high scale accelerometer HDR with full-scale of 400 g was acquired in all the three axes. The HDR data sampling was set at 1600 Hz. Unfortunately, the HDR acquires different samples at maximum 1000 Hz, but automatically copy some samples when it is not able to acquire (at the end HDR acquire at 1600 Hz with some samples present twice).

Once the part of snow/foam to test is selected, the impactor is moved above it and the *MUSE* is switched on.

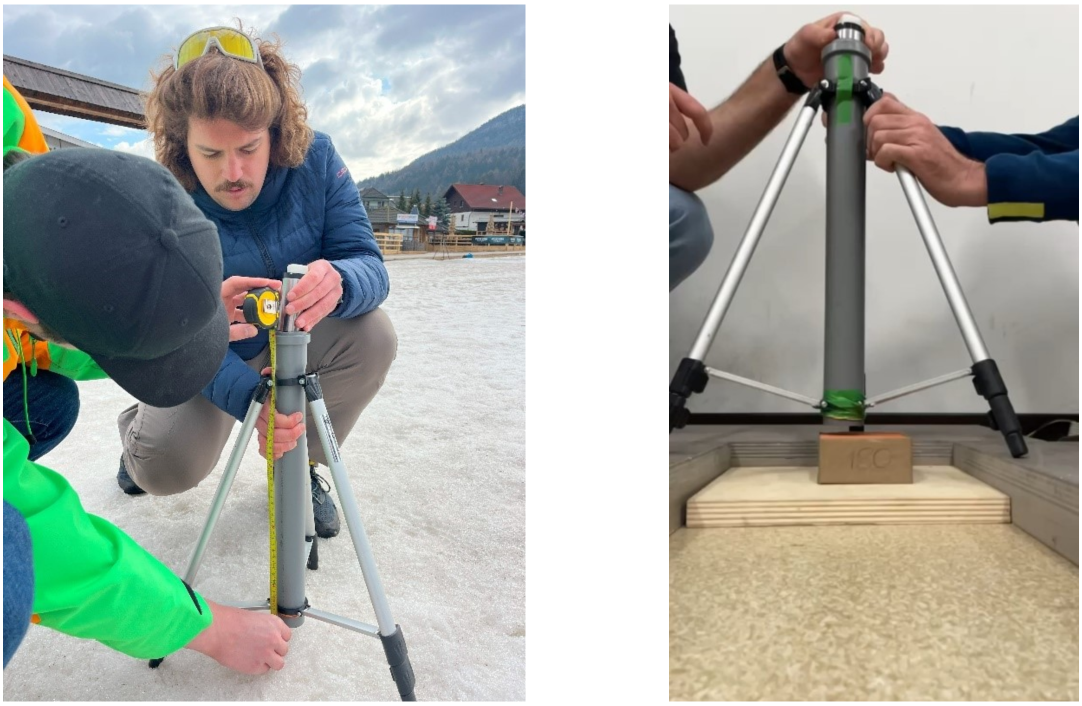

Figure 2.19: impact test on snow in Kranjska Gora and impact test on foams in Padova

Then is measured the height from the ground to the top of the pipe to derive later the velocity of the dart at the start of the impact. When the measure is written down and the dart is located on the top of the pipe, the acquisition can be started with the button and the dart is let fall. Then the pipe is removed, the acquisition is stopped with the button and picture of the darts on the snow and of the holes are taken.

Data are then imported and elaborated with *MATLAB*. Only the acceleration in the direction of the impact (Z axis) is taken in consideration. Doubled samples were substituted with the mean values of the previous and successive samples and a plot without step at sampling rate of 1600 Hz was obtained. From the acceleration plot were manually selected the start of the impact i.e. when the acceleration starts to grow. The velocity at the start of the impact was obtained from the formula of the kinetic energy and potential energy as:

$$v_0 = \sqrt{2 \cdot g \cdot h_o}$$

where h_o is the distance from the tip of the probe and the ground and g is the gravitational acceleration.

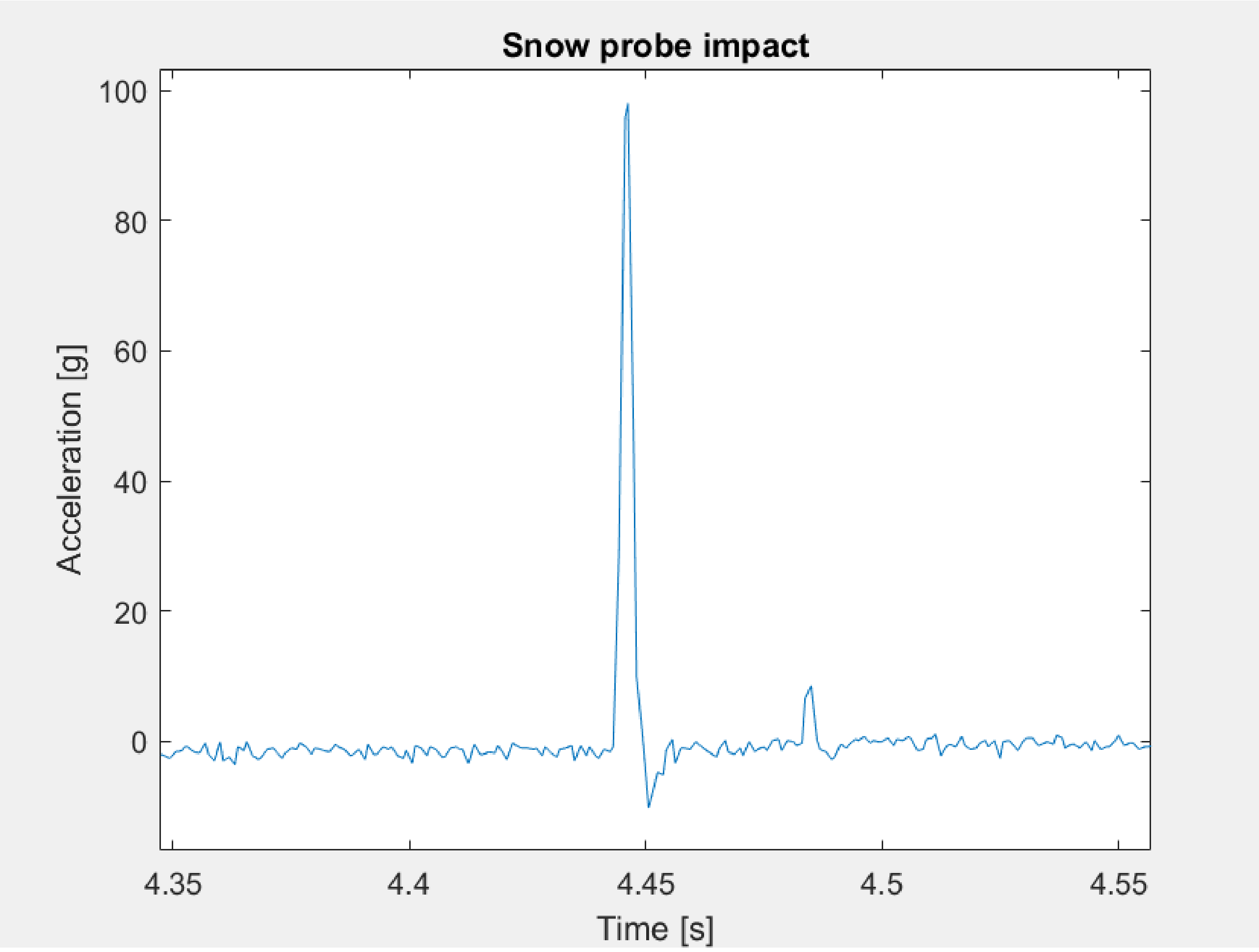

Figure 2.20: example plot of MUSE accelerometer signal on Z axis

The acceleration is integrated over the time impact to get the velocity of the impact, then the stop of the impact was set when the differences between v_0 and the velocity obtained with the integral crossed zero. Only the time impact acceleration and velocity are saved. The penetration of the dart in the snow/foam was obtained integrating again the velocity of the impact.

Then the force during the impact was obtained multiplying the values of the acceleration for the mass of the dart (1 Kg) and the gravitational acceleration (9,81 m/s^2) as:

$$Force = a_z \cdot g \cdot m_{dart}$$

Finally force-penetration plots for all the tests were obtained and the comparison between snow and foams can be done.

Impact tests were done on different type of snow in *Kranjska Gora* and on phenolic foams at different density in *Padova*. On each type of snow three impact were tested, while number of tests on phenolic depended on the density. For each snow and foams, the most representative curve was visually chosen observing geometry of the curves, peak force (maximum force) and penetration depth (maximum penetration).

Impact test on snow were carried on during *ISEA WinterSchool* in *Kranjska Gora*. Four different types of snow were tested:

1. Ice of an ice-skating track.
2. Medium grain snow of the slope in *Kranjska Gora*. Slopes were closed for the skiers, but some snow was still present.
3. Hard snow nearby the ice-skating track.
4. Soft snow nearby the ice-skating track.

Force-Penetration curves of the three tests are plotted to show how the most representative curve are chosen for the snow.

It must be said that the MUSE accelerometer acquire data at 1600 Hz and the impact window does not present a huge number of samplings. The low number of samplings with the double integration process to get the penetration of the dart complicated the post processing data and originated some differences in the curves. Force Peak and Maximum penetration of different curves are compared together and with the penetration of the hole made by the dart on the snow to choose the most realistic curve of each snow.

Impact test on phenolic foams were carried on indoor in *Padova* laboratory to search a foam density able to mimic the snow behavior. Samples of phenolic foams were taken from *POLIFEN*, a company that produces thermal insulation for houses. Phenolic foams were chosen because are made of expanded closed cells that crash when loaded, simulating the crash of the snow when loaded.

Six samples of phenolic foams of different density are tested: 35, 60, 80, 120, 160 and 180 kg/m^3. For each foams different impact were plotted. For each foams force-penetration curves of alle the impacts are plotted and the best ones was chosen as representative of each foam. The choice was based on curve shape, peak force and penetration depth.

2.5 Ski subjective evaluation

Another step of this work consisted in the subjective evaluation of the three pair of *Blizzard ZeroG 85, 95* and *105*. Testing ski on the bench and with load cells gave quantitative numbers to evaluate the skis characteristics, but also subjective evaluation is important to evaluate skis performances. A ski test with the three skis were done and the skiers feedback were collected.

A questionnaire evaluating few basic ski performances was developed, defining seven ski evaluation parameters with their description and scale values to allow a uniform evaluation. Usually ski tester search different sensation when evaluate skis and give back discursive feedback of all of them; summarizing a huge number of this feelings in marks of few parameters is an effort and some misunderstandings can happen. It is important then to define scrupulously each parameter to simplify testers understanding of them. The questionnaire developed to evaluate skis is reported below.

Figure 2.21: subjective evaluation collection in Madonna di Campiglio

SKI – EVALUATION PARAMETERS

1 – EDGE SWITCHING QUICKNESS:

evaluate the quickness of the ski in switching from one edge to the other

10 – excellent: the ski releases very easily the old edge and moves very quickly to the new one
8 – good: the ski releases easily the old edge and moves quickly to the new one
6 – sufficient: the ski releases hardly the old edge and moves slowly to the new one
4 – poor: the ski remains bond to the old edge and moves very slowly to the new one

2 – EDGE CATCHING QUICKNESS:

evaluate the readiness of the ski in catching the edge and entering into a turn.

10 – excellent: very short time for catching the edge and entering into the turn
8 – good: short time for catching the edge and entering into the turn
6 – sufficient: long time for catching the edge and entering into the turn
4 – poor: very long time for catching the edge and entering into the turn.

3 – CARVING PRECISION:

evaluate the precision of the ski in following the desired turning radius without skidding

10 – excellent: very high precision – no skidding at all
8 – good: good precision – no evident skidding
6 – sufficient: sufficient precision – the skidding can be controlled
4 – poor: poor precision – the skidding is evident and can hardly be controlled

4 – REACTIVENESS AT THE END OF THE TURN:

evaluate the capacity of the ski in "pushing" the athlete out of the turn, helping the edge change

10 – excellent : ski exits the turn in a very short time with maximum "push".
8 – good: ski exits the turn in a short time with good "push".
6 – sufficient: ski exits the turn in a long time with enough "push".
4 – poor: ski exits the turn in a very long time with no "push".

5 – ENERGY REBOUND:

evaluate the capacity of the ski in giving back the energy used to deform the ski when pops back to unbent state

10 – excellent: the ski gives back a huge energy and increase a lot its speed
8 – good: the ski gives back a big energy and increase its speed
6 – sufficient: the ski gives back a sufficient energy and increase few its speed
4 – poor: the ski is gives back low energy and doesn't increase its speed

6 – VIBRATION DAMPING:

evaluate the capacity of the ski in damping the vibrations during straight skiing or edge change

10 – excellent: the ski does not present any perceivable vibration.
8 – good: the ski presents some perceivable vibrations.
6 – sufficient: the ski presents evident vibrations.
4 – poor: the ski presents high vibrations affecting his performances

7 – FLOATING:

evaluate the ability of the ski to stay above the snow in off piste conditions

10 – excellent: the ski does not sink and stays all above the snow
8 – good: the ski sinks a little and stays mostly above the snow
6 – sufficient: the ski partially sinks but stays sufficiently above the snow
4 – poor: the ski sinks a lot and stays below the snow

LOC: ______________________________ DATE: ________________

Subject: SURNAME___________________NAME______________________

AGE__________HEIGHT(m)___________MASS (kg) ______________

SKILL LEVEL____

TYPE OF SNOW ________________________ HOUR_____________

4 (poor) 6(sufficient) 8 (good) 10 (excellent)

SKI	**EVALUATION**						
	4	**5**	**6**	**7**	**8**	**9**	**10**
1. EDGE SWITCHING QUICKNESS							
2. EDGE CATCHING QUICKNESS							
3. CARVING PRECISION							
4. REACTIVENESS AT THE END OF THE TURN							
5. ENERGY REBOUND							
6. VIBRATION DAMPING							
7. FLOATING							
Note:	____________________________________ ____________________________________ ____________________________________						

In April subjective evaluation for the *Blizzard ZeroG 85, 95* and *105* were collected in *Madonna di Campiglio*. Four ski instructor and a ski instructor student were available for the ski test. From the early morning were given 45 minutes to each subject to try all the skis. At first the questionnaire was presented to the subject to let them focus on the described parameters. After test for each ski was filled the questionnaire using *Google Forms* to rapidly collect data.

Weather conditions were foggy with some weak snowfall, while the snow was compact and hard during all day and allowed all the subjects to ski with similar conditions. The floating parameter was not evaluated because the skis were only tested on slopes due to the foggy conditions. The collected data were then analyzed and plotted via *Excel*. Despite skitouring skis are thought for off-piste conditions, test with *Slytech edge load bench* and with load cells system were carried on hard snow conditions. Then also the subjective evaluation was done on hard snow.

2.6 Correlations

The last step of this work consisted in searching possible correlation between subjective evaluation made with questionnaire and objective evaluation made with *Slytech* test bench and with load cell system. A possible correlation would validate the use of bench tests and in field tests with load cells to evaluate the performance of a ski. In order to search these correlations, the following parameters are defined to be correlated with mean vote obtained by questionnaire:

1. **Tip Area:** obtained from the *Slytech* bench as the ratio between the load under the tip over the load under all the ski over the distance between the tip peak and the ski tip by 1000 at 40°.
2. **Tail Area:** obtained from the *Slytech* bench as the ratio between the load under the tail over the load under all the ski over the distance between the tail peak and the ski tail by 1000 at 40°.
3. **Tip speed of growing area:** obtained from the *Slytech* bench as the derivative of the tip area over the angulation of the ski. Can represent how fast the ski is able to catch the ground on the tip
4. **Tail speed of growing area:** obtained from the *Slytech* bench as the derivative of the tail area over the angulation of the ski. Can represent how fast the ski is able to catch the ground on the tail
5. **M_y peak:** obtained from the load cells test in *Kranjska Gora,* it is the maximum value of M_y in a mean turn cycle for the ski.
6. **M_x peak:** obtained from the load cells test in *Kranjska Gora,* it is the maximum value of M_x in a mean turn cycle for the ski.
7. **F_y peak:** obtained from the load cells test in *Kranjska Gora,* it is the maximum value of F_y in a mean turn cycle for the ski.
8. **F_z peak:** obtained from the load cells test in *Kranjska Gora,* it is the maximum value of F_z in a mean turn cycle for the ski.

The parameters above represent the data extracted from test results of each ski. Via *Excel* these parameters were correlated with mean vote results from questionnaire using the coefficient of correlation r. Absolute values of r higher than 0.85 expressed good correlations.

Furthermore, parameters obtained from test bench, from load cell in field tests and from the questionnaire results were analyzed searching correlation with skis building parameters to understand which skis building parameters affect a particular phase of skiing. Building parameters are parameter related to ski geometry or ski stiffness able to describe a physical characteristic of the ski.

Ten building parameters were taken from *Soothski* online database, an online database with measured ski data obtained from a machine able to collect information about ski geometry, ski profile, ski bending and torsional stiffness and the ski weight with precision and accuracy. The working principles of the machine are described in Truong, Jonas & Brousseau, Camille & Desbiens, Alexis. 2016. *A Method for Measuring the Bending and Torsional Stiffness Distributions of Alpine Skis*. Procedia Engineering. 147. 394-400. All the data in *Soothski* database are open source and can be find online.

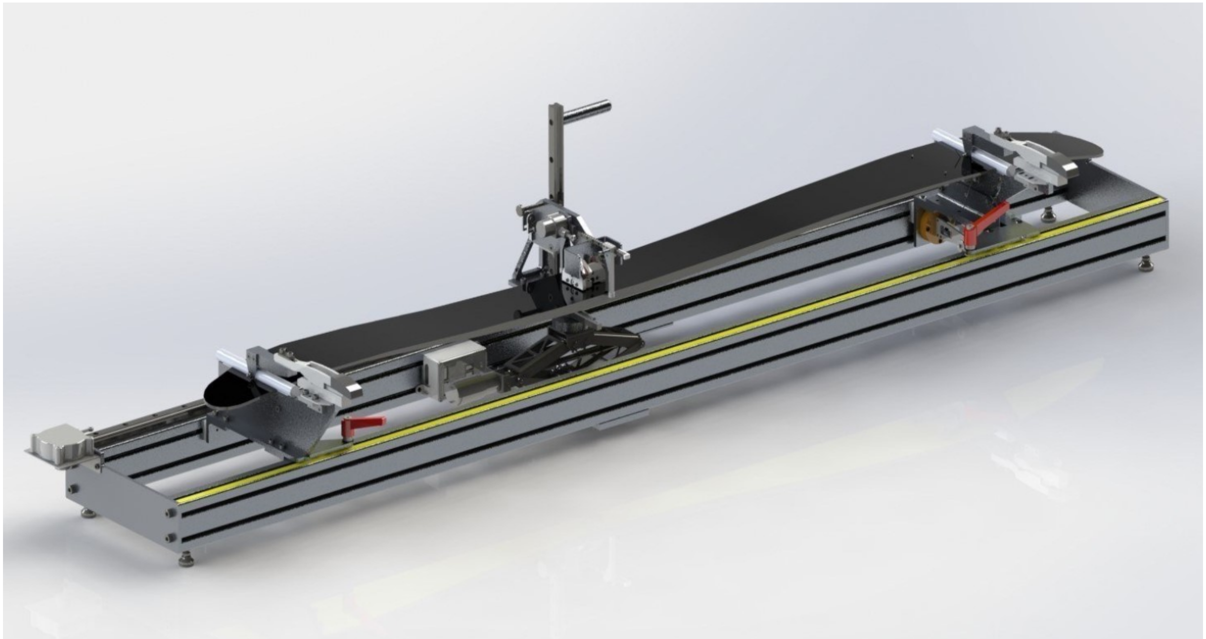

Figure 2.22: Soothski ski measuring technology

The building parameters extracted from *Soothski* are the following:

1. **Tip width:** is the measure of the largest part of the ski's shovel.
2. **Tail width:** is the measure of the largest part of the ski's tail.
3. **EI mean:** is the measure of how hard it is to flex a ski. The Average bending stiffness is the average value over the whole tip, center and tail of the ski.
4. **GJ mean:** is the measure of how hard it is to twist a ski. The Average torsional stiffness is the average value over the whole tip, center and tail of the ski.
5. **Weight:** is how much a single ski weighs without bindings.
6. **Surface over weight:** is obtained by dividing the ski's base area by its mass.
7. **Tip rocker length:** is the length of the upturned part of the front of the ski. It is measured as the distance between the front contact point and the tip of the ski.

8. **Tail rocker length:** is the length of the upturned part of the rear of the ski. It is measured as the distance between the rear contact point and the tail of the ski.
9. **Camber:** is the gap under the binding when a ski is laid on a flat surface.
10. **Sidecut radius:** is the average curve of the hourglass-shaped part of the ski.

In *Excel* a matrix with the coefficient of correlation r between building parameters extracted by *Soothski* and evaluation parameters extracted by indoor and outdoor test was obtained. Absolute values of r higher than 0.85 expressed good correlations.

3. Results

In this chapter results of the tests are presented following the same order in which the setups and test methodologies were presented in *Chapter 2*.

3.1 Indoor bench tests results

The Edge Load profiles of each ski and the comparison of the three skis are plotted below for each force and inclination.

<u>0° edge angle and 50 kgf Edge Load profiles</u>

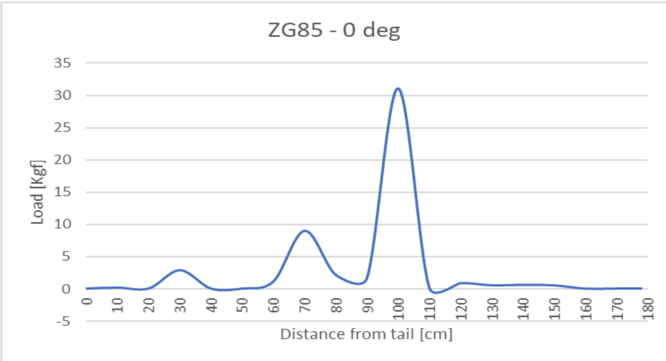

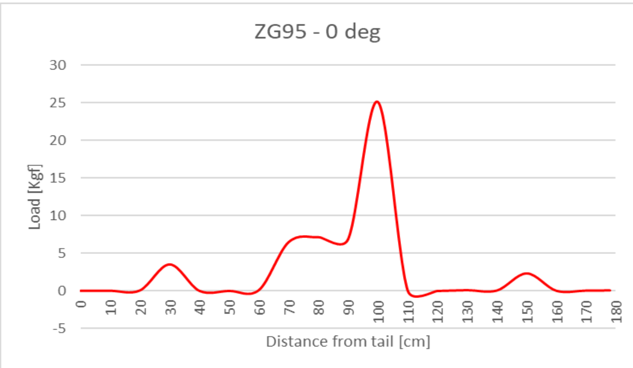

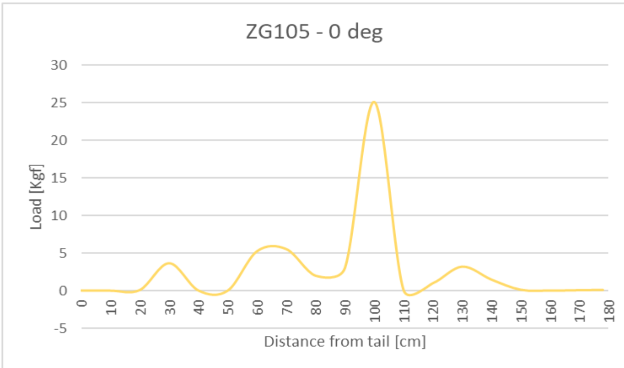

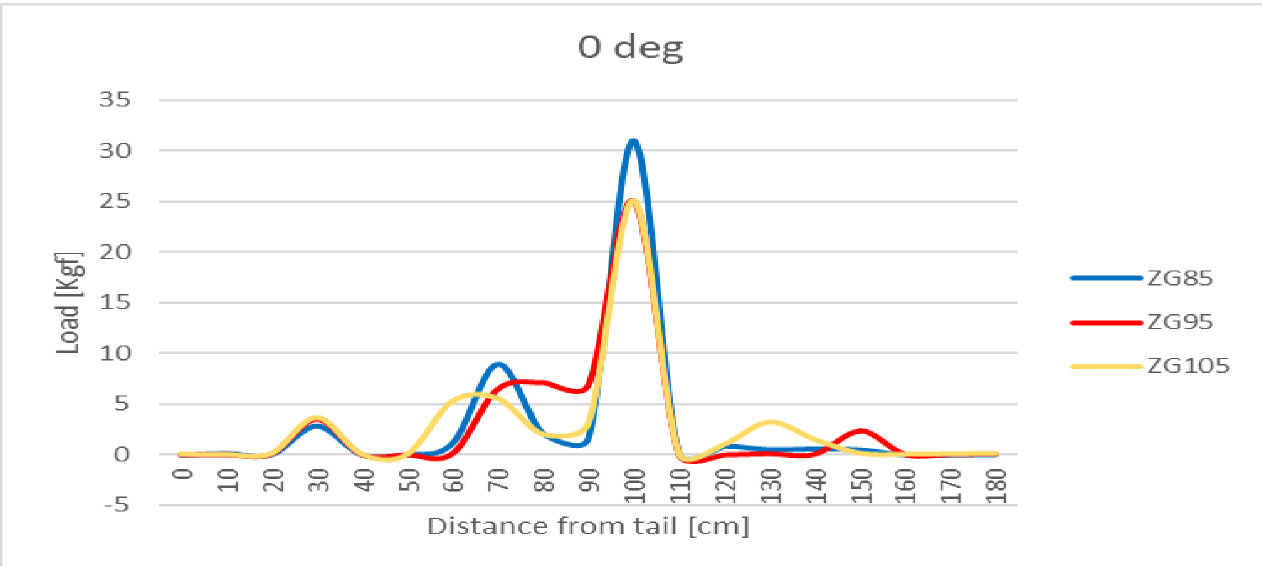

<u>10° edge angle and 60 kgf Edge Load profiles</u>

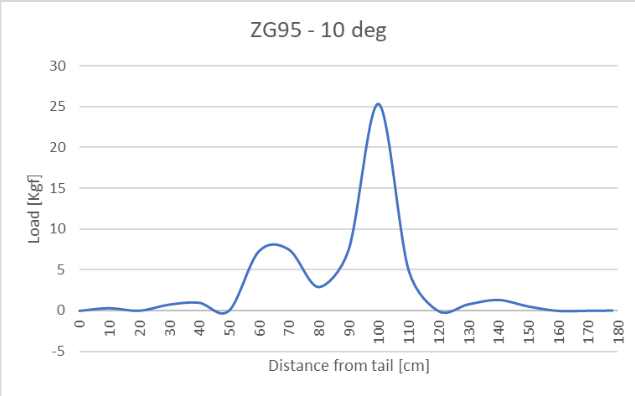

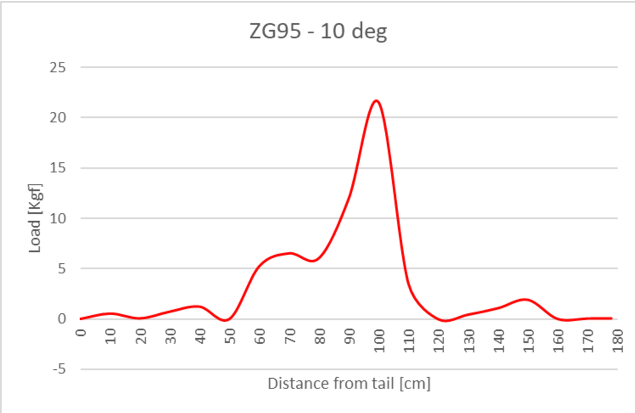

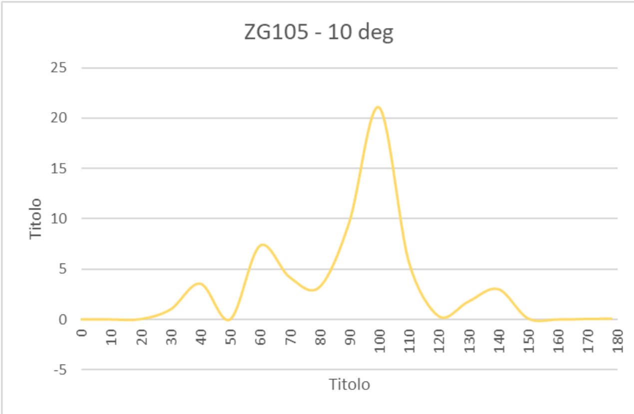

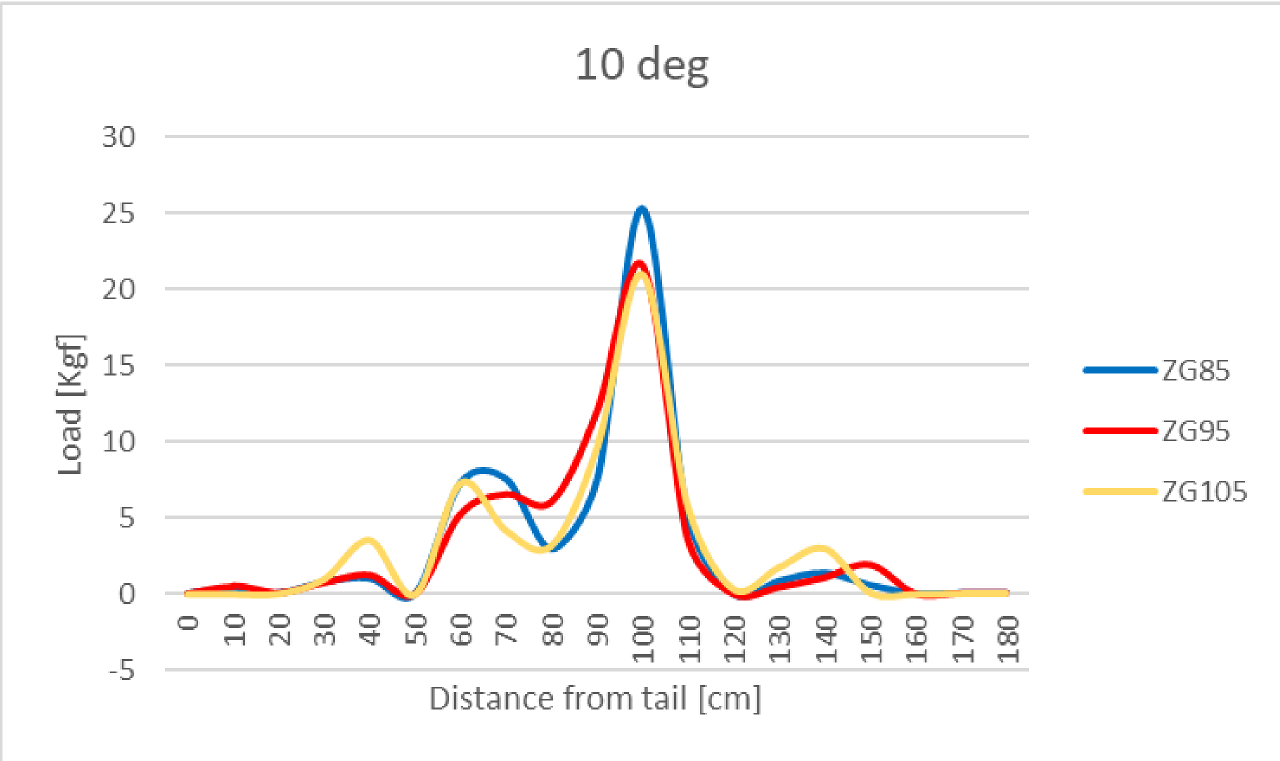

20° edge angle and 70 kgf Edge Load profiles

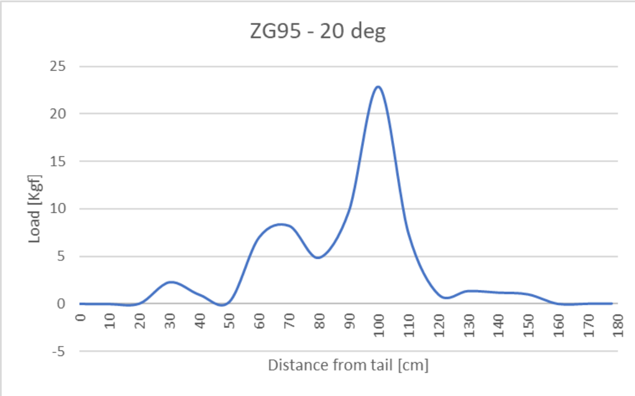

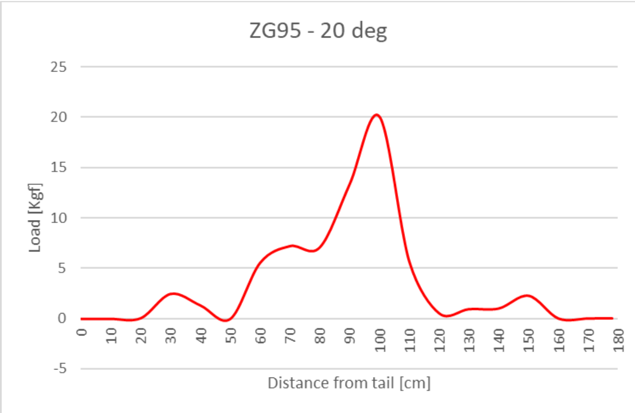

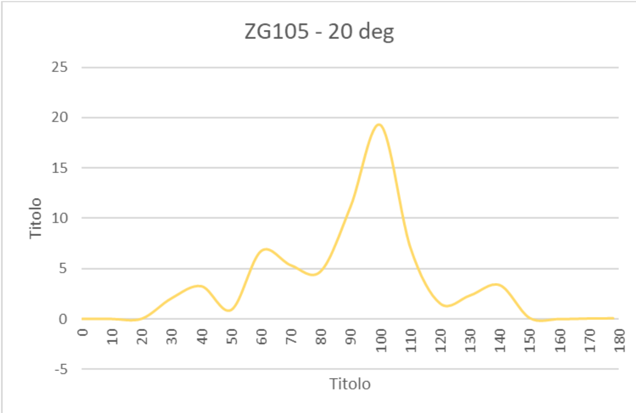

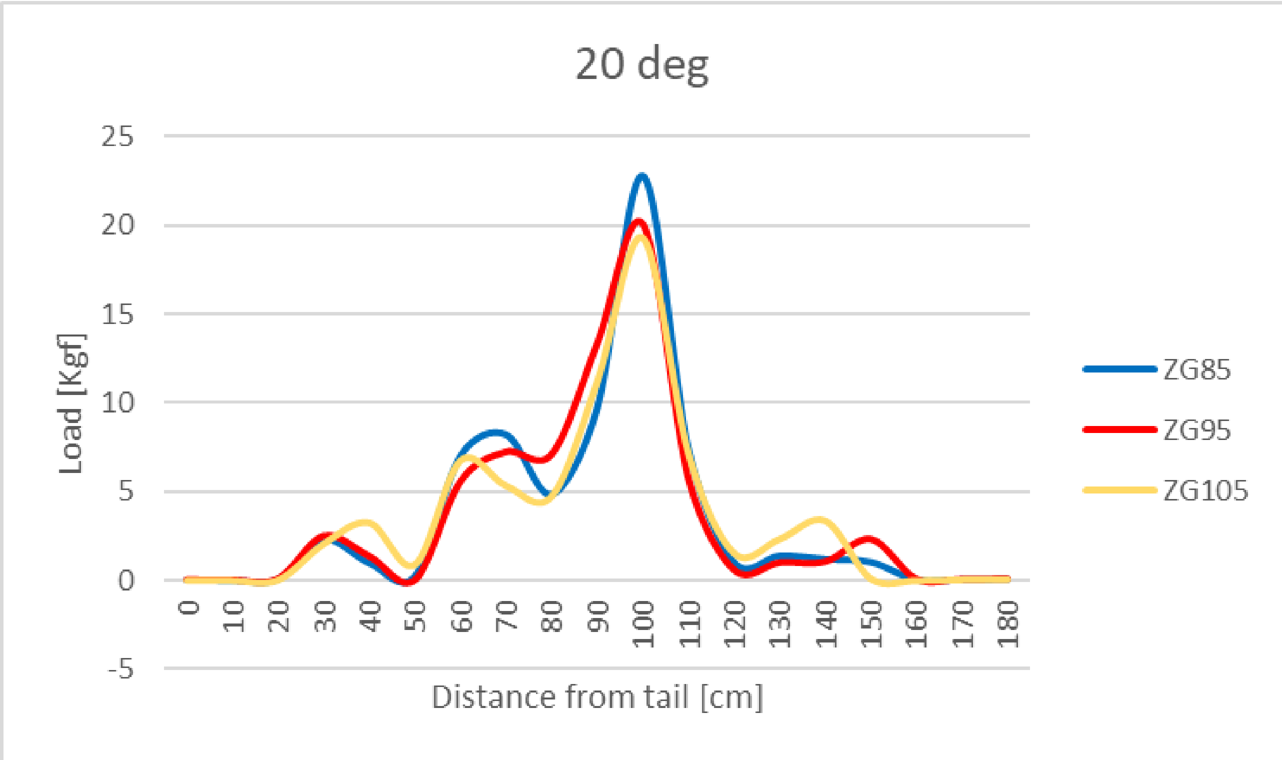

30° edge angle and 85 kgf Edge Load profiles

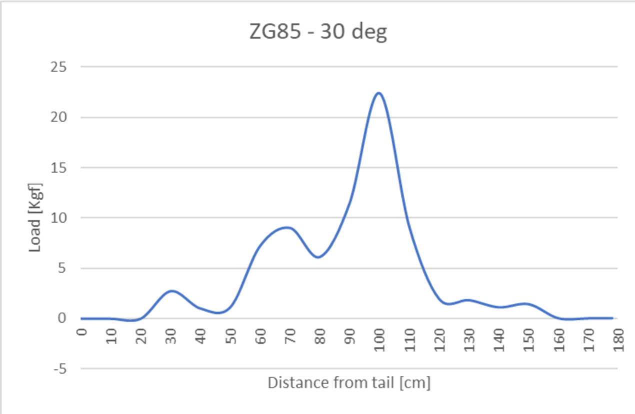

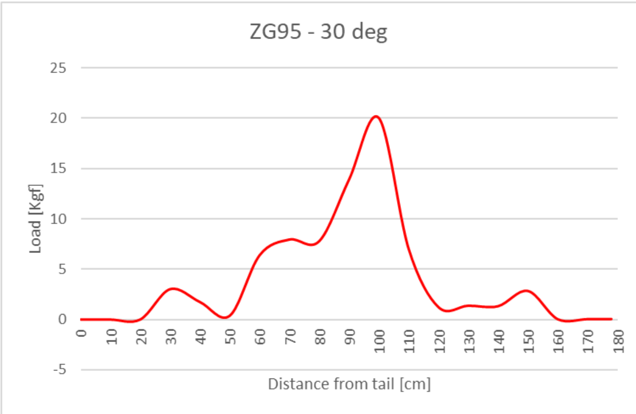

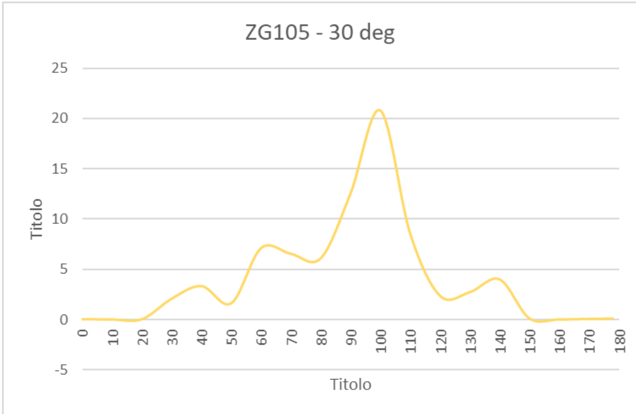

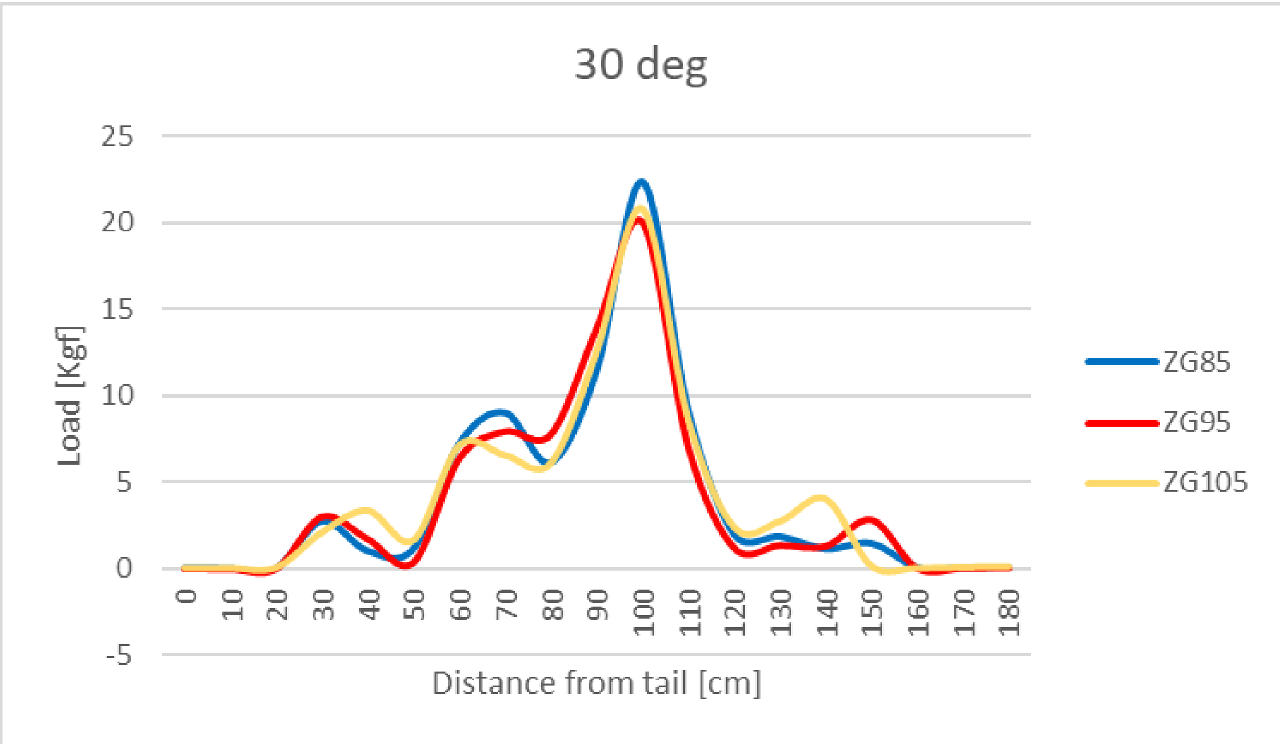

40° edge angle and 100 kgf Edge Load profiles

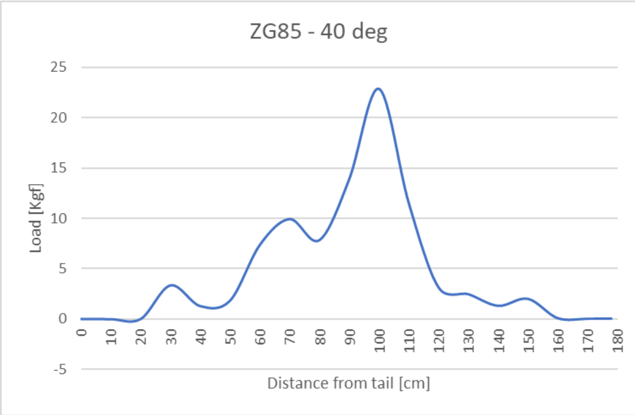

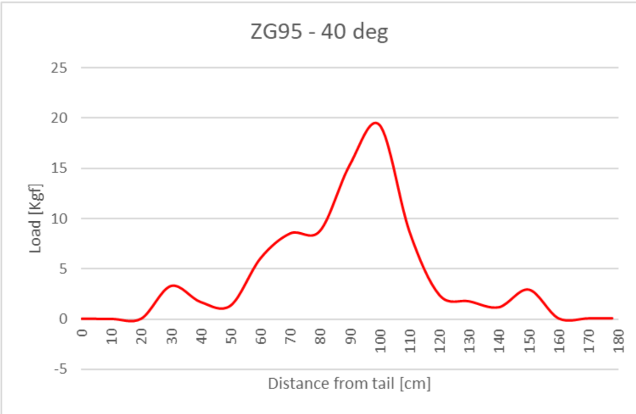

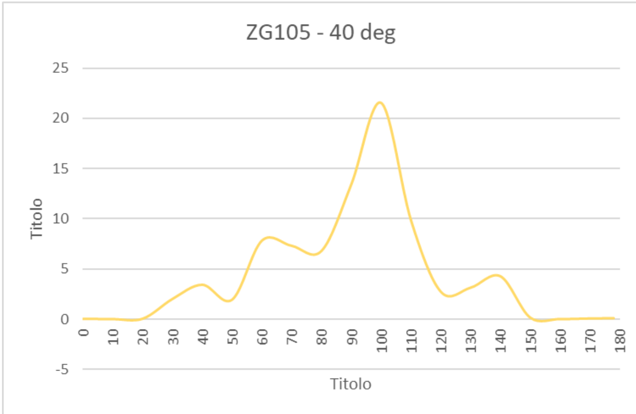

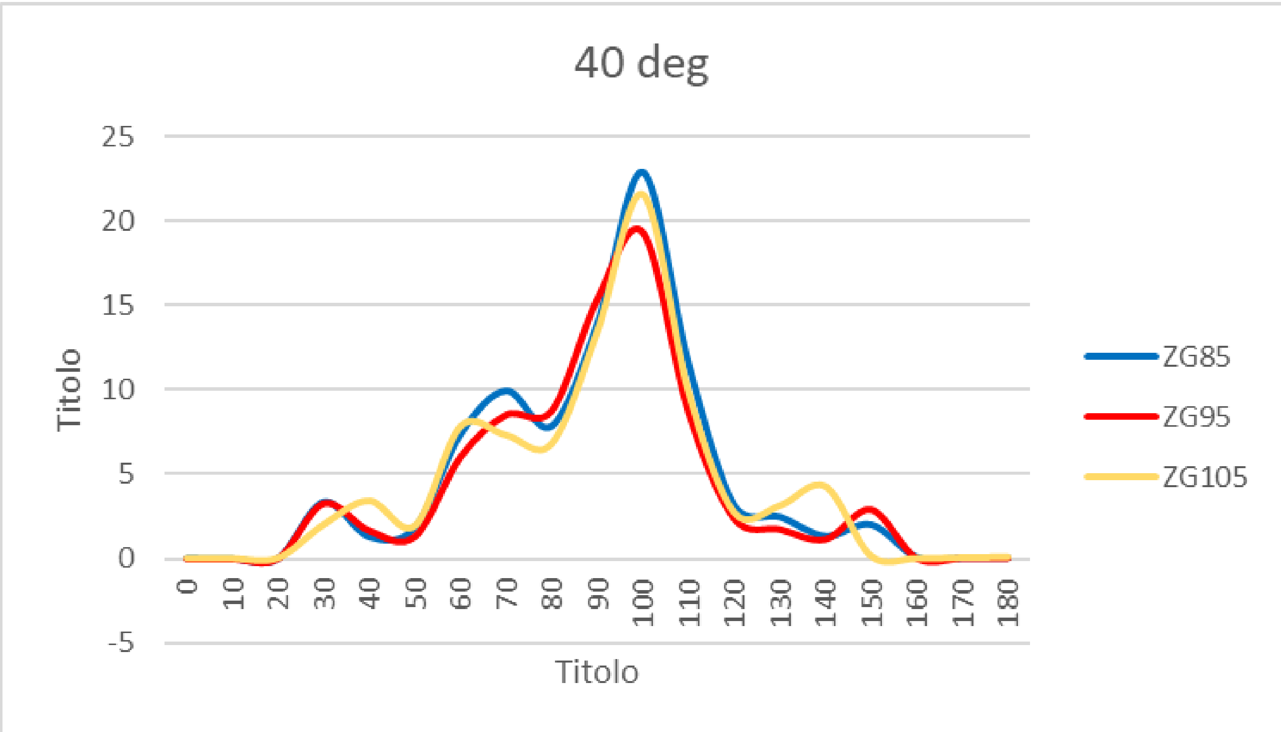

__**50° edge angle and 120 kgf Edge Load profiles**__

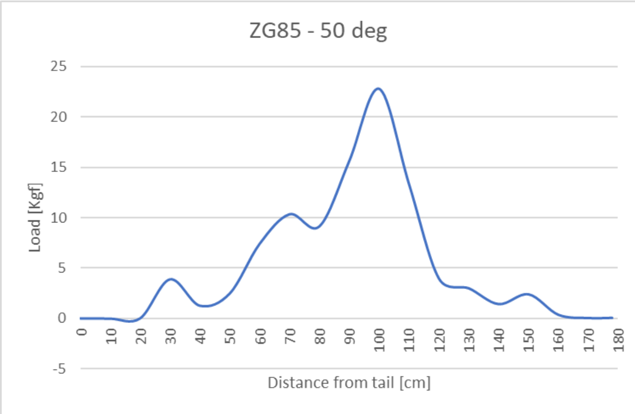

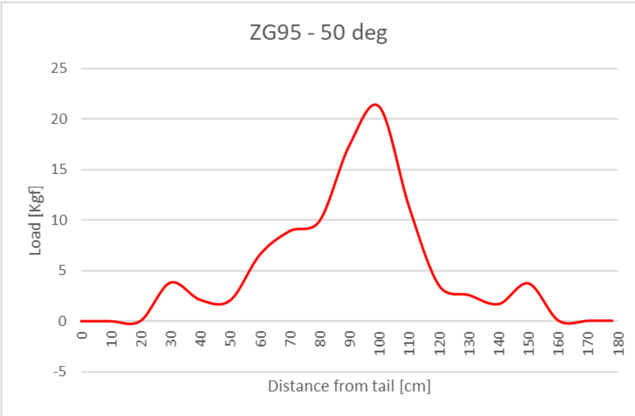

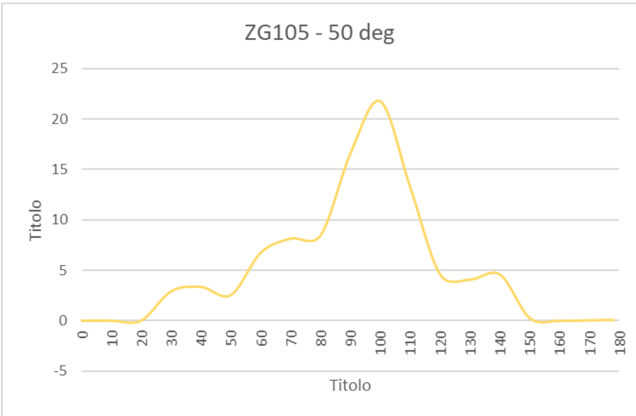

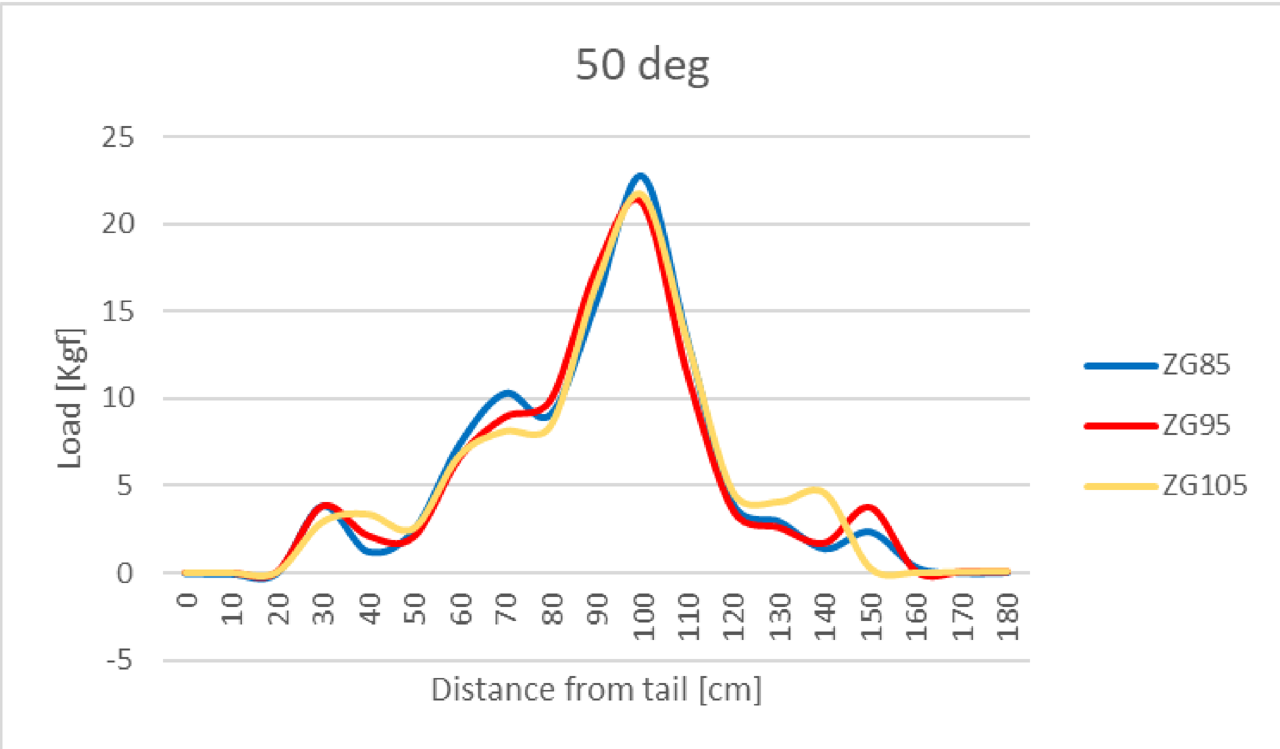

60° edge angle and 140 kgf Edge Load profiles

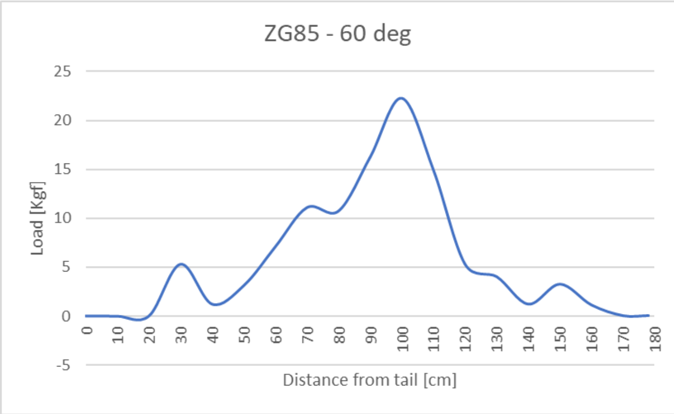

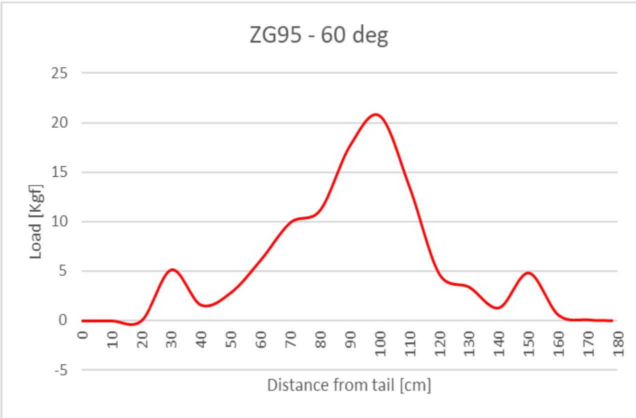

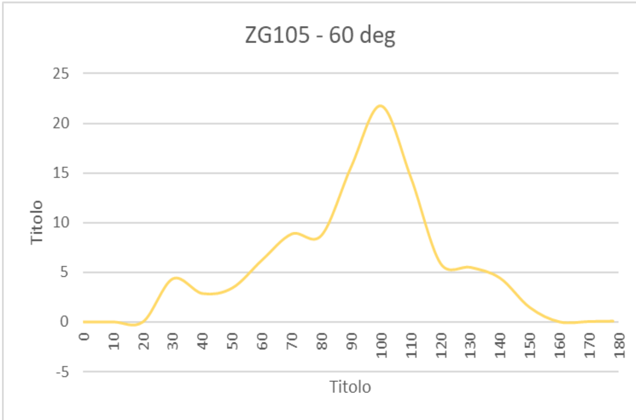

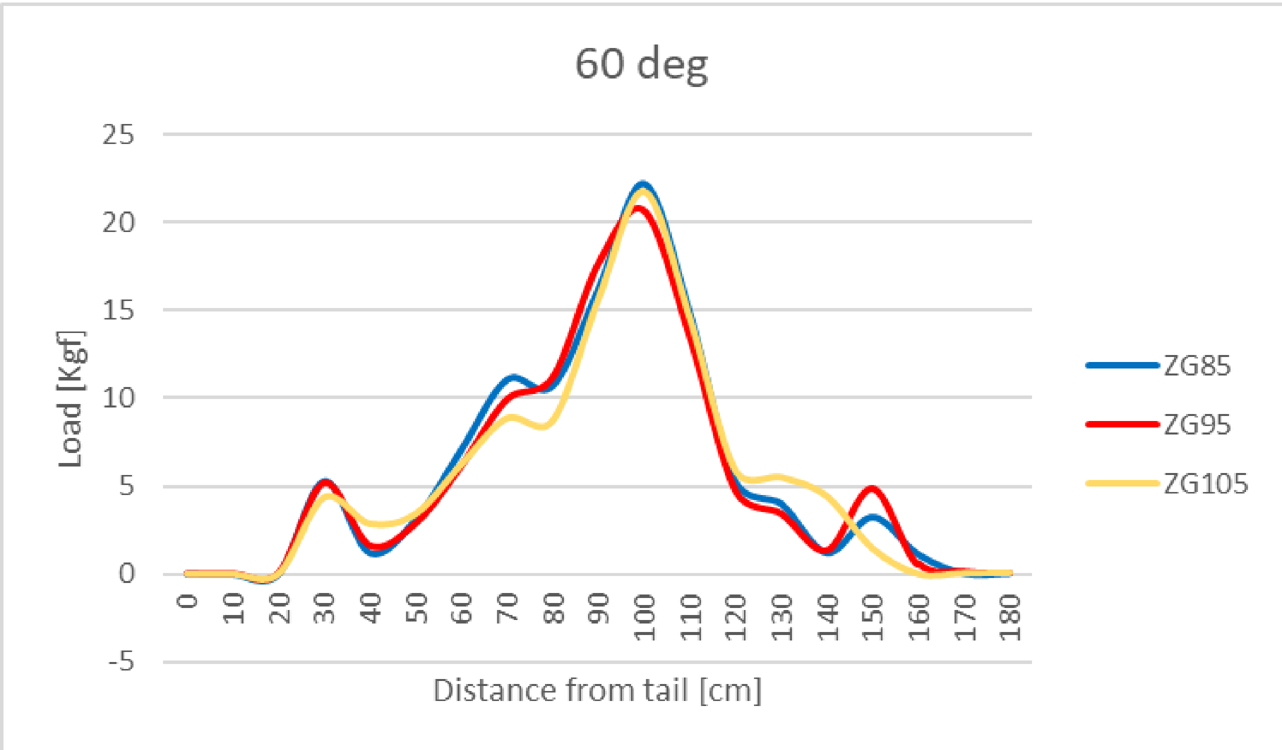

The Edge Load profiles of the three skis *Blizzard ZeroG 85, 95* and *105* shows interesting trends. As the actuator press the ski in the middle at 85 cm from the tail, skitouring bindings transfer more load on the front binding (at 100 cm from the tail) than on the rear binding (at 70 cm from the tail). Peak above front and rear bindings are observed at all edge angles. To better compare the results, tail of the ski is defined as the area on the ski from 0 cm to 60 cm length, center of the ski is defined as the area from 60 cm to 120 cm length while tip of the ski is defined as the area from 120 cm to 180 cm.

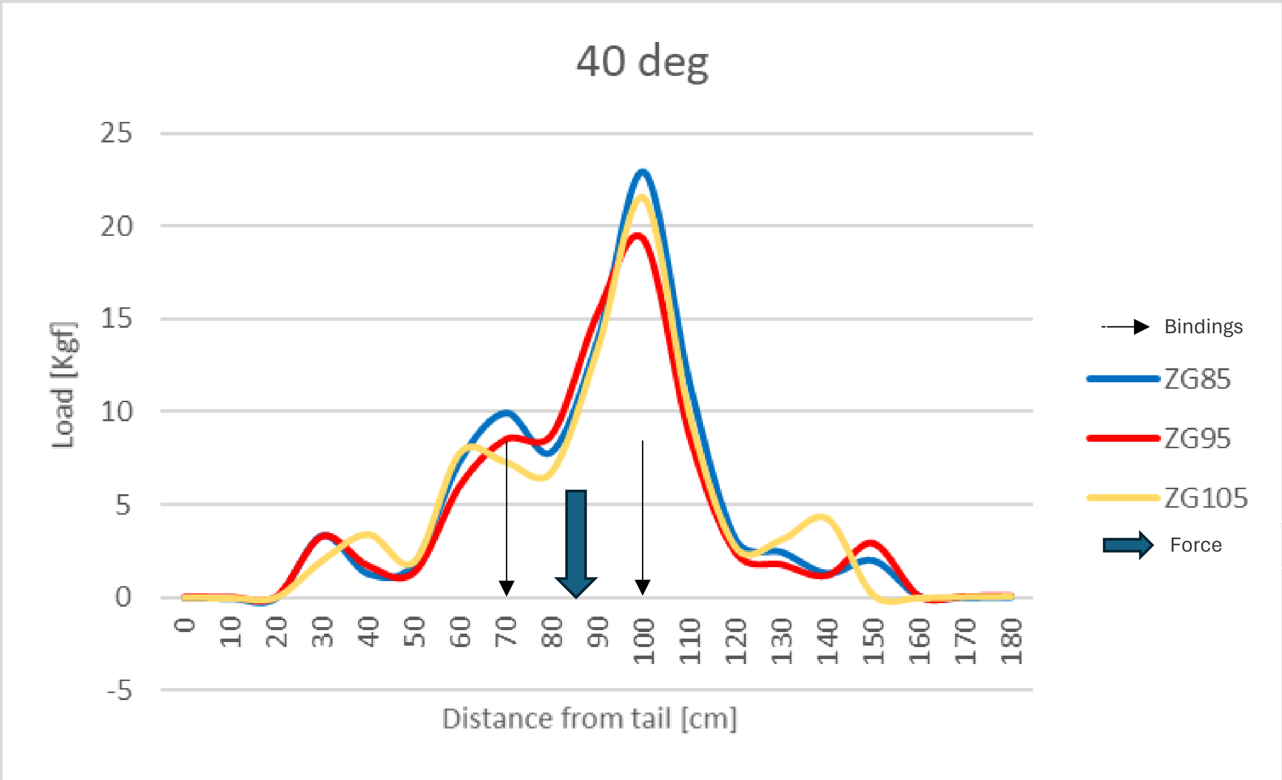

ZG85 and *ZG95* has tip and tail peaks in the same position while *ZG105* has the peaks closer to the ski center zone. These peaks are also far from the start and the end of the ski: this means the working part of the ski (i.e. the part of the ski pushing the para surface) is 120 cm for the *ZG85* and *ZG95* and 110 cm for *ZG105* according to the *40deg* plot. In fact, skitouring skis are designed to perform in off-piste conditions as powder snow and are not optimized for hard snow. *Slytech* bench perform test on hard snow conditions and can identify the inefficient behavior on-piste of skitouring skis due to the small working part of the ski. Moreover, *ZG85* has higher values of load under the bindings (70 cm and 100 cm from tail) while *ZG105* has lower values.

Blizzard ZeroG 85 presents also a plateau in the tip at lower inclinations from 0° to 30°. *Blizzard ZeroG 95* has more continuity under the boot, because at 80 cm from the tail the curve decreases less than for the other skis.

All *ZeroG* skis at every edge angle Edge Load profiles

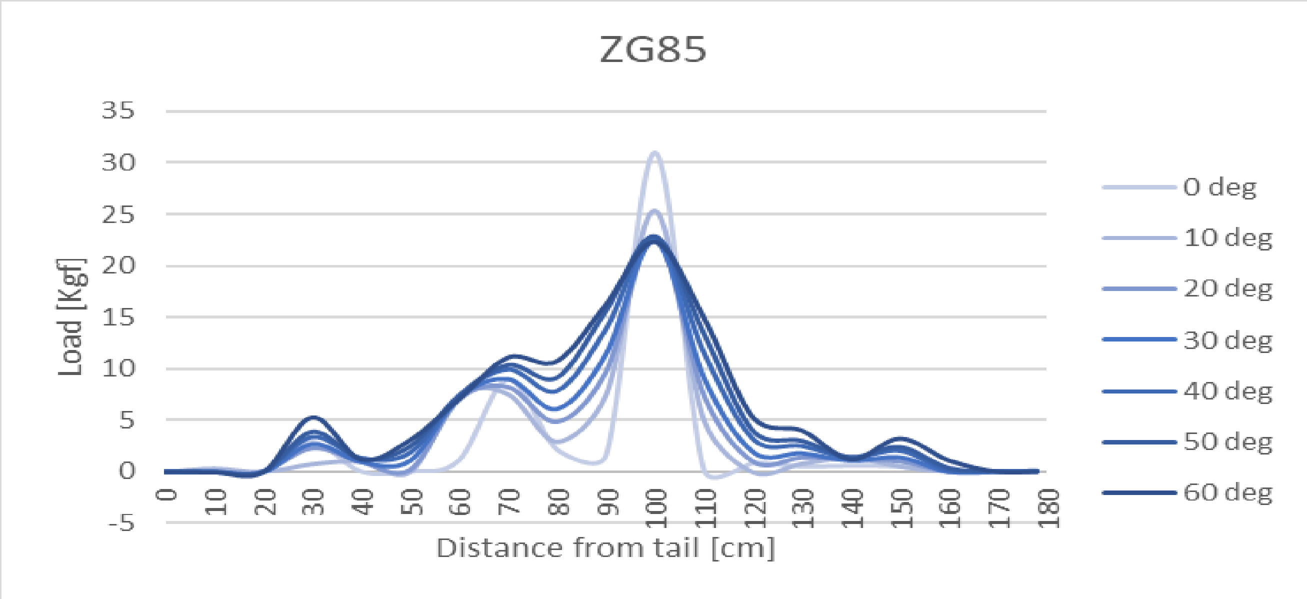

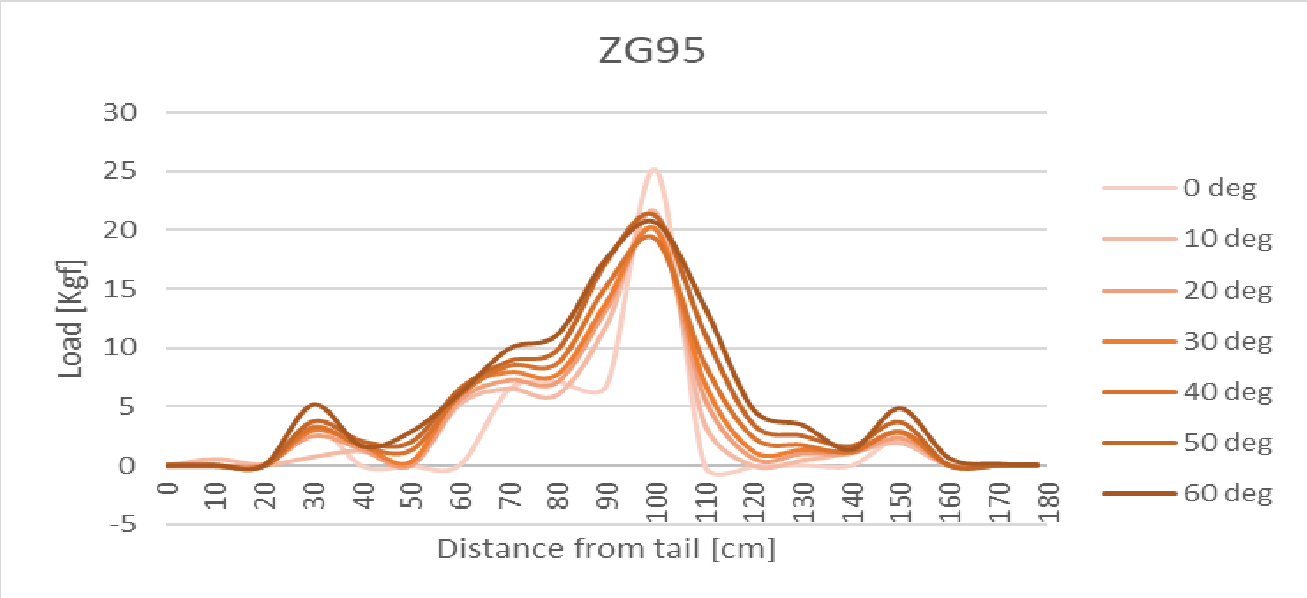

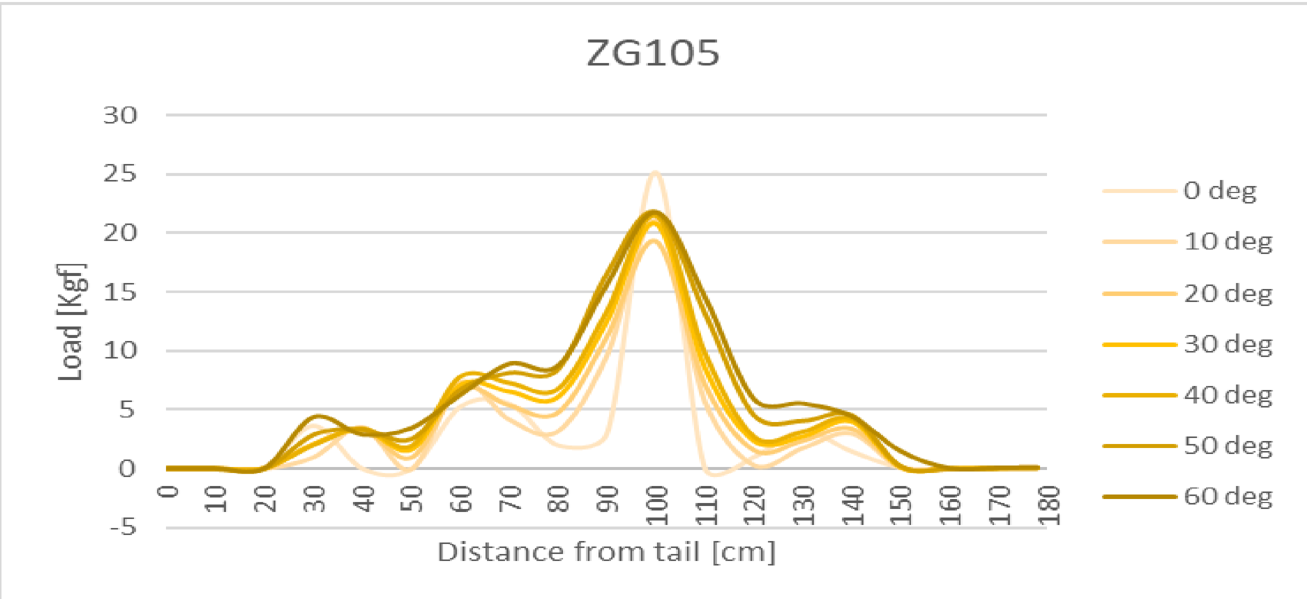

The three graphs above highlight the behavior of the skis as the edging angle increase: from 10° to 60° the edge load profile move upper and became smoother. As the actuator force increase the ski bend itself and cover better all the load cells, smoothing the curves. Moreover, as the edge angle increase, tip and tail peaks increase and slightly slide towards the extremity of the ski.

<u>Tip and Tail ratio for *ZeroG* skis at every edge angle</u>

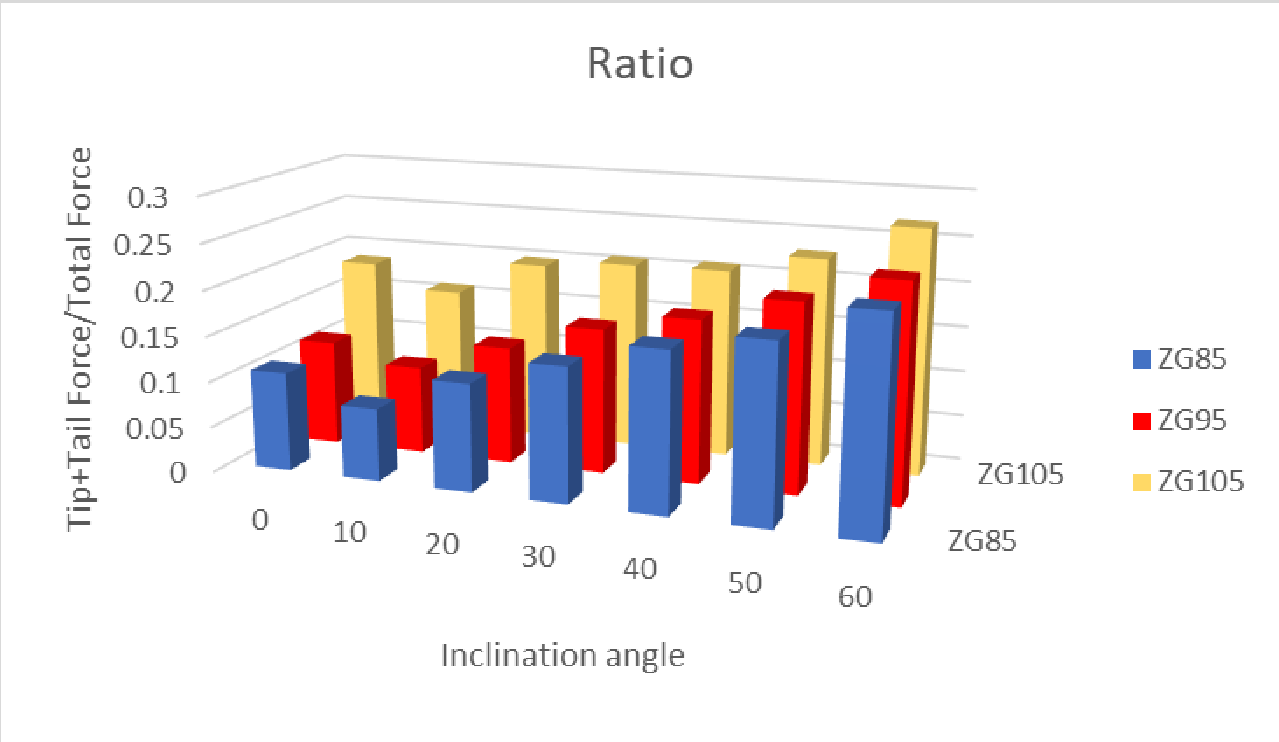

To show how fast the area under the tip and tail ski section increase, a ratio is defined. At first area under the curve for tip, center and tail were calculated. Then the ratio was obtained as:

$$Ratio = \frac{Area\ under\ the\ tip + Area\ under\ the\ tail}{Area\ under\ the\ tip + Area\ under\ the\ tip + Area\ under\ the\ center}$$

The ratio of the three skis was calculated for each edging angle and then plotted in a 3D graphs. At 20° peaks start to become significative, while at 40° noticeable effect can be seen. Area under tip and tail for skitouring ski are low compared to the whole area under the curve (ratio always lower than 0.3). This means that skitouring skis are not aggressive on slope but are stable under the boots.

3.2 Outdoor load cells measurements results

For each run the mean F_x, F_y, F_z and M_x, M_y, M_z of the Ground Reaction loads are obtained. One example of mean load during a run is reported below.

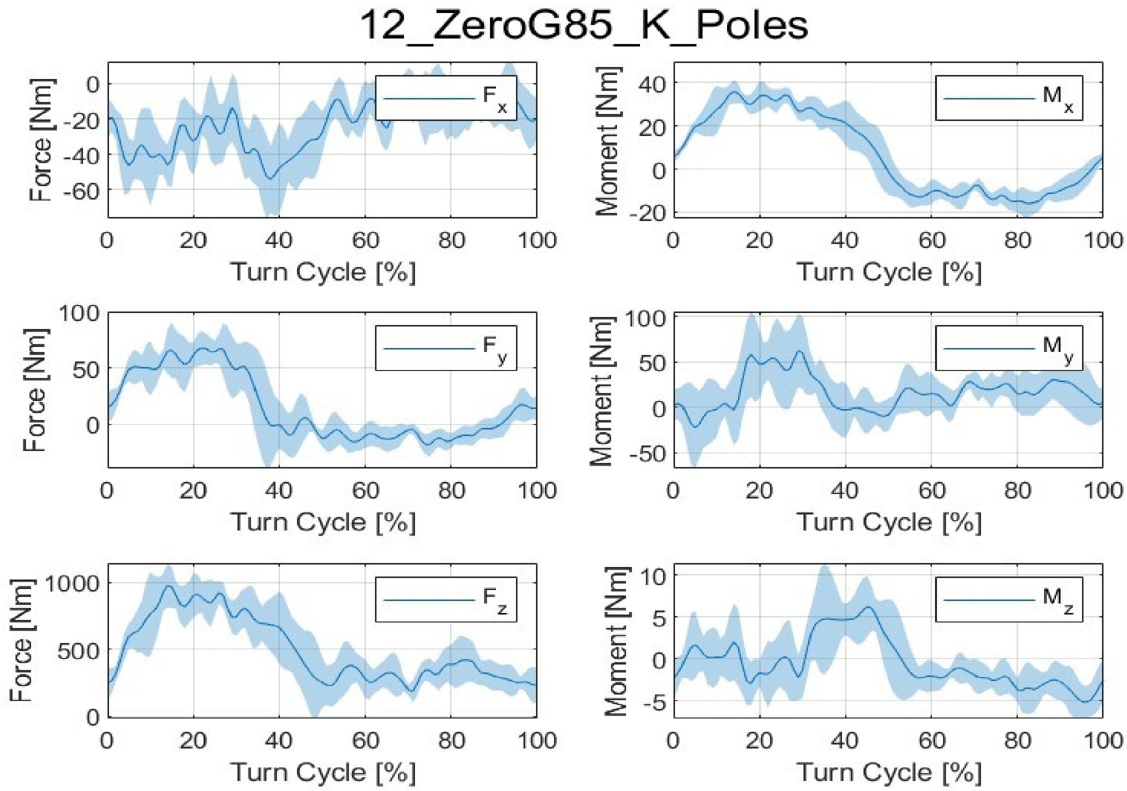

Figure 3.1: example plot of mean Fx, Fy, Fz, Mx, My and Mz of run 12 of Subject 2 with their standard deviations

Figure 4.2 shows the GRF and GRM of run n° 12 of Subject 2 with *Blizzard ZeroG95* with poles conditions. Turn cycle can be divided in left turn and right turn looking at M_x values. When M_x cross zero values the ski is flat on the snow, the turn is finished, and a new one will start. Thus, values from 0% to 50% of Turn Cycle are values during left turn, while values from 50% to 100% of Turn Cycle are values of right turn. Forces and moments are higher during left turn when the instrumented ski is the external one and the more loaded.

F_x represent the force along ski longitudinal axis. As the ski goes down from the mountain, F_x work as friction force. Vectorial sum of F_y and F_z is the force applied from the skiers to the right skis. M_x represent the roll moment of the ski, i.e. the moment impressed from the skier to edge the ski. M_y represent the moment around Y axis. It is positive if more weight goes on the front bindings than in the rear one. M_z represent the moment around the Z axis of the ski.

F_y, F_z and M_x are thus the most interesting loads to compare.

Subject comparisons

Differences in the ski performance of the two subjects are analyzed in this part. Graphs of all forces and all moments for each ski width and each type of ski (with poles and with free turns) are collected and compared for Subject 1 and Subject 2. Differences in loads trends are then analyzed.

Subject comparison on ZG85 with poles

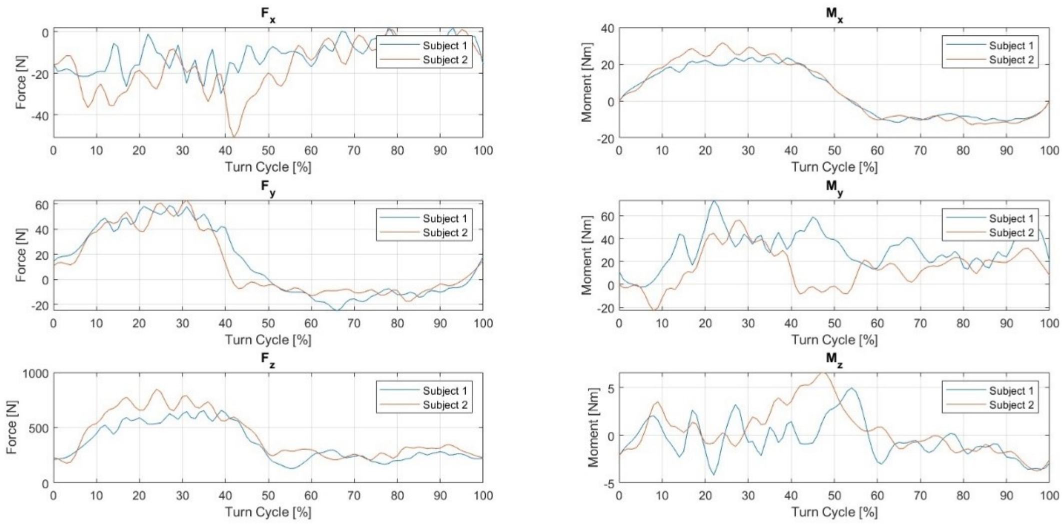

With *ZG85* and poles conditions the system collected higher absolute values of F_x for subject 2 than for subject 1. The same trend is present in M_x where subject 2 values are higher than subject 1 value. F_y data are instead similar for the two subjects while M_y values are now higher for subject 1 than for subject 2. Differences between maximum and minimum M_y values are anyway similar for the two subjects. F_z collected for the second subject are above the ones collected for the first, same for M_z data. Overall subject 1 showed higher loads.

Subject comparison on ZG85 with free turns

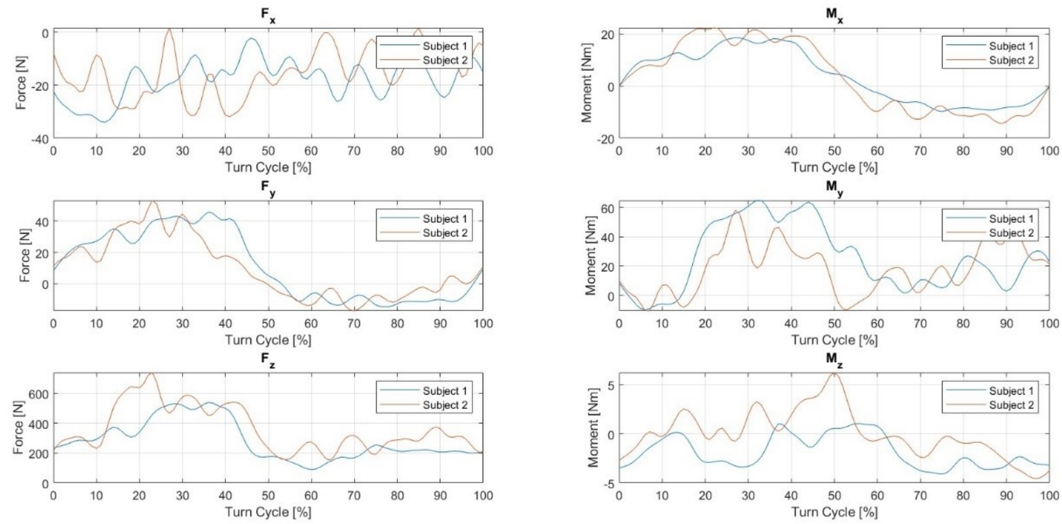

With the same ski but in free conditions F_x collected are similar for the two skiers, while M_x remain higher for subject 2 than for subject 1, but differences between the two are lower. Force in the Y axis is now similar between the two skiers but M_y values are higher for subject 1 than for subject 2. F_z and M_z are again higher for the second subject. Overall subject 1 showed higher loads.

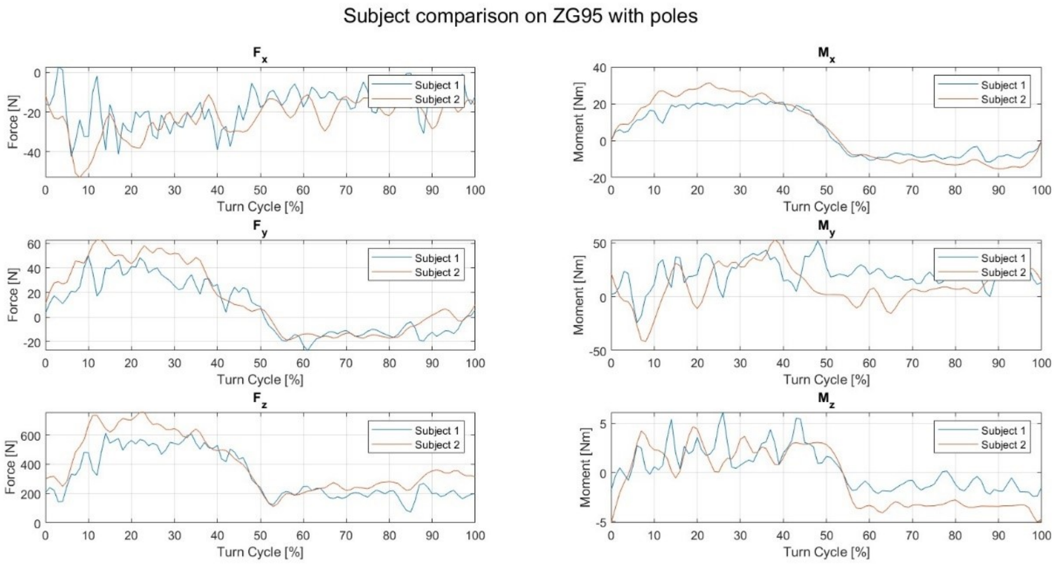

Data collected on *ZG95* during poles runs show similar values between the two subjects in F_x. Instead M_x values are higher for subject 2 than for subject 1. F_y follow the same pattern with higher values for the second skier, while the moment on Y axis is similar for the two subjects. Higher values of Z forces are collected for the second skiers respect to the first, though the Z moments have similar values. Overall subject 1 showed higher loads.

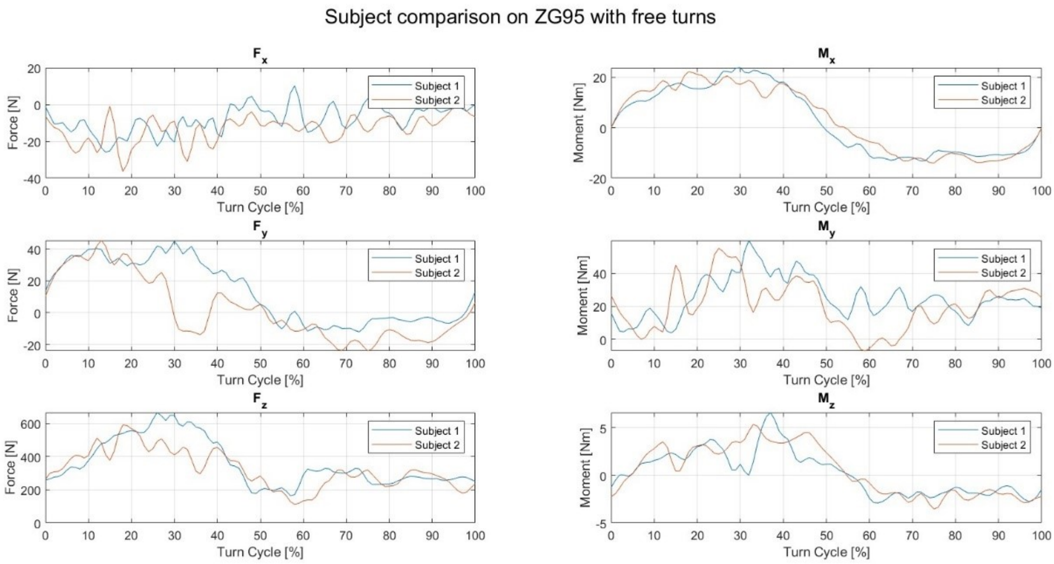

Analyzing loads for the same ski in free turns conditions can be observed as F_x are now similar between the two subjects, and same for M_x values. Forces values on Y axis are lower for subject 2 than for subject 1, while M_y values are similar between the two subjects with some values lower for subject 2. Forces on Z are now lower for the first subject than for the second, while M_z are similar. Overall subject 2 showed higher loads.

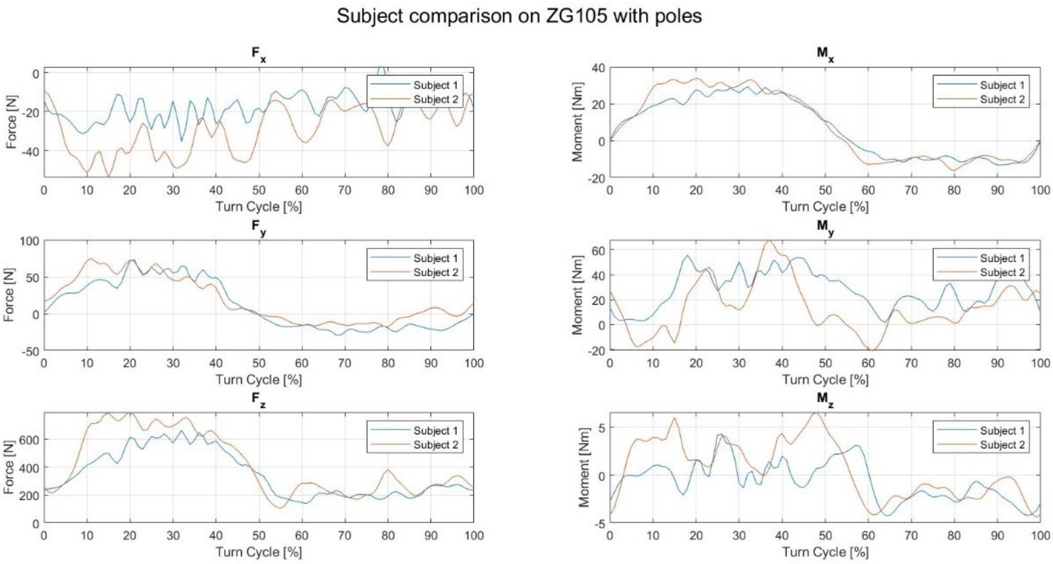

Durin *ZG105* runs with poles all the collected loads are higher in absolute values for subject 2 than collected loads for subject 1, except F_y and M_y. In fact forces collected on Y axis are similar between the two skiers while moments collected on Y axis are similar between the two subjects as mean values, but higher as maximum and minimum values for the second subject. Overall subject 1 showed higher loads.

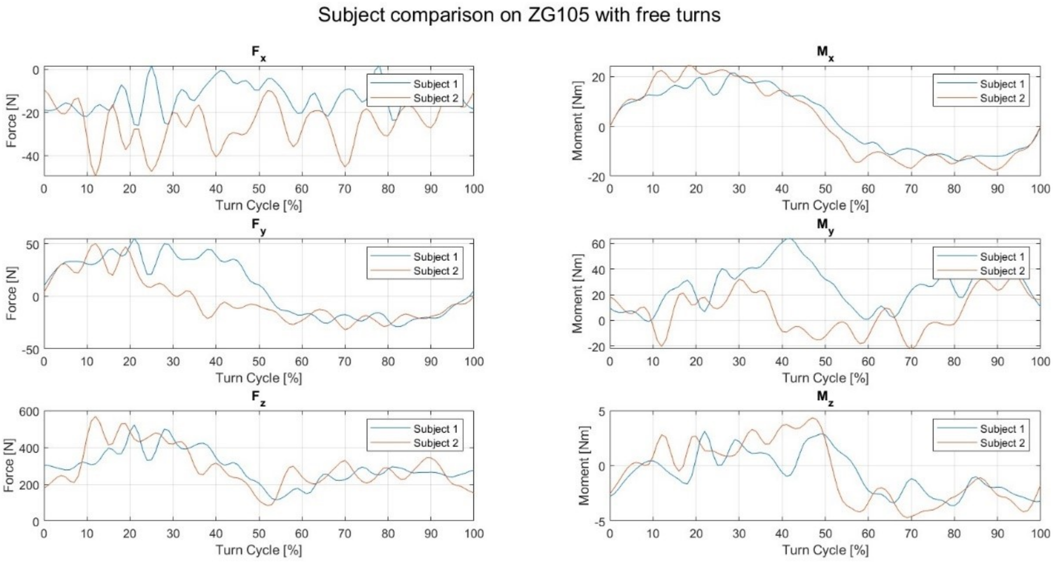

With the same ski in free turns conditions loads collected shows different patterns. Absolute values of F_x are higher for subject 2 than for subject 1, same for M_x values but differences are lower. Subject 2 F_y and M_y values are lower than F_y and M_y values for subject 1. Force on Z axis are than similar for the two skiers while moments on Z axis are higher for subject 2. Overall subject 2 showed higher loads.

Poles vs Free turns comparisons

Differences between poles and free turns loads during mean turn cycle are investigated in this part. After calculating mean turn forces and moments during the turn cycle of different runs, loads during poles runs are overlapped to loads during free turns runs to search differences in the curves patterns. As the previous results showed higher loads during subject 2 runs, graphs of poles runs and free turns runs are reported only for the second subject.

F_x acquired for subject 2 runs with *ZG85* were higher in absolute values for poles runs than for free turns and same was for M_x. Forces in the Y direction were also higher during poles runs, while M_y were similar. F_x is higher for poles runs than for free turns runs and M_z values are similar for the two conditions. Overall loads measured *ZG85*during poles runs are higher than loads measured during free turns runs.

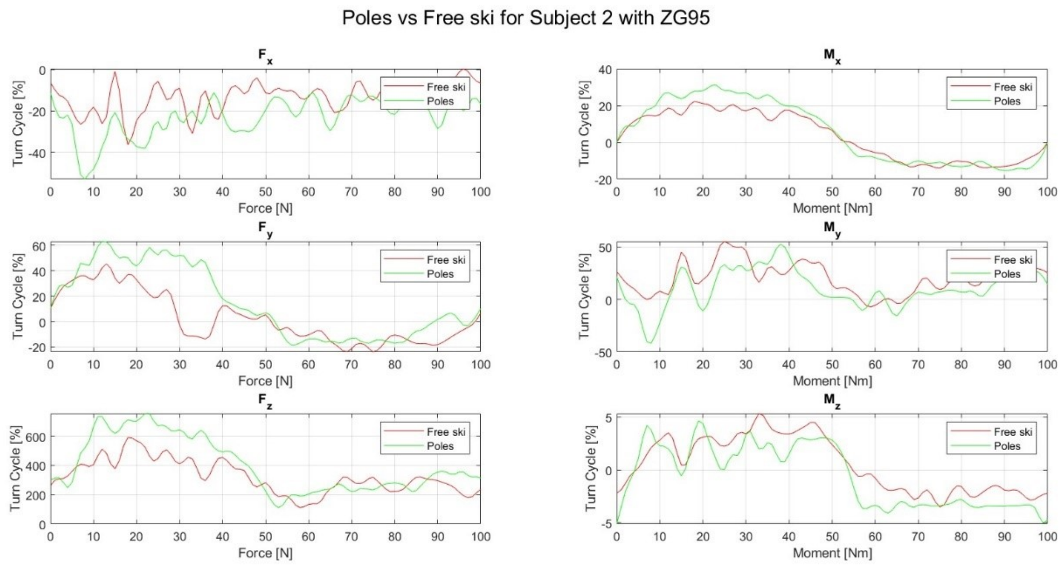

Loads acquired during runs of subject 2 on *ZG95* are similar to the ones collected on *ZG85*. F_x values during poles runs are higher than values during free turns runs, same for M_x and F_y. Moments on the Y axis had similar maximum values during poles and free turns runs but minimum values are much lower during poles runs: the differences between maximum M_y values and minimum M_y values were way higher during the poles runs. F_z shows again higher values for poles runs, while M_z shows similar results between poles runs values and free turns values. Overall loads measured on *ZG95* during poles runs are higher than loads measured during free turns runs again.

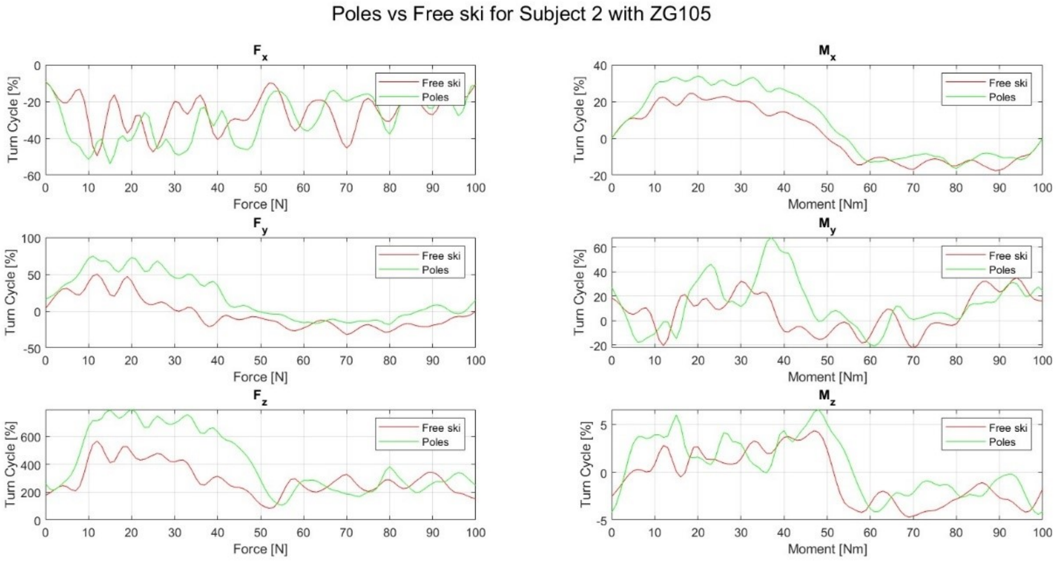

With *ZG105* shows again similar trends with the runs with the two other skis. F_x collected are similar between the two skis. M_x, F_y, M_y and F_z collected during poles runs are higher than M_x, F_y, M_y and F_z during free turns. M_z values were similar during poles runs and free turns runs. Overall loads measured on *ZG105* during poles runs are higher than loads measured during free turns runs again.

Different skis comparison

After the evaluation of differences in skiing loads between different subjects and in skiing loads between different ski conditions, differences in the loads between the three *Blizzard ZeroG* skis are also searched. Differences are searched between the mean values of F_y, F_z and M_x during the ski turn cycle: the mean loads between all the runs were calculated from the mean forces and moments of the turn cycle for each run. Differences in the loads between the three skis are searched only in F_y, F_z and M_x as they are the most interesting loads to compare.

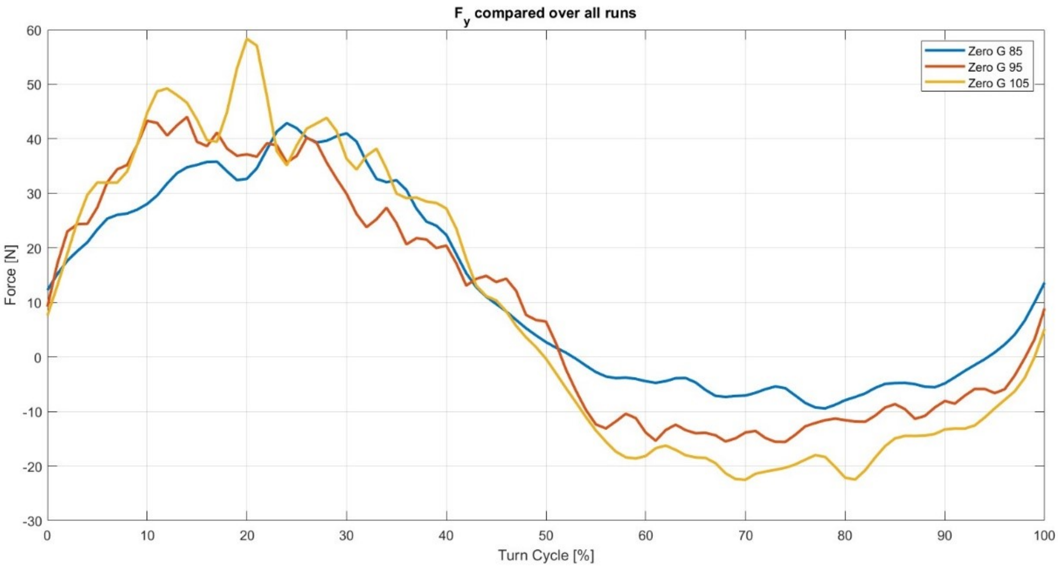

Figure 3.2: Mean Fy from all runs

The mean F_y values obtained from the load does not show significative trend in the first 50% of Turn Cycle. During the left turn *ZG85* and *ZG95* have the same mean values (around 35 N) while *ZG105* show higher mean values (around 40 N) also thanks to the presence of two peaks altering the force trend. In the second part of the Turn Cycle instead a clear decreasing force trend is observed (*Figure 4.3*). *Blizzard ZeroG 105* has the lower force, *Blizzard ZeroG 85* has the highest while *Blizzard ZeroG95* is in the middle. Clear differences in the F_y are present in the right turns between the three skis but are not present during the left turn when the absolute values of the forces are higher.

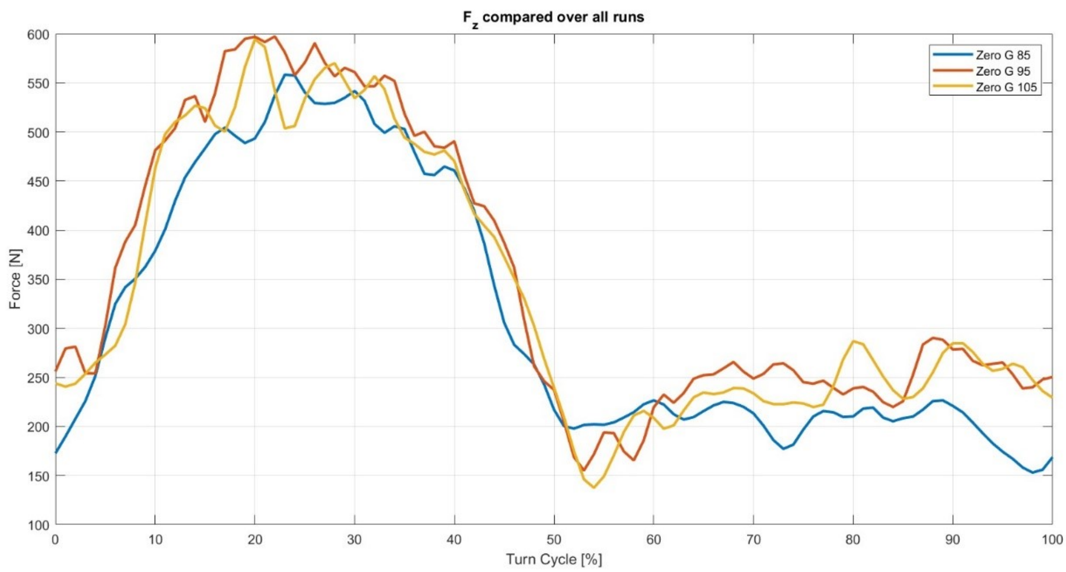

Figure 3.3: Mean Fz from all runs

F_z values during the Turn Cycle show small differences between the three skis. In the left turn forces on the Z axis collected under the *ZG85* are the lowest compared to the forces on the Z axis of the other skis. In fact, F_z collected under *ZG95* and under *ZG105* are the highest between the three skis and has similar values. In the second 50% of the Turn Cycle and so during the right turn the trend is the same with lower values: *ZG85* show the lowest values of force on the Z axis, while *ZG95* and *ZG105* showed the highest forces. Also, during right turns F_z values for *ZG95* and *ZG105* are similar. Differences in Z forces collected under the skis are present between different pair of skis but these differences are small.

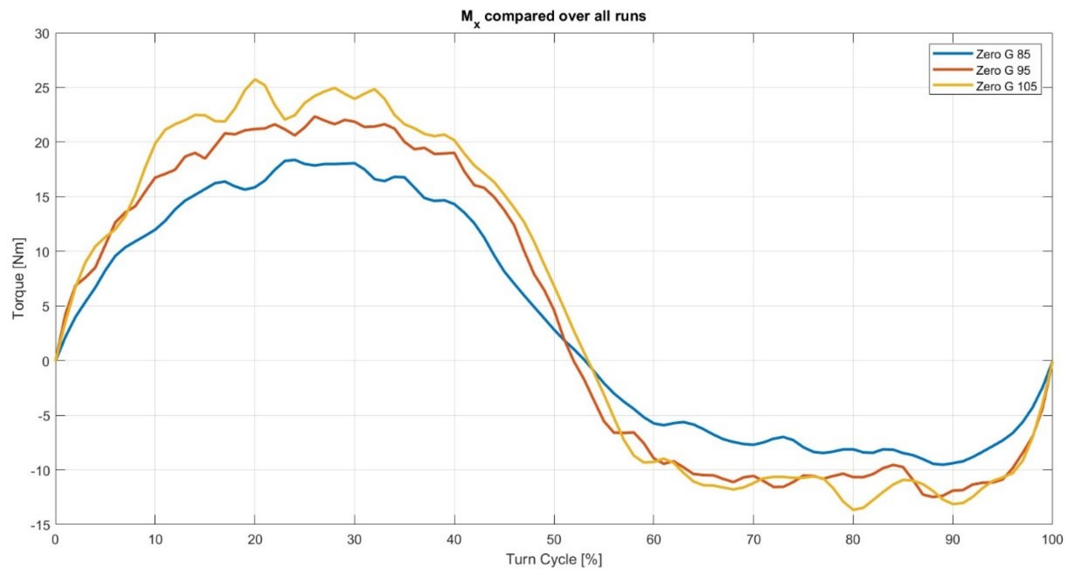

Figure 3.4: Mean Mx from all runs

In the 50% of the Turn Cycle the moments on the X axis collected for the three skis are different. The values obtained for the *ZG105* are the highest, followed by the values of the *ZG95* and *ZG85*. Clear differences between the curves can be observed. During the right turn the same trend is observed with the absolute values (the moment on the X axis during the right turn is below zero): values obtained for the *ZG105* are the highest, followed by the values of the *ZG95* and *ZG85*. A clear trend is seen analyzing M_x values: M_x absolute values collected by the load cell system increase as the ski width increases.

3.3 Impact test on snow and foams results

Impact tests were conducted to evaluate impact forces and penetration depth of the dart over different snow and foams conditions. After obtaining the force-penetration curves for each impact, the most representative curves for every snow condition and type of foam were extracted taking in consideration the average values of force peak and penetration depth obtained during the impacts on each material. When the obtained curves had huge differences, the real penetration measured in the hole made by the dart in the material was compared to the penetration of the curve to choose the most representative one.

After obtaining the most representative curves of each material, each snow curve was overlapped to all the foams curve to choose a foam able to mimic the behavior of that particular snow.

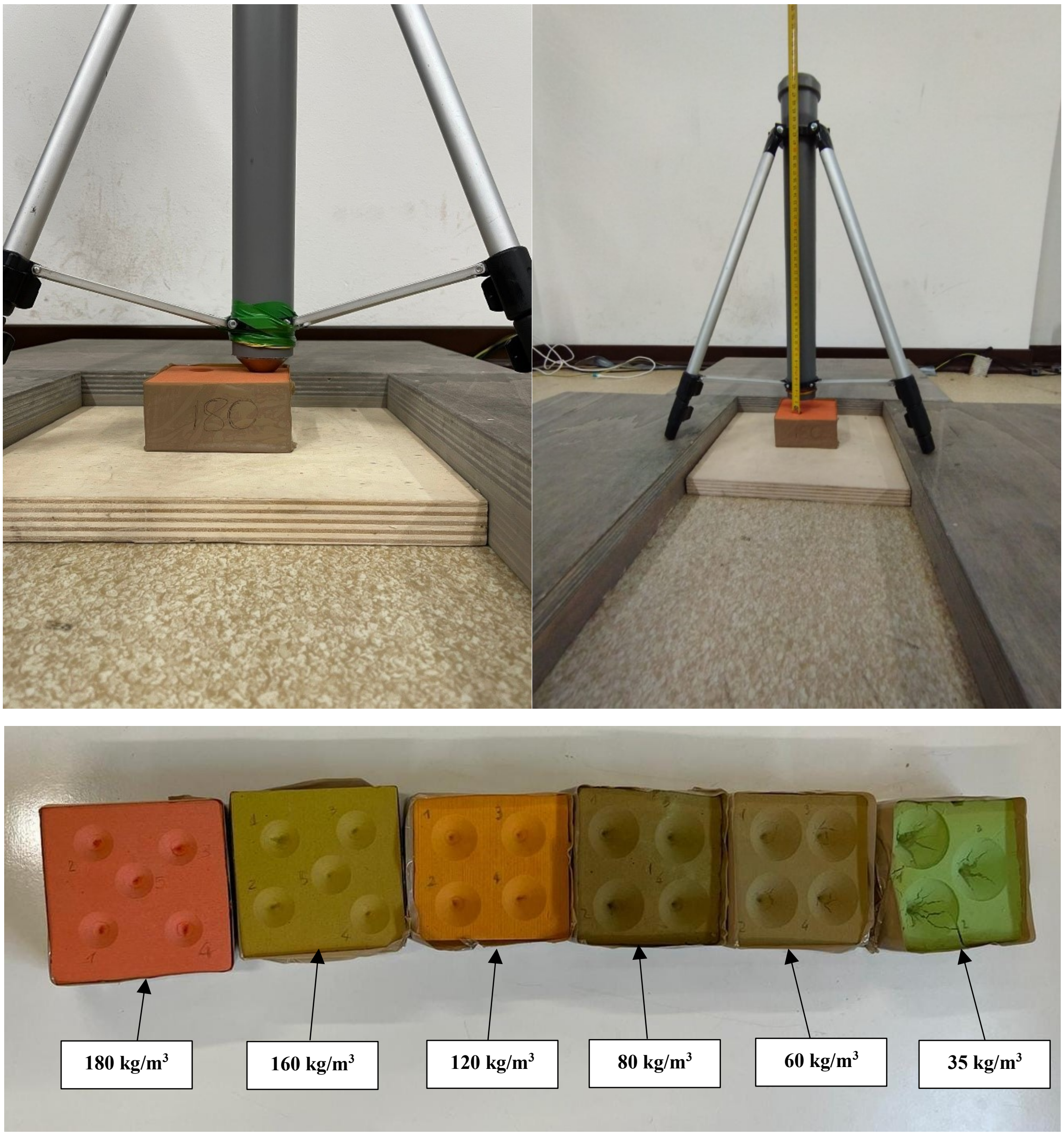

Figure 3.5: test setup in Padova laboratory and impact on foams with their density

Snow impacts force-penetration

Impact test on snow were carried on during *ISEA WinterSchool* in *Kranjska Gora*. Four different types of snow were tested with impact from 50 cm:

1. Ice of an ice-skating track.
2. Medium grain snow of the slope in *Kranjska Gora*. Slopes were closed for the skiers, but some snow was still present.
3. Hard snow nearby the ice-skating track.
4. Soft snow nearby the ice-skating track.

For each type of snow is presented a graph containing the force-penetration curves of all the impact carried out on that snow. The most representative curve of each snow will be selected considering the peak forces values, the penetration depths and the geometry of the curves. Real measured penetration depth is considered in the choice of the most representative curve.

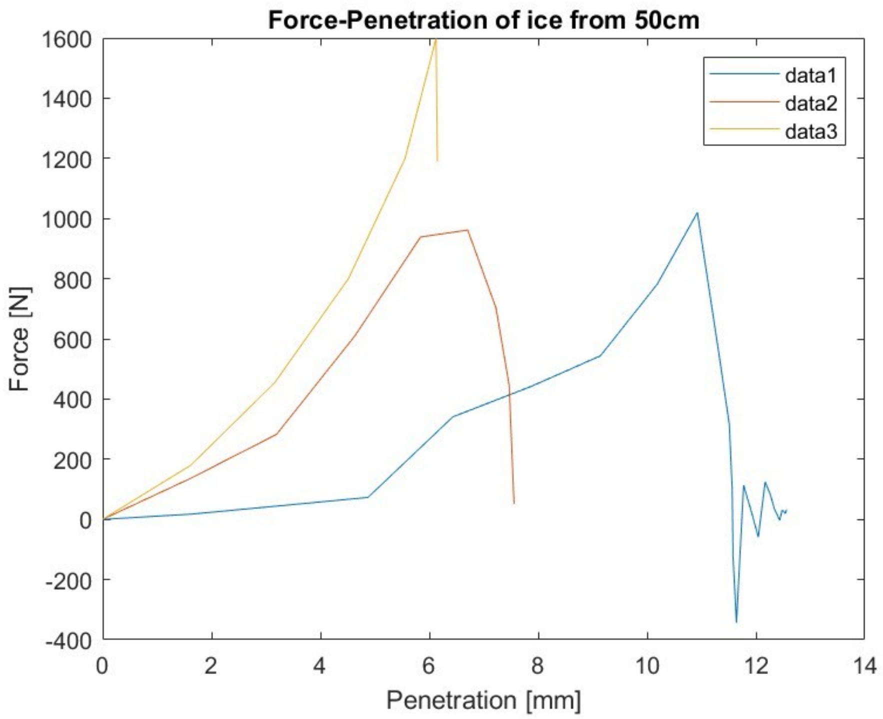

On ice three tests were successfully performed. The three force-penetration curves on ice shows different values in the peak forces, with the first two impact having a value of around 1000 N and the third around 1600 N. Also the penetration depths are different for the three curves: the first one is over 12 mm, the second is 7,5 mm and the third is 6mm. Moreover, the first curve has some problems in its final part. Considering all this information the second curve is chosen as representative of the snow, having peak values equal to the mode of the peak values and a penetration depth comparable with the one of the third impact and to the real one.

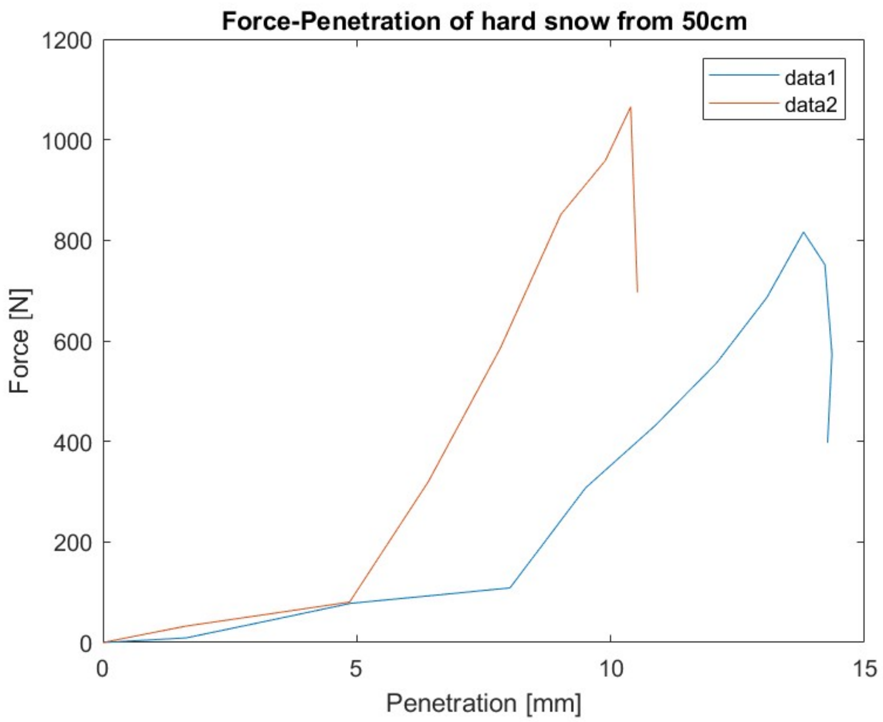

Unfortunately, only two impacts were recorded on the hard snow tested in Slovenia. The two curves of the impacts are not similar and differences in both peak values and penetration depth are present. In this case the choice of the most representative curve was made only considering the penetration depth of the curves and comparing it with the real ones. The first curve (blue one) had penetration depth comparable to the real penetration depth and was chosen as representative of the hard snow found in Slovenia.

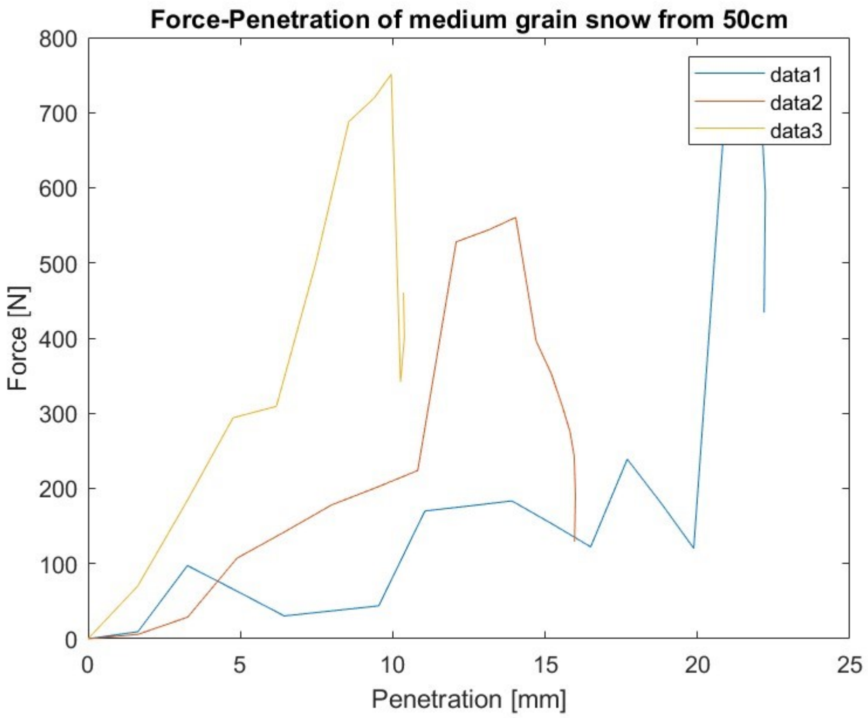

On grain medium snow three impact were made. The first one and the third one has similar values of peak force, around 750 N and are repetitive. Instead, the three curves have very different penetration depths (22mm, 15 mm and 10 mm). Despite the second curve has peak values different form the mode of the peak values of this snow, it has a reasonable penetration depth if compared with the real one. The curve of the second impact was chosen as representative curve of the grain medium snow tested in Slovenia.

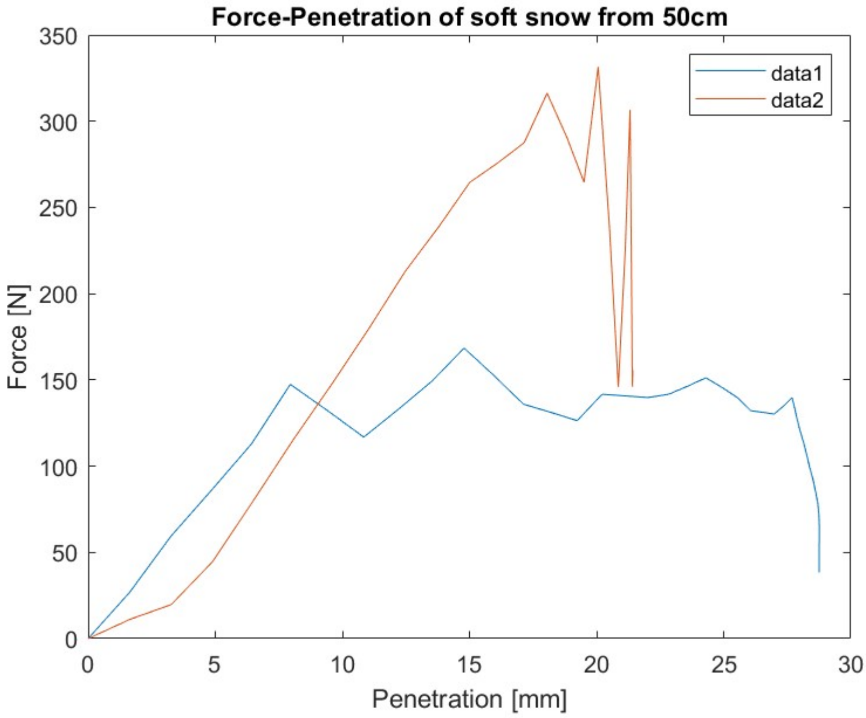

Unfortunately, also for soft snow only two impact tests were recorded. As in the hard snow case the two curves of the impacts are not similar and differences in both peak values and penetration depth are present. Choice of the most representative curve was made again considering the penetration depth of the curves and comparing it with the real ones. The first curve (blue one) had penetration depth comparable to the real penetration depth and was chosen as representative of the hard snow found in Slovenia.

With this technique a visual measure of the hardness of different snow (ice, hard snow, medium grain snow and soft snow) is obtained and can be compared later to visual measurement of the hardness of phenolic foams.

Foams impacts force-penetration

Phenolic foams were tested in the laboratory of *Padova* with impact test to visually measure their hardness and try to compare with snow. In laboratory six samples of phenolic foams taken from *POLIFEN* are tested. The tested foams samples had density of 35, 60, 80, 120, 160 and 180 kg/m^3. The same process used in snow impact to extract the most representative curve for each type of snow is repeated in this case with foam. Fortunately, the six foams presented more repeatable curves and choice were made also considering the curve with the mean values of peak force and penetration depth for the current density.

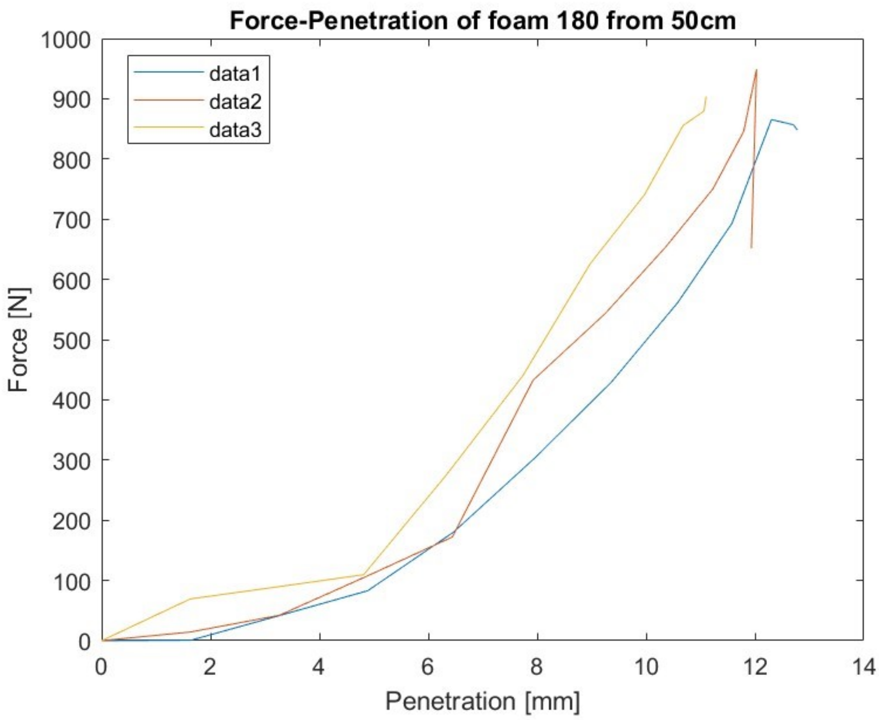

On foam 180 only three impacts were correctly recorded. The three curves have similar shape, similar values of peak force and similar values of penetration depth. As the second impact had a better shaped curve and its penetration is close to the mean penetration of all the three curves, it was chosen as representative of foams 180.

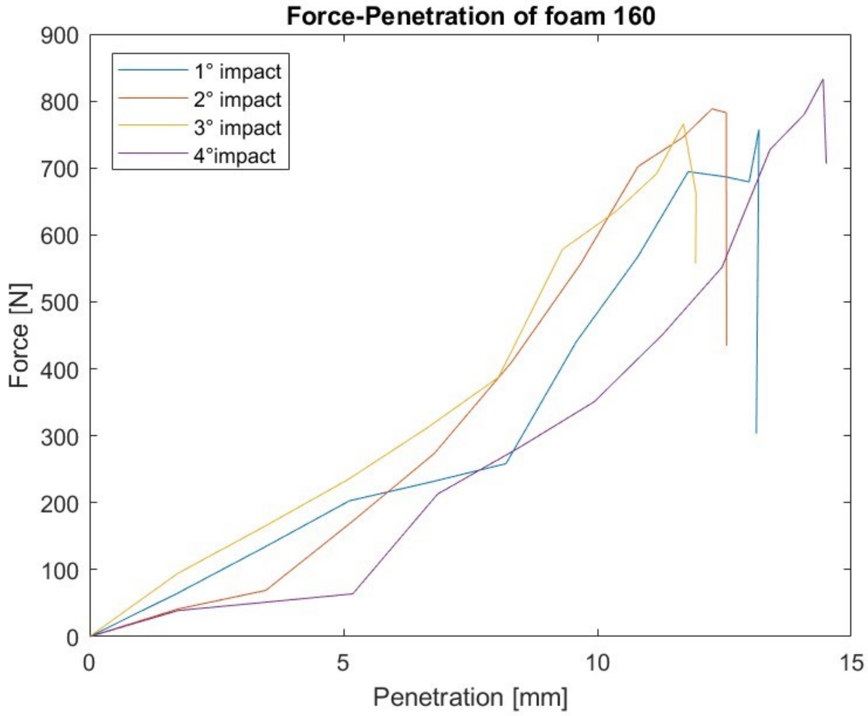

On foam 160 all the four impacts performed were correctly recorded. All the four force-penetration curves of the impacts present similar values of the peak force (around 800 N) and differs little in penetration depth. Comparable curves and small differences allowed to choose the characteristics curve taking in consideration the mean penetration between all the curves. With this method the second impact curve (red one) was chosen as representative for the foam 160.

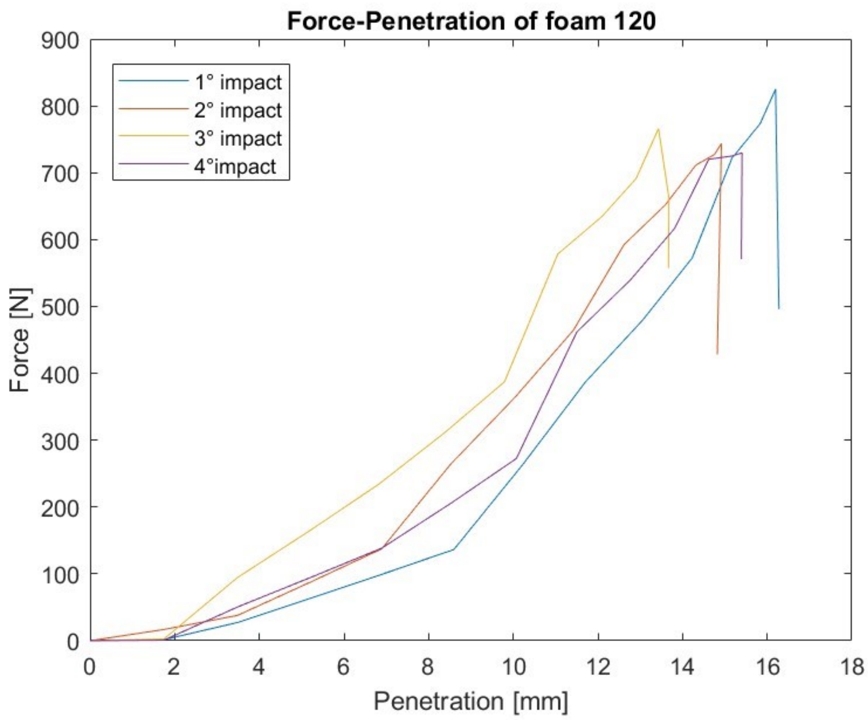

On foam 120 all the four impacts performed were correctly recorded. Once again peak forces values of the force-penetration curves are similar (750 N) and penetration depth differs little. Comparable curves and small differences allowed to choose the characteristics curve taking in consideration the mean penetration between all the curves. With this method the second impact curve (red one) was chosen as representative for the foam 120.

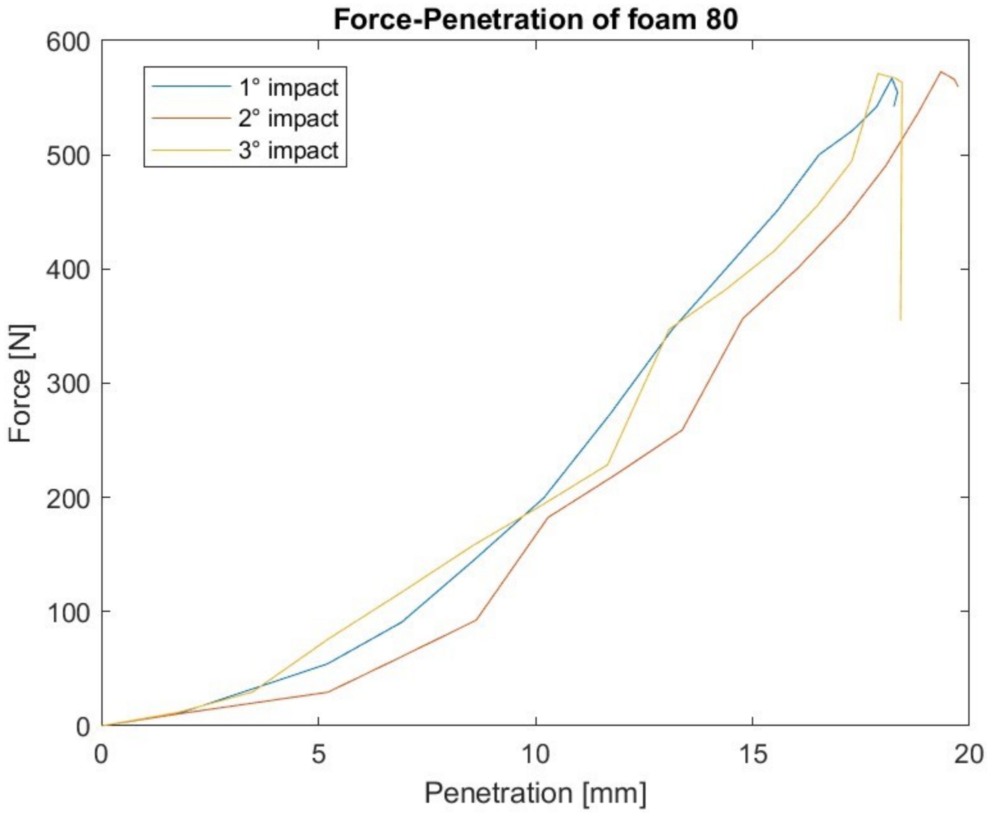

On foam 80 all the three impacts performed were correctly recorded. The three curves are very similar, show peak force of around 550 N and very similar penetration depth. The third curve was chosen as representative of foam 80 because of it has penetration depth near the mean of the penetration depth values of all the curves.

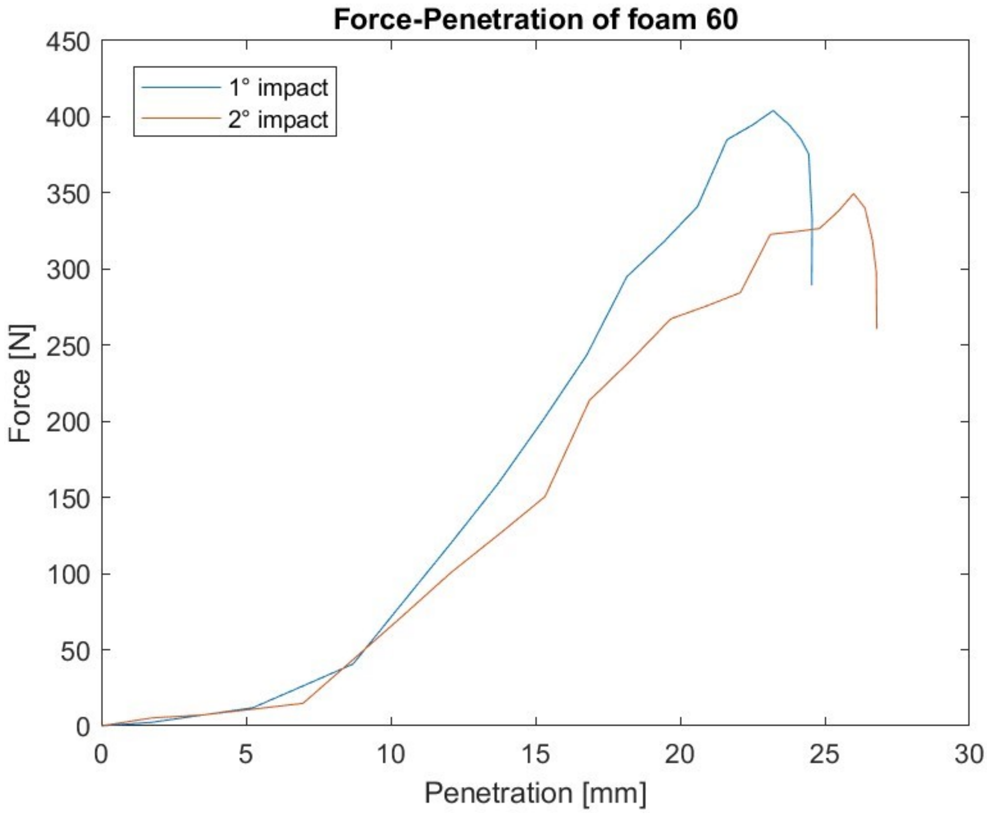

Unfortunately for 60 only two impacts of the three performed were recorded. The two curves are not as similar as the curves obtained with the previous foams. They show difference in peak values (400 N and 350 N) but smaller differences in the penetration depth values. Considering the real penetration depth of the impact, impact one was chosen as representative of foam 60.

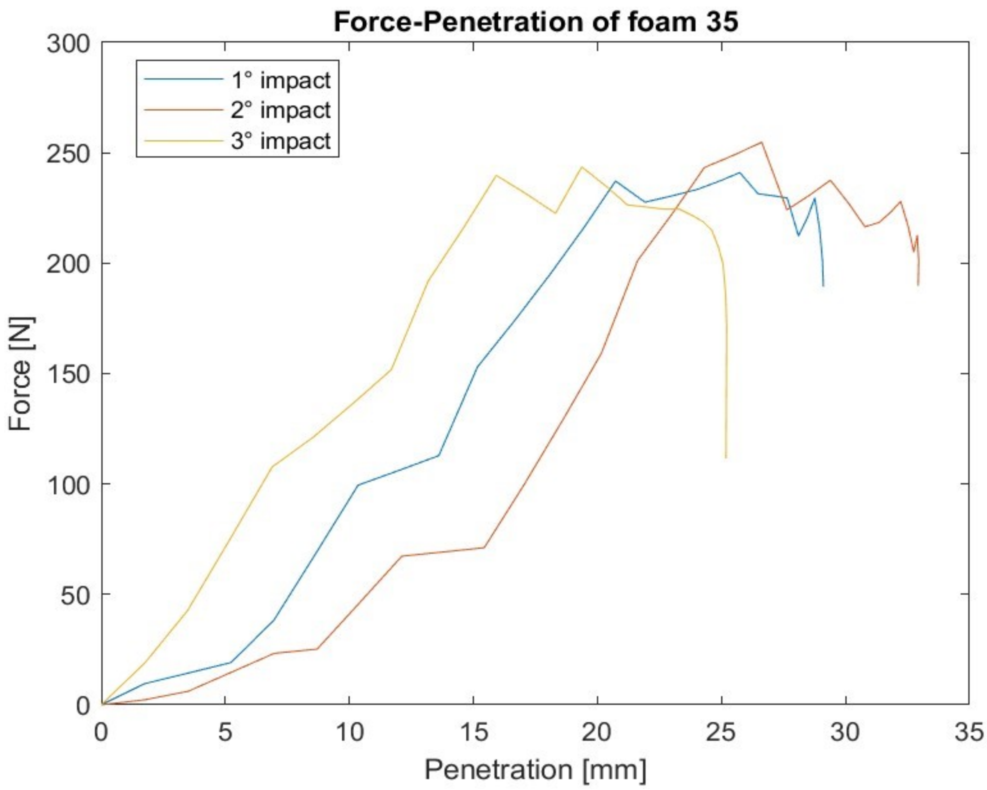

On the foam 35 all the three impacts performed were recorded. All the curves present a first growing phase ending with a plateau achieving a similar force peak of 250 N. The three curves differ in penetration depth. In this case the choice of the curve was made taking the curve in the middle, considering it as the mean curve of the three. The first curve (blue curve) is chosen as representative of foam 35.

Finally, after obtaining the force-penetration curves of all the foams a graph containing all of them was plotted to see how they differ in shape, peak force and penetration depth.

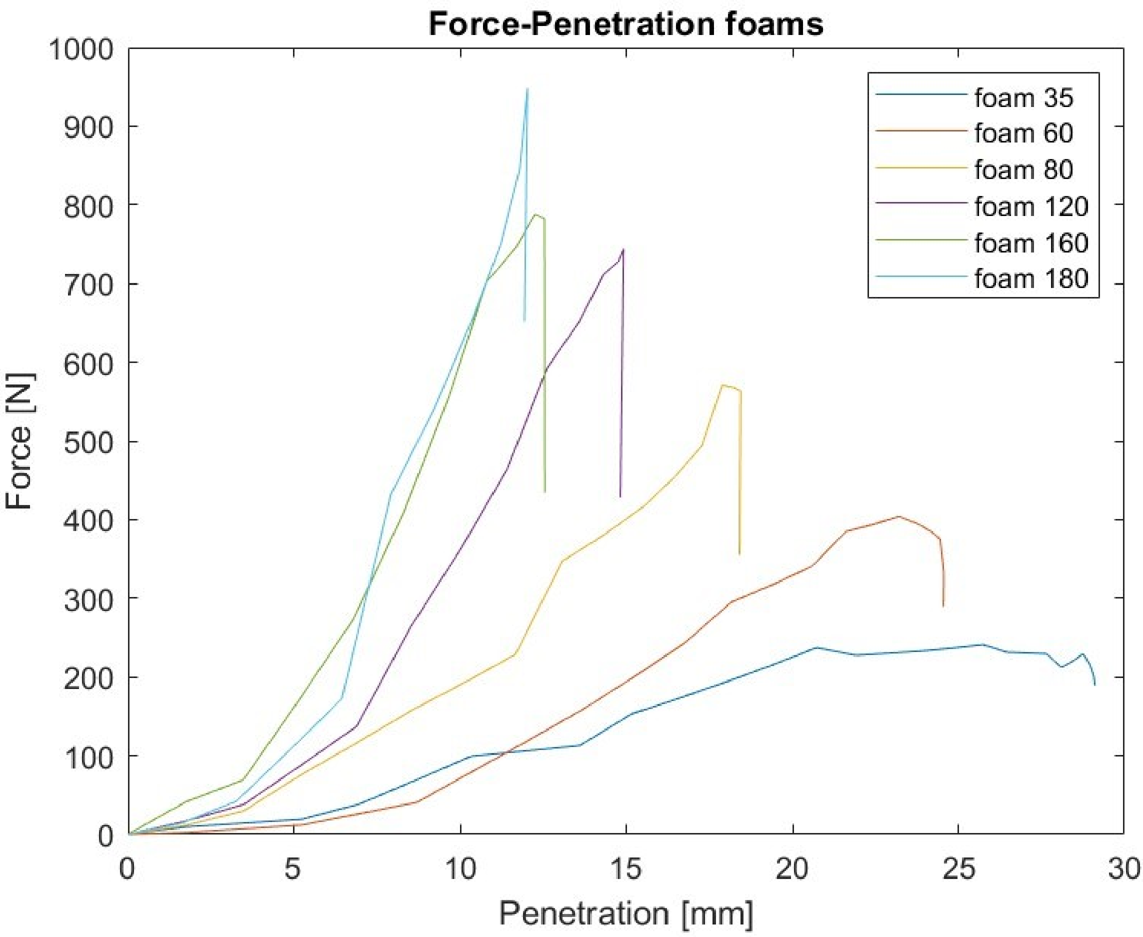

It can be observed that peak force values following the decreasing density trend of phenolic foams: more dense foams show higher peak forces while less dense foams show lower peak forces. Moreover, penetration depth values follow the decreasing density trend of phenolic foams as well: more dense foams show lower penetration depth while less dense foams shows higher penetration depths. A clear trend can be observed.

Different snow over All foams force-penetration comparison

After obtaining force-penetration curves of phenolic foams and force-penetration curves of different snows, each snow curve is now overlapped at the graph with the curves of all the foams to see if snow curve resembles one of the curves of the foams. Snow force-penetration curves are compared to the foam's ones analyzing similitude in shape, peak forces and penetration depths.

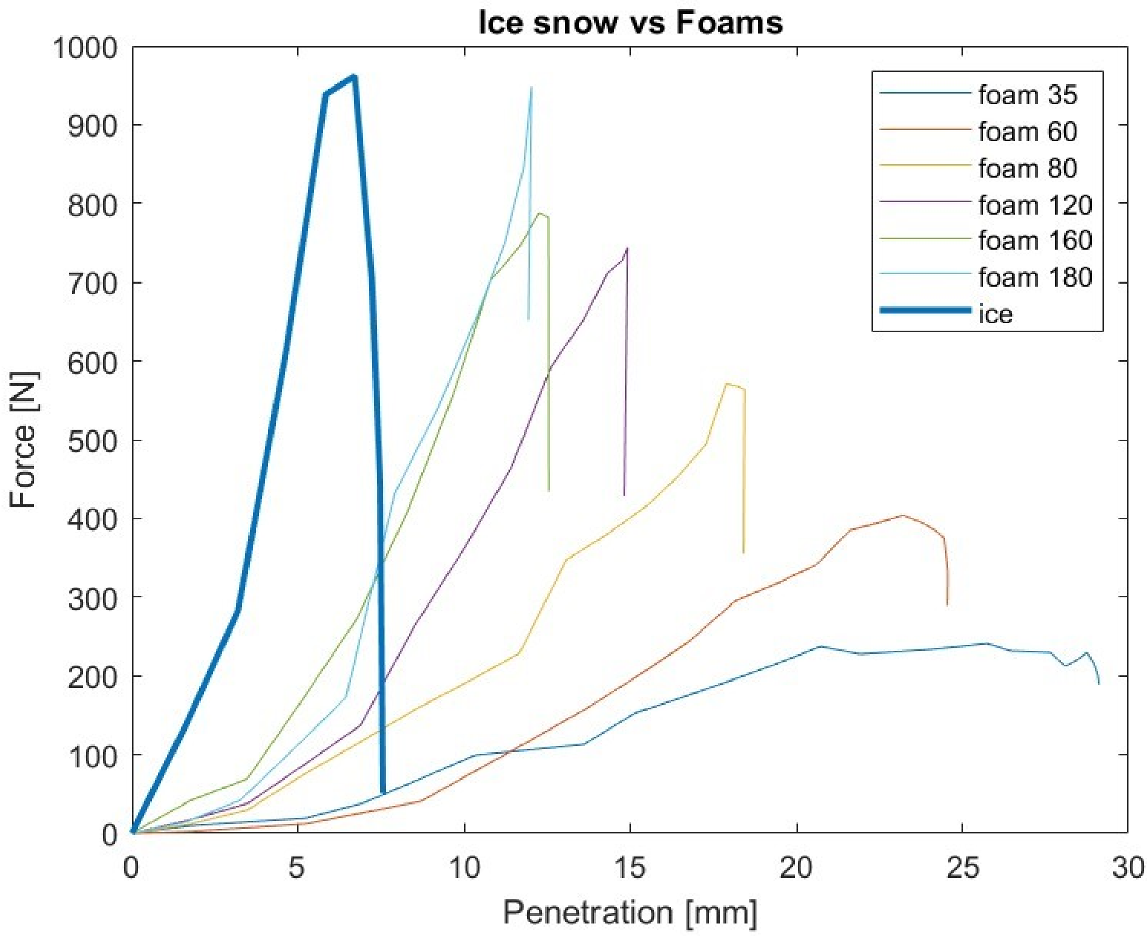

The curve of the impact on ice shows a growing phase ending with a peak. The final peak represent also its peak force (950 N). The penetration depth of the ice is instead 7.5 mm. The curve of foam 180 has similar shape of the curve of the ice and its peak force is like the peak force of ice curve. Unfortunately foam 180 has penetration depth values way higher (11 mm) than the penetration depth values of ice. Despite that foam 180 is the foam with force-penetration curve like the force-penetration curve of the ice

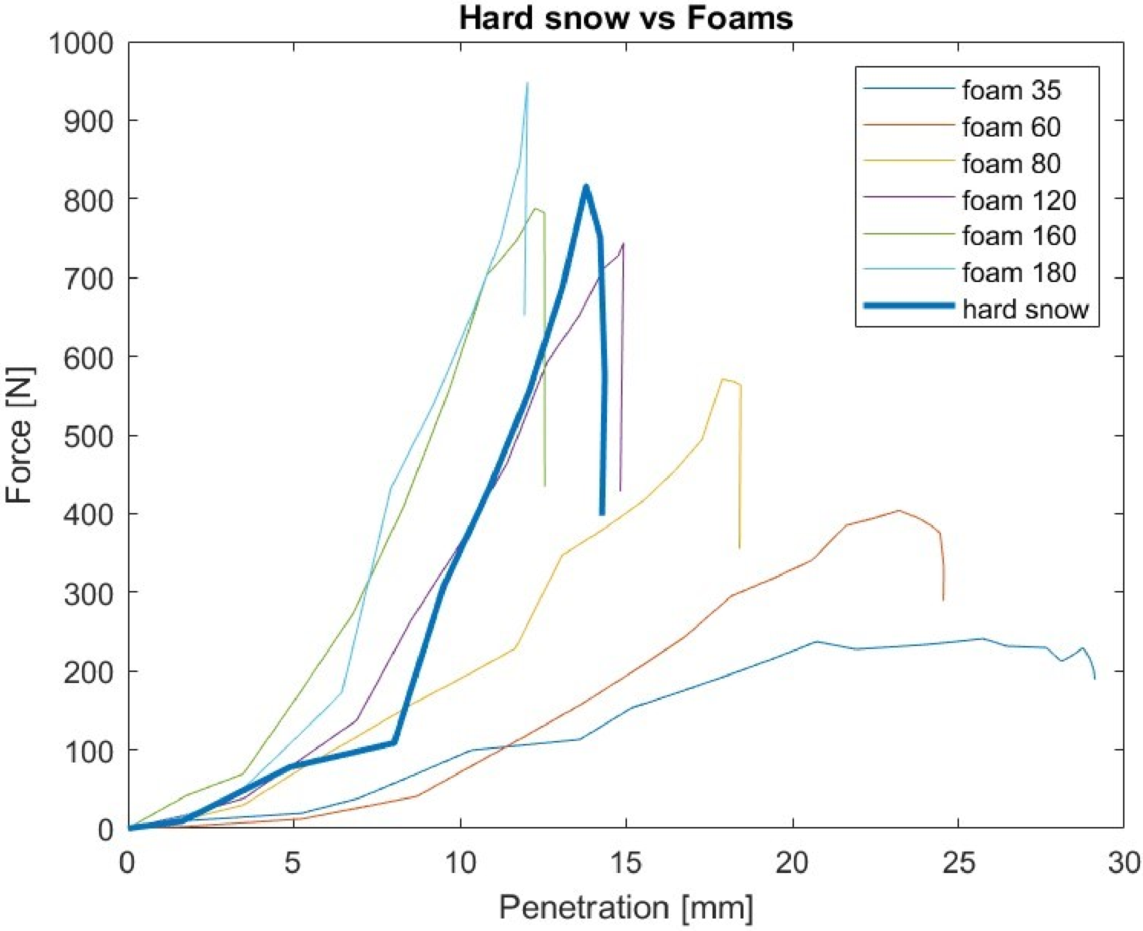

The force-penetration curve of the impact on hard snow is shaped with a growing phase ending with a peak. Peak force value of the hard snow is around 800 N while the penetration depth reached on the impact is 14.5 mm. The curve of foam 120 has shape very similar to the one of the hard snow curves. Moreover, the peak force of the curve of foam 120 is close to hard snow peak force (750 N and 800 N). Penetration depth value of the foam 120 curve is 15 mm. Considering the three parameters, force-penetration curve of foam 120 is very similar to force-penetration curve of hard snow tested in Slovenia.

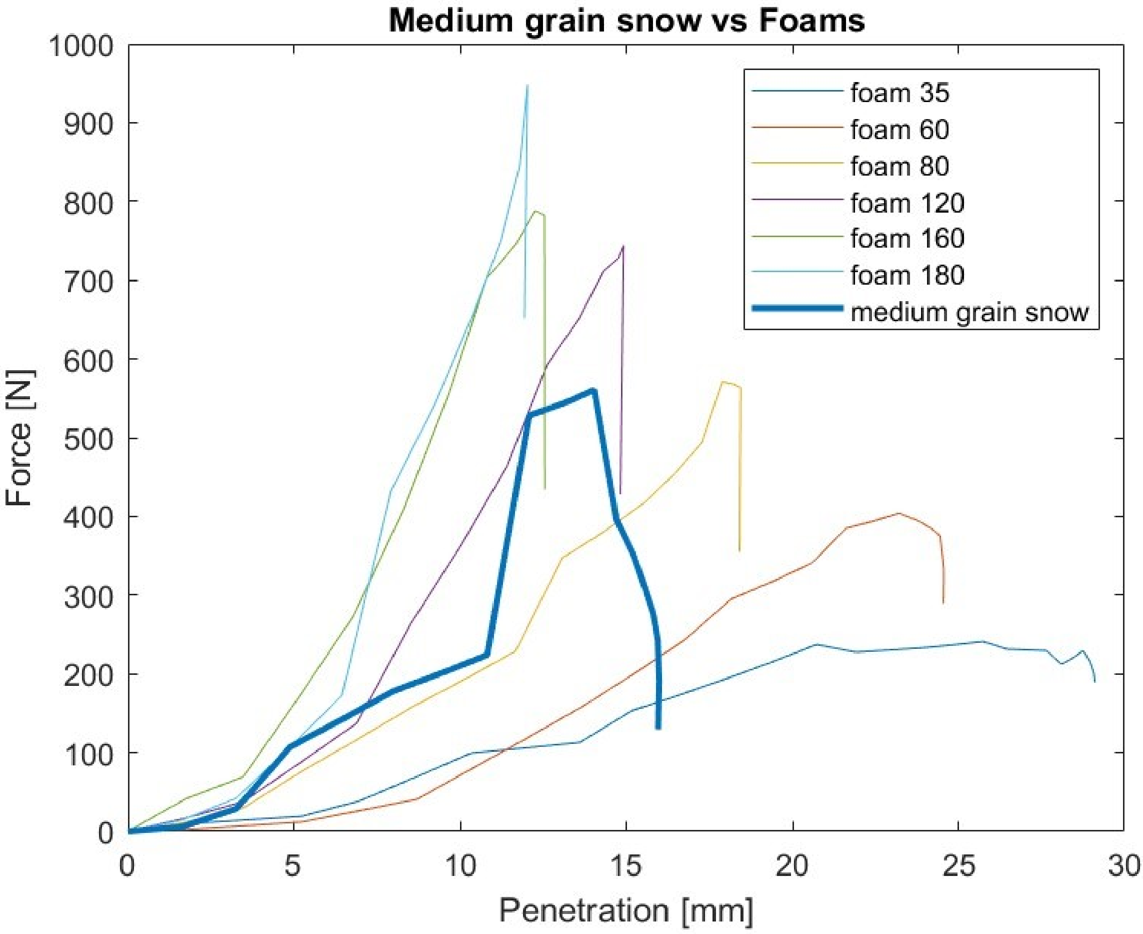

Impact in Slovenia on medium grain snow shows a force-penetration graph with a growing phase ending in small force plateau between 500 N and 600 N. Peak value of medium grain snow is near to the peak value of foam 80 (550N). Also the geometry of the curve of the snow is more similar to the foam 80 because of the small force plateau present at the peak force. Instead, the penetration depth of medium grain snow (16 mm) is near to the penetration of foam 120 (15 mm). Considering the three parameters, force-penetration curve of foam 80 is like force-penetration curve of medium grain snow, despite small differences in penetration depth.

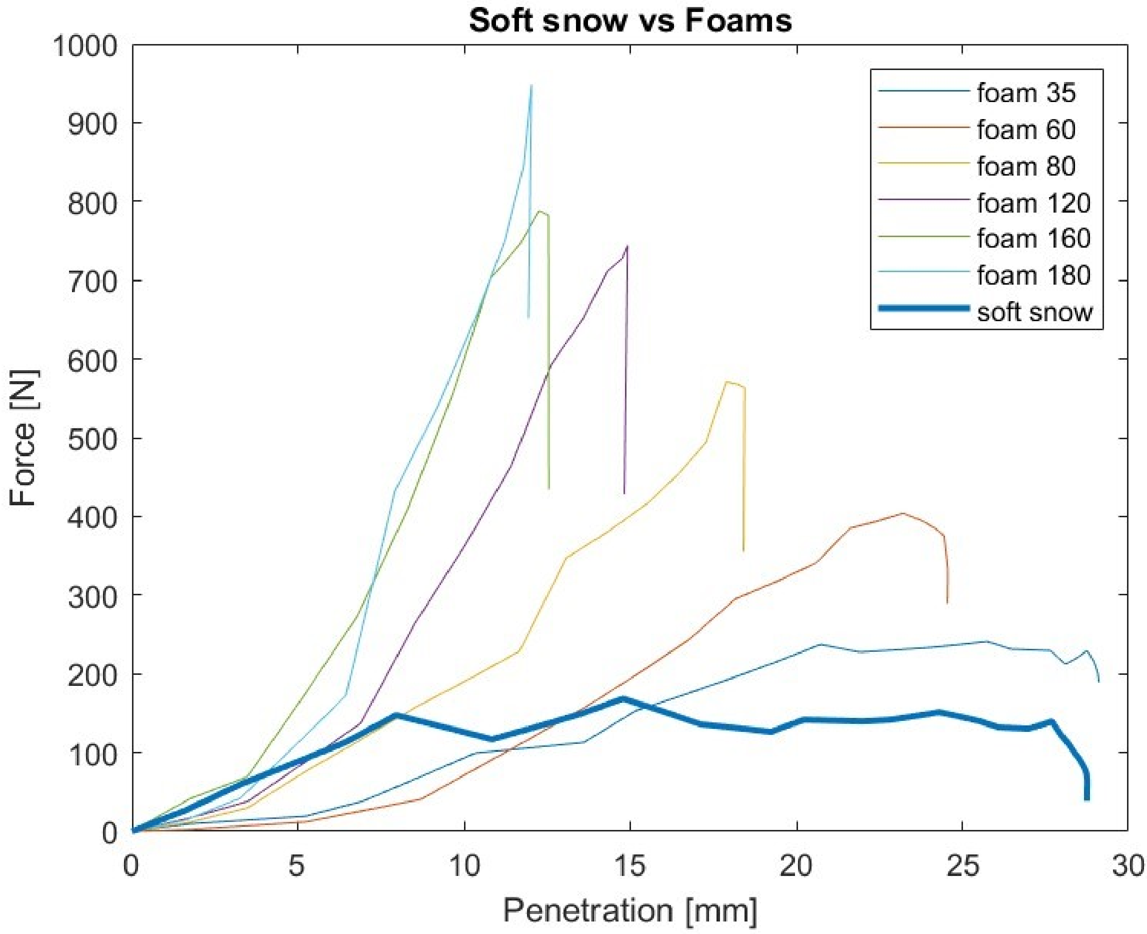

Soft snow force-penetration curve shows a different geometry than others snow. It has a smaller growing region in the first phase but a large force plateau in the final phase. Its peak force values arrive in the plateau at 150 N and its penetration depth reach 28 mm. Foam 35 has a similar geometry with an initial small growing phase and a plateau in the final zone. Peak force value of foam 35 is around 250 N, higher than peak force value of the soft snow. Soft snow has smaller peak force (around 150 N) than the foam 35 but same penetration (28 mm). Foam with density 35 kg/m^3 has a similar behavior of the soft snow.

3.4 Subjective evaluation results

A ski test was made in *Madonna di Campiglio* with five testers to fill the questionnaire already presented and giving a subjective evaluation of six ski parameters: edge switching quickness, edge catching quickness, carving precision, reactiveness at the end of the turn, energy rebound and vibration damping. Once the answers were collected, mean vote of each category and overall vote were calculated for each ski. Results were then plotted in histograms and commented.

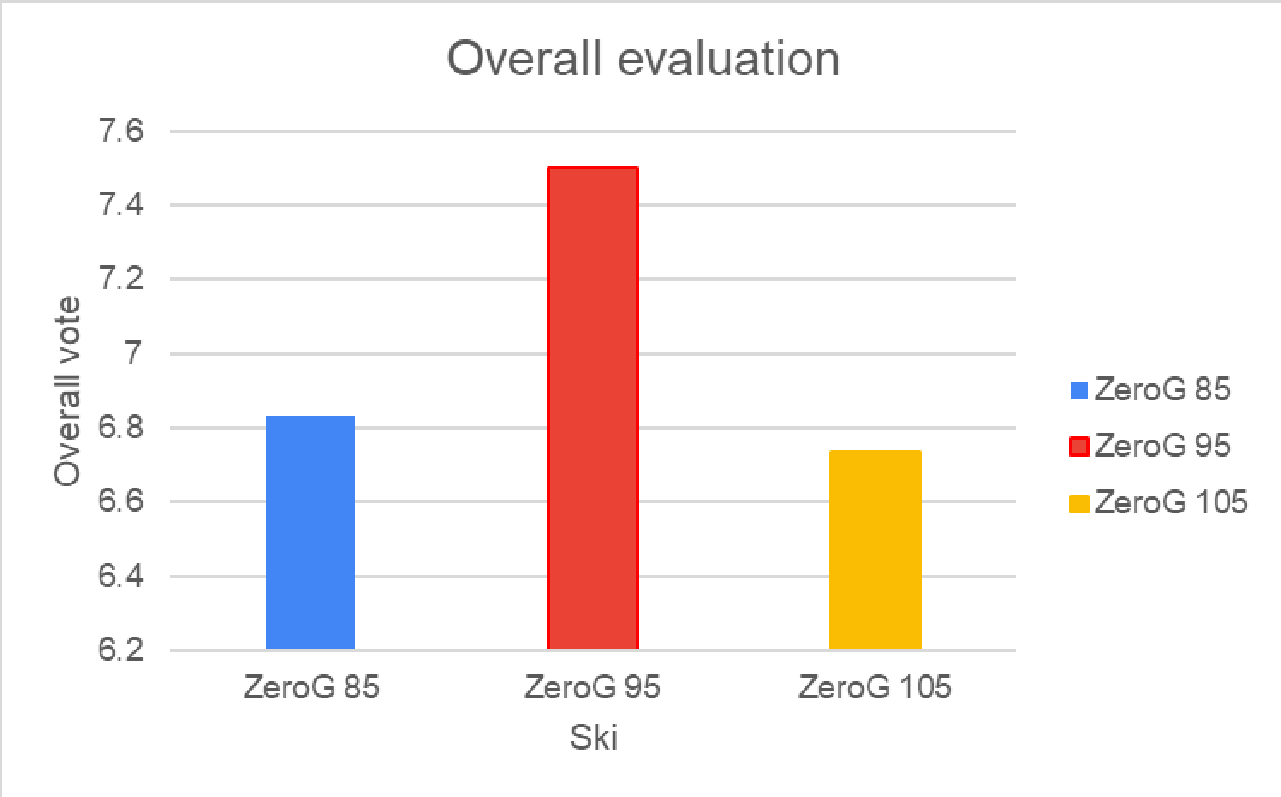

Figure 3.6: overall evaluation of the three ZeroG skis

The *Blizzard ZeroG 95* was the best ski for all the testers and received a medium vote for all the parameters of 7,5. *Blizzard ZeroG 85* and *Blizzard ZeroG 105* were similar as overall mean evaluation with a compressive vote of 6,83 and 6,73.

Singular categories evaluation are presented in the graph below.

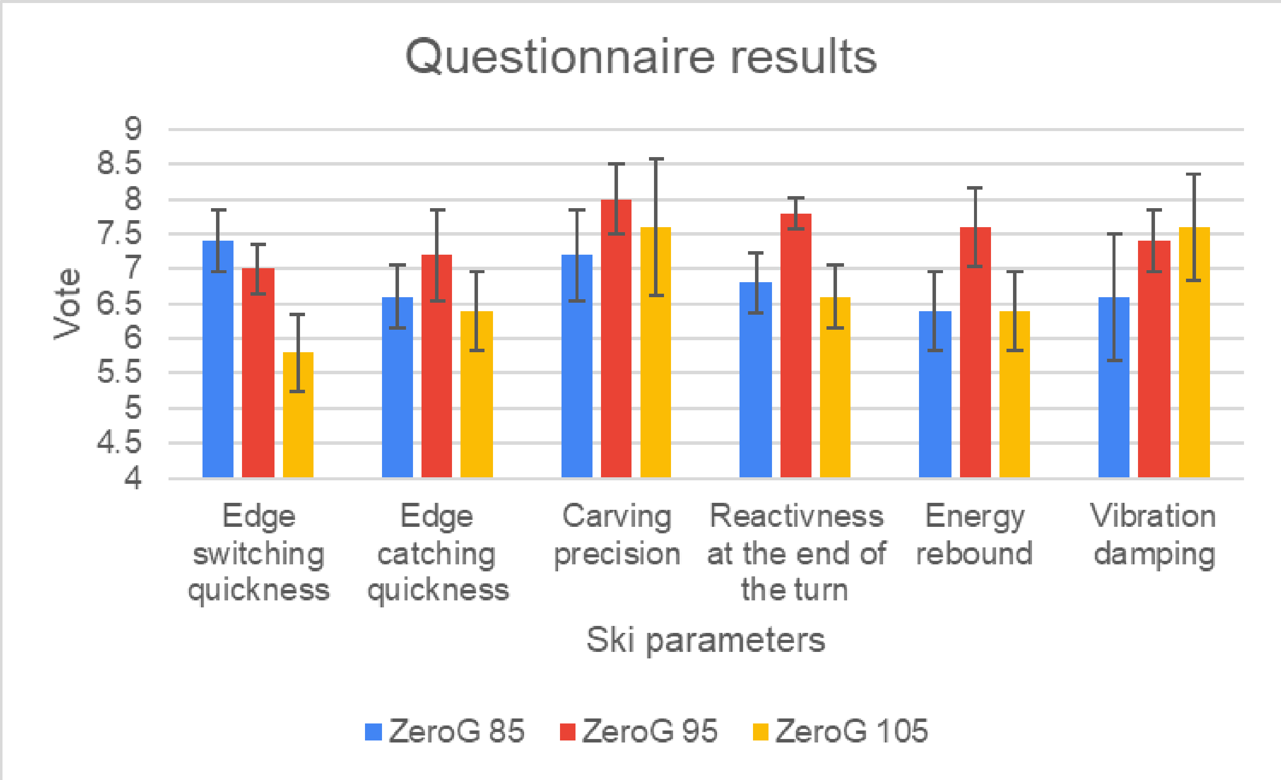

Figure 3.7: mean vote results from subjective evaluation

The edge switching quickness parameter decreased as the width of the ski increases: the *ZG85* had a medium vote of 7.4, the *ZG95* had a medium vote of 7 while the *ZG105* had a medium vote of 5.8. Wider skis needed more effort to switch edge according to skiers feedbacks. The edge catching quickness had a different vote trend, with the *ZG95* collecting the highest vote (7.2) above *ZG85* and *ZG105*. For the skiers *ZG95* was the fastest ski in edge catching. *ZG95* is first as carving precision with the highest mean vote collected (8), behind it are present *ZG105* and *ZG85*. Reactiveness at the end of the turn had the same trend as the edge catching quickness, with the *ZG95* in the first position, *ZG85* in the second position and *ZG105* in third. *ZG85* and *ZG105* collected the same mean vote in Energy rebound: 6.4. Also for this evaluation parameter *ZG85* and *ZG105* ranked below *ZG95* (collected again the highest vote). Trend change for the Vibration damping parameter, where wider skis felt less vibration. In fact, *ZG105* collected the highest vote in vibration damping (7.6) before *ZG95* and *ZG85***.**

Overall, the *Blizzard ZeroG 95* collected highest votes and was considered the best ones in four of six categories. *Blizzard ZeroG 85* and *Blizzard ZeroG 105* classified first in only one category, collected similar overall vote but show differences in single categories.

3.5 Correlations results

Data collected during with bench tests and with load cells system are compared with vote obtained from subjective evaluation to see if correlations are presents between the two. All the data extracted from indoor and outdoor tests were reported in the table below.

		Ski		
		ZG85	*ZG95*	*ZG105*
Tests results	Area tip	3.37101	3.376729	3.033925
	Area tail	2.403031	2.569921	2.12321
	Growing spee	2.074286	2.066063	1.926763
	Growing spee	1.090966	1.002609	1.161445
	My Peak [Nm]	43	38	44
	Mx Peak [Nm]	19	22	25
	Fy Peak [N]	48	44	58
	Fz Peak [N]	600	597	594
	Edge switchin	7.4	7	5.8
	Edge catching	6.6	7.2	6.4
	Carving precis	7.2	8	7.6
	Reactivness a	6.8	7.8	6.6
	Energy rebour	6.4	7.6	6.4
	Vibration dam	6.6	7.4	7.6

Coefficient r between the objective and subjective evaluation were calculated with *Excel* and collected in another table highlighting in orange absolute values of r higher than 0.85.

		Ski subjective evalutaions					
		Edge switc	Edge catcl	Carving pr	Reactivnes	Energy reb	Vibration d
Objectiv	Area tip	0.967123	0.703799	0.014568	0.639881	0.512563	-0.64357
	Area tail	0.813163	0.910639	0.369681	0.871593	0.784733	-0.32882
	Growing s	0.981442	0.656788	-0.04959	0.589277	0.456438	-0.69134
	Growing s	-0.6741	-0.97673	-0.55511	-0.95459	-0.89663	0.124906
	My Peak [	-0.42342	-0.99627	-0.77771	-1	-0.98783	-0.17637
	Mx Peak [	-0.96077	-0.24019	0.5	-0.15554	0	0.944911
	Fy Peak [N	-0.86603	-0.86603	-0.27735	-0.81966	-0.72058	0.419314
	Fz Peak [N	0.960769	0.240192	-0.5	0.155543	0	-0.94491

The correlations between subjective evaluations and objective parameters are numerous for edge switching quickness, edge catching quickness, reactivity at the end of the turn, energy rebound, and vibration damping parameters. Instead, for carving precision, there are no correlations with an absolute value of $r > 0.85$. The quality of all these correlations will be further discussed in the subsequent chapter of this thesis.

Moreover, correlations are searched between test results and the construction parameters obtained from *Soothski* database. In table below are presented the construction parameters extracted from the database.

		Ski		
		ZG85	*ZG95*	*ZG105*
Construction	Tip width [mm	116	127	133
	Tail width [mm	100	111	117
	EI mean [Nm^	219	227	221
	GJ mean [Nm	73	87	86
	Weight [g]	1157	1236	1530
	Surf/Weight [c	1.41	1.46	1.31
	Tip rocker leng	220	293	220
	Tail rocker len	132	185	232
	Camber [mm]	9	4	5
	Sidecut radius	22.5	22.3	24.1

The same process applied in the correlations research between objective and subjective evaluations were applied at correlations research between building parameters and test results. Coefficient r between the objective and subjective evaluation were calculated with *Excel* and collected in a table highlighting in orange absolute values of r higher than 0.85.

		Construction parameters									
		Tip width [	Tail width [	EI mean [N	GJ mean [	Weight [g]	Surf/Weigh	Tip rocker	Tail rocker	Camber [n	Sidecut radius [m]
Tests results	Area tip	-0.76072	-0.76072	0.291317	-0.43043	-0.97657	0.949579	0.512563	-0.84039	0.313527	-0.996220778
	Area tail	-0.47971	-0.47971	0.61288	-0.08078	-0.83591	0.998979	0.784733	-0.5923	-0.04518	-0.961844371
	Growing speed tip	-0.80078	-0.80078	0.229363	-0.48743	-0.98836	0.927516	0.456438	-0.87342	0.373783	-0.988599118
	Growing speed tail	0.286433	0.286433	-0.76402	-0.1286	0.703256	-0.96766	-0.89663	0.411481	0.252263	0.883761024
	My Peak [Nm]	-0.01203	-0.01203	-0.92155	-0.41822	0.459505	-0.84856	-0.98783	0.121251	0.529107	0.704210555
	Mx Peak [Nm]	0.985887	0.985887	0.240192	0.83224	0.948838	-0.65465	0	0.999401	-0.75593	0.810884854
	Fy Peak [N]	0.562956	0.562956	-0.53294	0.177555	0.885432	-0.99863	-0.72058	0.668013	-0.05241	0.983933098
	Fz Peak [N]	-0.98589	-0.98589	-0.24019	-0.83224	-0.94884	0.654654	0	-0.9994	0.755929	-0.810884854
	Edge switching qui	-0.90078	-0.90078	0.038462	-0.64582	-0.99919	0.838628	0.27735	-0.95059	0.544705	-0.941379836
	Edge catching quic	-0.07429	-0.07429	0.884615	0.338288	-0.53442	0.891042	0.970725	-0.20644	-0.45392	-0.762842281
	Carving precision	0.637927	0.637927	0.960769	0.896258	0.20096	0.327327	0.866025	0.529682	-0.94491	-0.101360607
	Reactivness at the	0.012027	0.012027	0.921551	0.418219	-0.4595	0.848555	0.987829	-0.12125	-0.52911	-0.704210555
	Energy rebound	0.167412	0.167412	0.970725	0.554416	-0.31576	0.755929	1	0.03462	-0.65465	-0.585205736
	Vibration damping	0.986374	0.986374	0.544705	0.967868	0.79321	-0.37115	0.327327	0.955677	-0.92857	0.574660625

The correlations between building parameters and tests results are numerous. Weight and Surface/Weight ratio are the building parameters with most correlation with r absolute value higher than 0.85 (6 correlations in total). EI stiffness modulus and Tip rocker length are also highly correlated with tests results showing 5 correlations in total. Tip width, Tail width and Sidecut radius has instead 4 correlations with $r > 0.85$. However, for carving precision, there are no correlations with an absolute value of $r > 0.85$. The quality of all these correlations will be further discussed in the subsequent chapter of this thesis.

4. Discussion

Tests carried out in this work had the final aim of functionally evaluating the behavior of ski touring skis. In particular three skitouring skis were evaluated: *Blizzard ZeroG 85, Blizzard ZeroG 95* and *Blizzard ZeroG 105*.

Edge Load Profile bench tests provided the distribution of forces along the ski edge at different load conditions and ski inclinations when pressed against hard surfaces. Results showed that for all three skis a good percentage of the force exerted on the ski is discharged on the part of the edge immediately under the front binding. The Edge Load Profiles of the three skis showed also how the curves rise with the rise of loads and inclination of the ski, especially increasing the values of the peak forces at the ends of the skis (tip and tail). This was underlined in the tip and tail ratio plot. It is also important to point out that forces are distributed across the edge up to 20cm from the ski tail and up to 30cm from the tip when the ski is pressed against a hard surface, and the working part of the ski is only 140cm long out of a total length of 180cm. Differences between the Edge Load Profiles of the three skis were analyzed at 40° of edging angle, with the actuator pushing 100 Kgf: *ZG105* showed a tighter working area on the edge (of 130cm), *ZG85* showed higher values of forces distributed under the bindings while *ZG95* showed the smoothest curve under the boots and higher and more external peak values in the tip and tail zone. As the Edge Load Profile bench reproduce and collect forces distributions of the ski pressed against a hard surface, differences in the skis collected with this test reproduce the real differences in the Edge Load force distribution between the three skis in hard snow conditions.

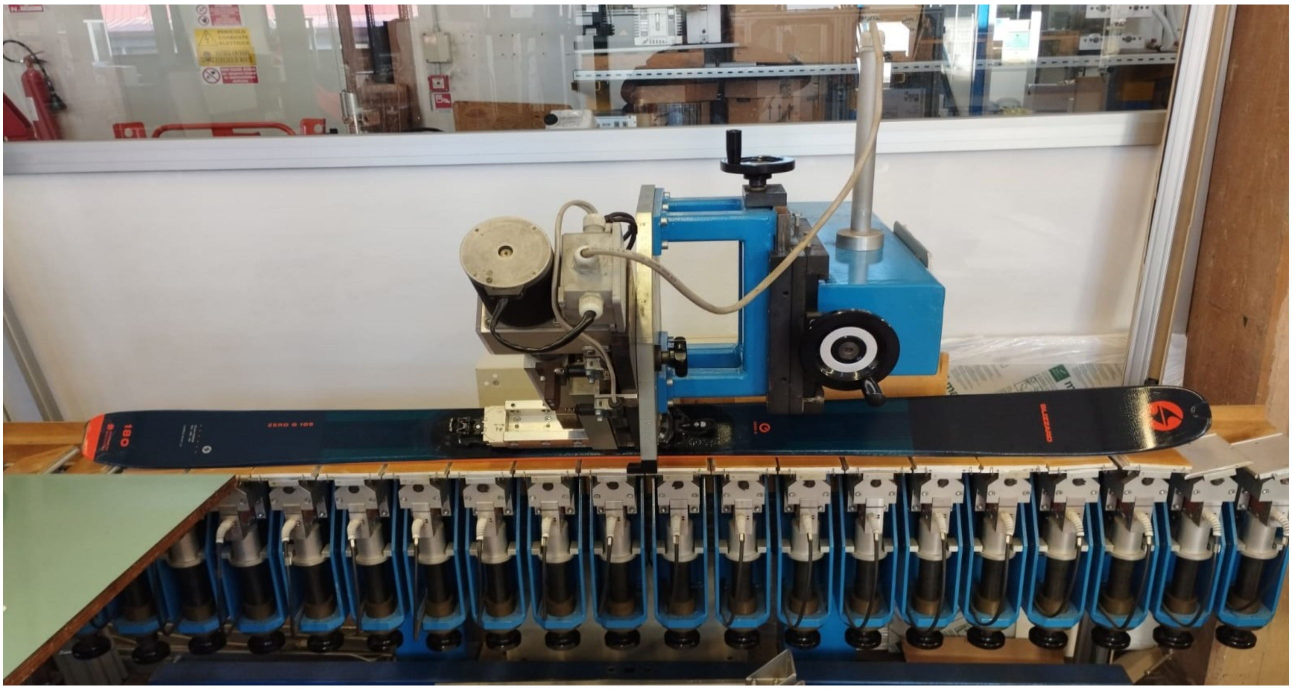

Figure 4.1: ZG105 edged on Slytech test bench

To simulate different snow conditions on the test bench, surrogate materials with similar characteristics were searched. Impact tests were performed on different types of snow and on phenolic foams to search similarities in the two materials.
Phenolic foams were selected for their composition of expanded closed cells, which collapse upon loading, mimicking the behavior of snow under pressure. Six samples of phenolic foams of different density were tested (35, 60, 80, 120, 160 and 180 kg/m^3) comparing their force-penetration curves with the ones of for different type of snow tested in Slovenia: ice, hard snow, medium grain snow and soft snow. Comparing the curves of the materials, ice can be reproduced indoor with some approximations with foam 180, hard snow can be reproduced with foam 120, medium grain snow can be reproduced with foam 80 while soft snow can be reproduced with foam 35. In future indoor tests with *Slytech* bench can be done with these foams to obtain the Edge Load distribution Profiles of the skis over different snow conditions.

Furthermore, tests conducted during *Winterschool* on the three skis instrumented with the load cells were useful in showing differences in the loads applied to the three skis. The tests conducted on the three skis were performed on two different subjects, both skiing with poles and skiing with free turns. The 6-axis load cells made it possible to obtain and compare forces and moments along the 3 axes acting under the center of the ski. The results showed higher loads during the tests of subject number 2, reflecting its greater experience. The results showed also higher loads collected during tests with pole conditions than the loads collected during tests with free curve conditions, which confirms the fact that during pole skiing the skier applies more effort. Finally, the differences in the loads collected on the three skis were analyzed. The forces collected along the Y-axis were quite similar for the three skis: the ZG85 and ZG95 skis behaved similarly to each other and with small differences from that of the ZG105 skis (which showed slightly higher peak values). The forces along the Z-axis of the skis showed subtle differences: the ZG105 and ZG95 had similar and slightly higher values than the ones of the ZG85. Therefore, the Fy and Fz forces of the three skis have very small differences and can be considered similar to each other. The moments along the x-axis of the three skis, on the other hand, showed an interesting trend. Wider skis collected higher values of roll moment, while narrower skis collected lower values. This is because for the same applied force, the arm on which this force acts are greater for the wider skis. A skier will therefore have to apply a greater moment to make a wider ski change edge.

Figure 4.2: particular of Blizzard ZeroG 85 during in field tests

Subjective evaluations of the skis were then collected via questionnaire with the help of four ski instructors and a ski instructor student. Questionnaire results showed how ski instructor preferred *Blizzard ZeroG 95* over the two other skis. The better shaped Edge Load Profile obtained with *Slytech* bench for *Blizzard ZeroG 95* reflect the result. In addition, questionnaires also collected evaluations of ski performance during different phases of the turn. These evaluations were then compared with data obtained from bench tests and load cell track tests to look for correlations between subjective and objective evaluations. With excel, the table containing the correlation coefficients r between subjective and objective evaluations was constructed. Looking for correlations between two quantities with only three points can lead to finding false results. For example it is false that the edge catching quickness is highly correlate with the area under the tip of the Edge Load distribution. Thus, in the final choice of correlations between subjective and objective quantities, both correlation coefficients and knowledge gained within this thesis were considered. Tables were therefore constructed showing graphical information about correlations, where **x** stands for a weak correlation, **xx** stands for a medium correlation and **xxx** represent a strong correlation.

		Ski subjective evalutaions					
		Edge switc	Edge catcl	Carving pr	Reactivnes	Energy ret	Vibration d
O	Area tip	x	xx				
b	Area tail				xxx		
j	Growing speed tip	x	x				
e	Growing speed tail				xxx	x	
c	My Peak [Nm]		x	x	x	x	
t	Mx Peak [Nm]	xxx					
i	Fy Peak [N]	x			x		
v	Fz Peak [N]	x					

With this methodology, it was observed that the angular momentum along the x-axis measured at the track with load cells is strongly correlated with edge switching quickness, that the sum of the forces on the tip of the edge obtained at the bench are strongly correlated with edge catching quickness, and that the reactiveness at the end of the turn is strongly correlated with the sum of the forces on the tail of the edge obtained at the bench and the rate of growth of the latter with respect to increasing angle. From *Slytech* bench tests results can be then evaluated the edge catching quickness and the reactiveness at the end of the turns for the skis. From load cells results can be evaluated for example the edge switching quickness parameters.

The same process was then applied at the comparison of building parameters and results obtained from vary tests. The table constructed showing graphical information about correlations is presented below.

		Building parameters									
		Tip width [	Tail width [	EI mean [N	GJ mean [	Weight [g]	Surf/Weigh	Tip rocker	Tail rocker	Camber [m	Sidecut rac
T	Area tip	xx									xx
e	Area tail		x								xx
s	Growing s	xx									xx
t	Growing speed tail		x								xx
s	My Peak [Nm]			xx							
	Mx Peak [	xx	x			x					
r	Fy Peak [N]					x					
e	Fz Peak [N	xx	x		x	x					
s	Edge switc	x	x			xx			xx		x
u	Edge catcl	xx		xx				xx			x
l	Carving precision			xxx	xx			x		x	
t	Reactivness at the end of the tur			xx					x		x
s	Energy rebound			xx							
	Vibration damping										

Results showed good correlations between the bending stiffness and the edge catching quickness, reactiveness at the end of the turn, energy rebound and with carving precision. Instead sidecut radius had interesting correlations with the Area under the tip, the area under the tail, the growing speed tip and the growing speed tail obtained by *Slytech* bench. Others good correlations are present and can be observed analyzing the table, confirming how building parameters affect the performances of the skis.

5. Conclusions

This work aimed to develop a methodology for the evaluation of ski responses during typical usage, helping the final customers in the ski choice but also ski constructor in the functional evaluation of prototype and final products. The differences in the ski loads and in the ski performance of skis with different widths were analyzed with this methos. At first the pressure distribution at the skis edge was evaluated using the Edge Load Profile testbench in the *University of Padova* laboratory. Through the testbench the edge load distribution, a peculiar "footprint" of the ski edge on the snow was determined for each ski at different inclinations and applied loads. This allowed us to observe how skis of different widths distribute the applied force along their length over a hard surface. To search materials able to mimic the snow behavior on the Edge Load Profile bench, impact tests over snow and surrogate materials were also carried on. Phenolic foams of different densities can reproduce different snow conditions: in future indoor tests with *Slytech* bench can be done with phenolic foams to obtain the Edge Load distribution Profiles of the skis over different snow conditions. Moreover, the ground reaction forces and moments under the skis were measured during in field tests, using load cells positioned between the skis and the front and rear bindings. Two different subjects skied in an outdoor in vivo session with the three *Blizzard ZeroG* skis. As the loads measured during this session directly correspond to the loads applied by skiers to the skis, these loads quantify the differences in skiing performance across skis of various widths but also across different subjects and different skiing situations. At the end subjective evaluation of the three *Blizzard ZeroG* skis were collected with a questionnaire on the ski performances from five ski instructor. While objective data provide fundamental information about the technical performance of skis, subjective evaluations complement this framework by providing a direct and intuitive experience of how the ski adapts to one's own style and ability. Sensations of stability, responsiveness, maneuverability, and comfort are difficult to quantify purely objectively and largely depend on the individual preferences of the skier. After data collection correlations between subjective evaluation and data measured in indoor and outdoor tests were searched. Strong correlation means that edge load profiles and load cell measurement are representative of the ski behavior in field. Furthermore, correlations are explored between the geometrical and stiffness parameters of skis and subjective assessments, edge load distributions, and load cell measurements. This analysis helped to understand which specific construction parameters like ski geometry and ski stiffness impact the ski's performance characteristics. Unfortunately, the correlations obtained between test results and construction parameters were not thoroughly analyzed, as having tested a low number of skis the correlation coefficients r may have been found to be out of whack. More skis should be tested in the future to assess the true correlation between test results and building parameters.

In addition, the tests on ski touring skis were conducted only in slope conditions. Load cells in fresh snow would have measured low load values and a slope approach was chosen. The bench tests and subjective evaluation tests were equalized with on-piste tests to obtain comparable results. Both outdoor and indoor off-piste snow tests may be conducted in the future, thanks to the snow surrogate materials found in this work.

Through this wide approach that includes indoor bench tests, on-slope load cell measurements, and on-slope subjective evaluations, a complete evaluation of the differences in loads and performances of skis with different widths is conducted. This methodology can be a valid help for ski manufacturer during the phase of prototyping evaluation and a valid alternative to testers feedback on different prototypes. The results obtained from the final product evaluation conducted through this approach can serve also as a valuable tool for the final customer. Ski selection by users can be informed not only by construction parameters but also by this comprehensive assessment of the ski's performance on the snow. Other research can be carried out with this system in order to provide winter sports enthusiasts with increasingly high-performance and modern materials.

Bibliography

[1] Zullo, G., Cibin, P., Bortolan, L., Botteon, M., & Petrone, N. (2023). An Innovative Compact System to Measure Skiing Ground Reaction Forces and Flexural Angles of Alpine and Touring Ski Boots. *Sensors*, *23*(2).

[2] M. Supej, V. Senner, N. Petrone, and H. C. Holmberg, "Reducing the risks for traumatic and overuse injury among competitive alpine skiers," Br. J. Sports Med., vol. 51, no. 1, pp. 1–2, 2017.

[3] N. Petrone, D. Vanzetto, G. Marcolin, B. Bruhin, and M. Gilgien, "The effect of foot setting on kinematic and kinetic skiing parameters during giant slalom: A single subject study on a Paralympic gold medalist sit skier.," J. Sci. Med. Sport, vol. 24, no. 10, pp. 1049–1054, Oct. 2021.

[4] N. Petrone, G. Marcolin, E. Centofante, and B. Atzori, "Analysis of the structural behavior of an innovative reinforced ski boot," Procedia Eng., vol. 2, no. 2, pp. 2599–2604, 2010.

[5] N. Petrone, G. Marcolin, and F. A. Panizzolo, "The effect of boot stiffness on field and laboratory flexural behavior of alpine ski boots," Sport. Eng., vol. 16, no. 4, pp. 265–280, 2013.

[6] N. Petrone, G. Marcolin, M. Cognolato, P. Hofer, and W. Nachbauer, "The effect of buckle closure and temperature on the in-vivo flexibility of ski-boots: A pilot study," Procedia Eng., vol. 72, pp. 630–635, 2014.

[7] G. Zullo, P. Cibin, and N. Petrone, "Torsion and bending loads on a ski-touring boot shell during uphill and downhill skiing [in press]," Sport. Eng.

[8] Campbell, J.R., Scher, I.S., Carpenter, D., Jahnke, B.L., & Ching, R.P. (2016). Performance of Alpine Touring Boots When Used in Alpine Ski Bindings. Journal of Applied Biomechanics, 33(5), 330–338.

[9] Truong, Jonas & Brousseau, Camille & Desbiens, Alexis. (2016). A Method for Measuring the Bending and Torsional Stiffness Distributions of Alpine Skis. Procedia Engineering. 147. 394-400.

[10] Neuwirth, C.; Snyder, C.; Kremser, W.; Brunauer, R.; Holzer, H.; Stöggl, T. Classification of Alpine Skiing Styles Using GNSS and Inertial Measurement Units. *Sensors* **2020**, *20*, 4232.

[11] Gosselin, Philippe & Truong, Jonas & Chapdelaine, Charles & Guilbert, Jean & St-Pierre, Étienne & Trahan, Xavier & Desbiens, Alexis. (2021). Effect of edged snow contact on the vibration of alpine skis. Sports Engineering. 24.

[12] Kabore, B. & Peters, Bernhard & Michael, Mark & Nicot, François. (2021). A discrete element framework for modeling the mechanical behaviour of snow—Part I: Mechanical behaviour and numerical model. Granular Matter. 23.

[13] Federolf, Peter & Auer, Mirco & Fauve, Mathieu & Lüthi, Anton & Rhyner, Hansueli. (2006). Subjective Evaluation of the Performance of Alpine Skis and Correlations with Mechanical Ski Properties.

[14] Petrone, Nicola. (2012). The use of an Edge Load Profile static bench for the qualification of alpine skis. Procedia Engineering. 34. 385–390.

[15] Han, Hongwei & Yang, Meiying & Liu, Xingchao & Li, Yu & Gao, Gongwen & Wang, Enliang. (2023). Study on the Constitutive Equation and Mechanical Properties of Natural Snow under Step Loading. Water. 15. 3271.

[16] Cherubin, E. (2016). Polymeric Foams: A New Method for Ski Edge Load Distribution Evaluation.

[17] La Chiesa, G. (2023). Characterization of snow impact properties and comparison with synthetic surrogates for the correct implementation of helmet safety standards

[18] Brousseau, C.; Desbiens, A.L. Alpine Skiing Recommendation Tool and Performance Prediction. Proceedings 2018, *2*, 316.